Development and Validation of a Human Blood Acyl-Specific Lipidomic Profiling Method for Clinical Applications

by

Juan José Aristizábal Henao

A thesis

presented to the University of Waterloo

in fulfillment of the

thesis requirement for the degree of

Master of Science

in

Kinesiology

Waterloo, Ontario, Canada, 2015

Author's Declaration

I hereby declare that I am the sole author of this thesis. This is a true copy of the thesis, including any required final revisions, as accepted by my examiners.

I understand that my thesis may be made electronically available to the public.

Abstract

Blood fatty acid levels have been used to determine dietary intakes of omega-3 highly unsaturated fatty acids, but also to examine the link between blood fatty acids, health and disease. However, these lipid analyses are gas chromatography-based and are dependent on derivatization of lipids to fatty acid methyl esters and do not provide information about the fatty acyl parent lipid species. The use of ultra high-performance liquid chromatography combined with tandem mass spectrometry (UHPLC-MS/MS) has the potential to do so. This thesis adapted a lipidomic approach to traditional blood fatty acid profiling to characterize lipids in their naturally-occurring state in human blood. Semi-quantitative methods using UHPLC-MS/MS were developed using a high-resolution Quadrupole-Orbitrap Hybrid Mass Spectrometer (Thermo Q-Exactive), and were validated for the determination of lipids in whole blood. Molecular species were confirmed for over 500 lipids, including phospholipids, sphingolipids, triacylglycerols, cholesteryl esters, free cholesterol and free fatty acids. Over 150 acyl-specific species were confirmed from all lipid classes. Following this, the method was used to validate dried blood spots for lipidomic profiling as this sampling technique offers several advantages, including minimally invasive sample collection, stability, and facilitated handling. Additionally, the UHPLC-MS/MS method was used to examine whole blood lipid remodeling that follows fish oil supplementation. Specifically, the blood lipidomic profiles of samples from a previous intervention trial comprising 20 participants that received eicosapentaenoic acid + docosahexaenoic acid (EPA+DHA) at 150 mg/d, 500 mg/d, and 1000 mg/d over a twelve-week period were determined. Notably, lipidomic profiling of whole blood suggests that three specific lipids (16:0/DHA phosphatidylcholine, 16:0/EPA phosphatidylcholine, and plasmenyl-phosphatidylethanolamine P-16:0/EPA) increase in a dose-dependent manner with increasing

doses of EPA+DHA supplementation. Finally, lipidomic analyses of whole blood, plasma, and erythrocytes of individuals that consumed low, intermediate, and high amounts of EPA+DHA were performed. These results support previous observations on the rapid responsiveness of 16:0/DHA phosphatidylcholine and 16:0/EPA phosphatidylcholine to varying levels of EPA+DHA intake. The mechanisms through which lipid remodeling occurs remain to be elucidated. The work presented in this thesis provides the foundation for the use of acyl-specific complex lipids as biomarkers for omega-3 highly unsaturated fatty acid status and the lipidomic profiling method developed may be extrapolated for the characterization of acyl-specific lipids in other biological matrices.

Acknowledgements

I would first like to say thank you to my supervisor, Dr. Ken Stark. Ken, I have you to look up to – the career I have chosen is a reflection of how much I admire all of your hard work and passion for research. Thank you for making Juanimal a fat head. I am thankful for all of the opportunities you've given me so far, the projects that I've been allowed to work on (yes, even Burkina), and the projects that we have in mind for the next four years. Also thank you for letting me come into your office to pick your brains on an almost daily basis. Oh, and for drinking almost as much coffee as me.

I'd also like to thank my committee members, Dr. Russ Tupling and Dr. Robin Duncan, for their support and guidance over the past two years. Thank you also to everyone past and present in the Stark Lab, my friends Kristin(a), Isaac, Alan, Dr. Alex Kitson, Dr. Ashley Patterson, her samples, and especially Dr. Adam Metherel for being a role model and teaching me how to do everything in the lab. Thank you to my friends in the Duncan Lab and everyone in Physiology, as well as Cheryl Kieswetter, Denise Hay, Jing Ouyang, Dr. Eric Bombardier and Marg Burnett. A special thank you to Dr. Richard Smith for his support and expertise on mass spectrometry. More thank-yous to Dr. Jim Rush for his encouragement and multiple reference letters, Sigma-Aldrich for providing the prototype UHPLC column that significantly helped my results, Thermo-Fisher for providing us with LipidSearch, and the Natural Sciences and Engineering Research Council of Canada for my USRA and Doctoral Scholarship.

A final thank you goes to my friends and family, la Mona, Ana (cabra papel hagamos algo), Howard and Braedon, and especially Ma, for being the bravest person I know and being my most constant and dedicated teacher throughout the last 24 years. Tqm.

Table of Contents

List of Figures

List of Tables

List of Abbreviations

APCI	Atmospheric Pressure Chemical Ionization
AUC	Area Under the Curve
BF_3	Boron Trifluoride
CE	Cholesteryl Ester
CI	Chemical Ionization
CL	Cardiolipin
DBS	Dried Blood Spot
DDA	Data-Dependent Acquisition
DHA	Docosahexaenoic Acid (C 22:6n-3)
EDTA	Ethylenediaminetetraacetic Acid
EI	Electron Ionization
EPA	Eicosapentaenoic Acid (C 20:5n-3)
ESI	Electrospray Ionization
FAC	Fatty Acid Composition
FFA	Free Fatty Acid
G3P	Glycerol-3-Phosphate
GC-FID	Gas Chromatography-Flame Ionization Detection
HCD Cell	Higher-energy Collisional Dissociation Cell
HPLC	High-Performance Liquid Chromatography
HPLC-MS/MS	High-Performance Liquid Chromatography-Tandem Mass Spectroscopy
m/z	Mass-to-charge ratio
MALDI	Matrix-Assisted Laser Desorption Ionization

MS/MS	Tandem Mass Spectrometry
NIST	National Institute of Standards and Technology
PC	Phosphatidylcholine
PDA	Photodiode-Array
PE	Phosphatidylethanolamine
PG	Phosphatidylglycerol
PI	Phosphatidylinositol
PS	Phosphatidylserine
PUFA	Polyunsaturated Fatty Acid
QTOF	Quadrupole-Time Of Flight
RT	Retention Time
SIM	Selected-Ion Monitoring
TAG	Triacylglycerol
TOF	Time Of Flight
UHPLC	Ultra-High Performance Liquid Chromatography
UV	Ultra Violet

Chapter 1

Introduction

Lipidomics is an emerging field of study driven by advancements of analytical tools, particularly increased real-world usability and commercial availability of mass spectrometry (MS) coupled to high-performance liquid chromatography (HPLC). Previously, changes in the fatty acid profile of whole tissues and lipid fractions in response to dietary intervention were obtained from more traditional methods, such as thin-layer chromatography and gas chromatography-flame ionization detection (GC-FID) (Metherel et al., 2013; Patterson et al., 2012). These techniques, however, provide an indirect examination of lipids due to sample processing as fatty acyls are removed from their parent lipid. High-performance liquid chromatography coupled with tandem mass spectrometry (HPLC-MS/MS) allows the characterization of lipid molecules in their naturally occurring state (Sandra et al., 2010). These techniques also enable the discrimination of lipid species such as glycerolipids that have isobaric molecular weights but different fatty acyl constituents. These lipidomic methods enable a thorough understanding of molecular remodeling events that take place on cellular lipids under dietary manipulation but also conditions such as pregnancy and metabolic diseases (Koulman et al., 2014; Uhl et al., 2013; Wang et al., 2014; West et al., 2013; Zhang et al., 2013), but their use remains relatively limited.

Most of the available literature employing a lipidomic approach for human blood focuses on the examination of either plasma or erythrocyte fractions. The use of whole blood for fatty acid determinations has increased recently as it is inclusive of cellular and lipoprotein lipids, and it also lends itself to rapid sampling techniques such as fingertip prick collection and dried blood spotting (Armstrong et al., 2008). While the use of whole blood in method development presents

a data-management challenge due to its complexity, it enables the examination of more lipid structures compared to isolated plasma or erythrocyte fractions. This thesis presents a comprehensive acyl-specific lipidomic profiling method for whole blood. The use of whole blood is validated and compared to lipidomic examinations of dried blood spots, plasma and erythrocyte fractions, as well as comparisons to traditional fatty acid profiling techniques. Additionally, there appears to only be one study (Uhl et al., 2013) using lipidomics to examine omega-3 supplementation and this was limited to a single dose of DHA (510 mg/day for 29 days); lipidomic discrimination of acyl-species was done in plasma and erythrocyte fractions separately. As such, this thesis aims to adapt lipidomic analyses to human whole blood, and provide a more thorough analysis of lipid remodeling events that occur in human blood with varying doses of omega-3 HUFA supplementation over a twelve-week period. Furthermore, this thesis aims to find appropriate experimental conditions through which a representation of the human whole blood lipidome can be achieved while minimizing sample runs and sample preparation. Specifically, the use dried blood spots will be examined as their use in research and clinical settings is increasing due to their minimally invasive nature, and their ease of storage and transport. Lipidomic discrimination of acyl species in dried blood spots has been validated in heel pricks of infants (Koulman et al., 2014), but not in an adult population. Moreover, this was limited to examinations of some phosphatidylcholine (PC), cholesteryl ester (CE), sphingomyelin (SM) and triacylglycerol (TAG) species while phosphatidylethanolamines (PE), phosphatidylserines (PS), phosphatidylinositols (PI), and sphingomyelins (SM) that are significant constituents of erythrocyte membranes (Wang and Gustafson, 1992) were excluded. The applications developed here can be extrapolated for the analysis of various biological samples, including other human and animal tissues.

Chapter 2

Background

2.1 *Lipidomics*

Lipidomics is an emerging field of study that aims to study all of the molecular moieties that can be characterized as lipids (i.e. the *lipidome*) in their naturally-occurring state, including fatty acids, glycerolipids, glycerophospholipids, sterol lipids, sphingolipids, prenol lipids, saccharolipids and polyketides (Fahy et al., 2009). This specialized discipline is part of the growing field of *metabolomics*, which together with transcriptomics, proteomics and genomics, constitute Systems Biology (Ellis et al., 2007). Technological advances in the biological sciences have enabled the rapid growth of these disciplines. Particularly, some of them have adopted methodological approaches that enable the identification and characterization of all of their subcomponents in a given sample (Schmelzer et al., 2007). Lipidomic profiling, like in other '-*omics*' fields, may be especially problematic in biological samples due to the dynamic ranges in concentrations and structures of lipid molecules. Nevertheless, the growth of lipidomics and its applications has greatly been supported by the development of invaluable methods that incorporate MS and, more recently, HPLC.

2.2 *Principles of High-Performance Liquid Chromatography*

HPLC, also known as high-pressure liquid chromatography, is an analytical method whereby a sample dissolved in a solvent is separated into its subcomponents based on physical and/or chemical interactions with mobile and stationary phases. HPLC relies on the basis of pumping the liquid sample at high pressures (up to 6000 psi for HPLC) through a narrow column. The column is lined in its interior surface with a solid compound, sometimes silica

beads of various sizes, which serves as the stationary phase. As the sample is introduced into one end of the column, a predetermined solvent system continuously pumps (isocratic or gradient) solvents at specified flow rates to help guide the sample through the column; this is the mobile phase. The nature of the constituents of the sample will cause them to interact differently with the mobile and stationary phases, where those with a higher affinity for the mobile phase will be eluted first. As the compounds elute, different detectors employing various technologies are able to identify the constituents. A common technique for compound identification involves the use of photodiode array to measure the wavelengths of light that pass through a sample. More robust technologies such as MS, however, enable the characterization of the molecular formulae of the compounds being detected.

In HPLC, the nature of the compound or compounds of interest will largely dictate the solvent system, column, and detector to be used. HPLC methods can be classified as normal-phase- or reversed-phase. Normal-phase HPLC was the first to be developed, and involves a non-polar mobile phase and a polar stationary phase. In contrast, reversed-phase HPLC uses an aqueous solvent system and a non-polar surface lining the inside of the column. Approximately 75% of all HPLC methods currently employ a reverse-phase approach, due to its higher reproducibility (i.e. reduced inter-sample variability) and broader applicability compared to normal-phase HPLC (Waters, 2014). Additionally, the use of a polar solvent system enables the use of materials such as formic acid, which improve chromatographic resolution by stimulating the molecular ionization process that is needed in MS. While the use of single columns is most common in the literature, two-dimensional techniques that use two columns connected in tandem offer a considerable potential to increase peak capacity and resolution (Stoll et al., 2007). While two columns of the same packing material can be used just to increase the total length of the

stationary phase (Byrdwell, 2011), columns of different stationary phase materials may be employed, enabling the separation of sample constituents based on multiple physical and/or chemical properties. These significant advantages have driven the development of two-dimensional liquid chromatography techniques, but a disadvantage is that sample run times can increase to hours to tens of hours (Stoll et al., 2007). More recently, advances in HPLC technologies have enabled ultra-high performance liquid chromatography (UHPLC) applications to be developed (Varma et al., 2011). The use of smaller particle-sized columns coupled with instruments that are capable of withstanding much higher pressures (up to 15000 psi) improve the chromatographic separation and resolution of compounds that would otherwise co-elute (Forcisi et al., 2013). Additionally, adjustments may be made to chromatographic protocols to reduce sample run times and increase throughput (Plumb et al., 2005). Moreover, nano-flow liquid chromatography techniques are emerging that offer improved sensitivity and can enable the analysis of compounds found in low abundance in complex matrices (Gama et al., 2013; Kirsch et al., 2008). Nano-flow liquid chromatography also requires significantly less sample and mobile phase solvents compared to HPLC and UHPLC applications (Gama et al., 2013).

2.3 *Principles of Mass Spectrometry*

Modern MS relies on three basic concepts: ion vaporization/creation, ion separation and ion detection (Matsuo and Seyama, 2000; Moreau, 2006). Traditional mass spectrometers achieve ion creation through direct electron impact (EI), where the compounds of interest are bombarded with high-energy electrons. This technique enabled the development and evaluation of extensive libraries (Ausloos et al., 1999; Dagan et al., 1995), which are still currently used (Lowenthal et al., 2013). The development of 'soft' ionization techniques such as chemical

ionization (CI) followed, in which a gas (such as isobutane or acetonitrile) is ionized with an electron source and it is then allowed to interact with the analytes to transfer the charge. For EI and CI, the analytes need to already be in the gas phase prior to ionization. As a result, these ionization techniques are generally associated with gas chromatography methods. The ionization and vaporization of liquids and solids was not possible until the development of techniques such as Electrospray Ionization (ESI) and Atmospheric Pressure Chemical Ionization (APCI) for liquids, and Matrix-Assisted Laser Desorption Ionization (MALDI) for solids (reviewed in detail by Isaac et al., 2007). ESI and APCI largely rely on a nebulizing gas to convert liquids to a fine mist. Ionization can take place either at the nebulizing source with the application of a high electrical current directly to the capillary (in the case of ESI), or via a corona discharge following mist formation (APCI). The size of the newly formed droplets is gradually reduced as the solvent evaporates, until only the charged subcomponents of the original sample are left charged and in the gaseous phase. Droplet evaporation is further stimulated by heating the capillary to several hundred degrees, usually 200-300°C (Banerjee et al., 2011). Lastly, MALDI takes advantage of the physical properties of certain compounds to ablate when struck by a pulsed ultra-violet laser. Specifically, the matrix materials commonly used in MALDI all have in common a conjugated pi-system that readily absorbs UV energy (Precup-Blaga et al., 2013). Upon ablation, the analytes are released from their solid state and are ionized, generally by protonation.

For the ion separation step, multiple technologies such as a Quadrupole, Time of Flight (TOF), or Orbitrap may be used (Eliuk and Makarov, 2015). To separate ions, they rely on the ratio of the molecular weight of analytes to their charge (known as mass to charge ratio, *m/z*). Quadrupole mass spectrometers consist of four cylindrical, parallel metal rods that are connected

as opposing pairs. Very specific radio-electrical currents can be applied to each opposing pair, creating electrical fields that only allow certain ions to pass through to the detector. TOF instruments operate by applying an electric field to ions, making them gain kinetic energy. Ions with different *m/z* ratios gain different amounts of speed, and the TOF is able to measure very accurately the time when they hit the detector. The first publications for quadrupole- and TOF-MS date back to the 1950s (Paul et al., 1958) and (Wiley and McLaren, 1955), respectively. These technologies generally employ the use of electron multipliers, Faraday cups, or photomultiplier conversion dynodes in order to detect ions. More recently, developments in engineering and mathematical modeling led to the birth of orbitrap mass analyzers that enabled high-mass accuracy MS, providing information beyond nominal mass (Makarov, 2000). The orbitrap is made up of two key components: a central spindle and a cylindrical electrode. It is designed to trap ions by inducing an electrostatic field that causes ions to orbit around the spindle. Ions with different *m/z* ratios orbit along and around the spindle with different rotational, radial, and axial frequencies, causing them to separate. Moreover, ion detection in an orbitrap occurs by measuring the oscillation frequencies across the three axes and the image currents generated using the cylindrical electrode. These frequencies are then converted to *m/z* ratio data via Fourier transformation.

Technological advances over the past few years have resulted in the exponential growth of the field of MS and its applications across the biological sciences (Careri, 2011). Notably, hybrid instruments have been developed, and incorporate two or more of the techniques for ion separation described above (Yost and Boyd, 1990). These have shown increased quantitative capabilities that are often sought for examinations of complex systems (Ståhlman et al., 2009). Popular hybrid instruments include the quadrupole-orbitrap, triple-quadrupole, Q-trap (linear ion

trap as the third quadrupole in triple-quadrupole instruments) and quadrupole-time of flight mass spectrometers, all of which take advantage of a first-pass quadrupole mass filter and enable the accurate characterization of very specific compounds. These are landmarks of selected ion monitoring and some data-dependent acquisition methods (Hao et al., 2012). Due to all of the instrument combinations that can be configured and that are currently commercially available, the full characterization of biological metabolomes is progressively more within reach.

2.4 *High-Performance Liquid Chromatography, Mass Spectrometry, and the Growth of Lipidomics Research in Biological Matrices*

Although the study of lipids using MS tools has been ongoing since the early 1950s, the shift towards global lipid analysis or 'lipidomics' of biological systems has only taken place within the last decade or so. Specifically, Han and Gross in 2003 were the first to use the term *lipidomics.* The evolution of the field since then has resulted in the emergence of various subdisciplines, but these are still within an -*omics* approach and rely heavily on MS. Particularly, the division of lipidomics can be generally interpreted in terms of methodological approaches to target specific lipid classes (e.g. sphingolipidomics and phospholipidomics deal with sphingolipids and phospholipids, respectively; Buré et al., 2013; Merrill et al., 2009), interests in specific lipids based on their metabolic activity (e.g. functional lipidomics, mediator lipidomics; Arita, 2012; Ferreri and Chatgilialoglu, 2012), and targeted lipidomics of specific biological tissues for lipid profiling (e.g. neurolipidomics; Han, 2007) and structural mapping (MALDI-imaging lipidomics; Goto-Inoue et al., 2011). Furthermore, lipidomic methods within these specialized subdisciplines may take a targeted approach if there are specific lipids of interest within selected lipid classes (Isobe and Arita, 2014), or an untargeted approach in global lipid

screening applications (Godzien et al., 2015). Finally, some lipidomic profiling methods may take a form of an untargeted approach known as "*shotgun*" lipidomics (Han and Gross, 2003). Here, lipid extracts are directly infused into the ionization source of a mass spectrometer without prior chromatographic separation. Though this approach can generate MS data in acquisition times of just a few minutes, the resolution of isobaric lipid species in global lipidomics can be problematic due to the vast number of molecular moieties than may be present in biological samples.

The joint use of HPLC, ESI, and tandem MS form a well-suited method to determine the lipidomic profile of a system. While complex proteins can have molecular weights in the range of kilo-Daltons (eg. the molecular weight of actin is approximately 45 kDa; Rees and Young, 1967), the weights of most mammalian cellular lipids are less than 1000 Da. This is well within the scan range of most mass spectrometers. Furthermore, lipids generally form singly-charged molecules in soft ionization techniques like ESI, which simplifies their identification based on their predicted precursor *m/z* ratios (Cassiday, 2014). These characteristics enable lipidomic profiling to be possible in a virtually unlimited array of matrices, with or without prior chromatographic separation (Schuhmann et al., 2012). Most lipidomic profiling methods take advantage of many mass spectrometers' capabilities to perform tandem MS. Tandem MS relies on the generation of fragments from a precursor ion, and at least two rounds of ion separation. In lipidomics, fragmentation of native lipids is often carried out in order to characterize their fatty acyl constituents. Generally, tandem MS methods for fragmentation of acyl-containing lipids generate fragments that represent the loss of a fatty acyl chain. For example, the fragmentation pattern for a TAG containing palmitate (C16:0), stearate (C18:0) and docosahexaenoate (C22:6n-3) in positive ESI would reveal three peaks: one corresponding to the *m/z* ratio for a 16:0/18:0

diacylglycerol (loss of docosahexaenoate), one corresponding to a 16:0/22:6n-3 diacylglycerol (loss of stearate), and a third corresponding to a 18:0/22:6n-3 diacylglycerol (loss of palmitate). More elaborate tandem MS methods can go a step further and carry out MS/MS/MS. In this manner, tandem MS can often take the form of MS^n, with *n* being the number of ion separations performed with rounds of fragmentation in between each one. Though there are several ways to perform fragmentation, most current mass spectrometers use collision-induced dissociation (CID). In CID, ions are vibrationally excited with the application of a radiofrequency voltage while in the presence of a gas, such as nitrogen (Olsen et al., 2007). The ions and the gas collide once a certain kinetic energy is reached, causing the dissociation of the precursor ion. Less commonly used fragmentation methods include in-source fragmentation, where sufficient energy is applied in the ionization process to cause fragmentation within the mass spectrometer (Pais et al., 1997); and photodissociation, where the energy required for dissociation is supplied by the addition of a laser by an ultra-violet laser (Williams et al., 1990).

As with other -*omics* disciplines, there are several challenges in lipidomics. The development of the field of MS and related analytical tools has coincided with shift away from early applications of simple compound identification towards applications involving comprehensive qualitative and quantitative analyses (Eliuk and Makarov, 2015). Advances in technological instrumentation and software have played a vital role in moving the field forward, and this has been accompanied by the desire to do more to keep pushing the limits of our instruments. In a sense, instrumental solutions to current methodological problems become the limits of future applications.

Comprehensive qualitative determinations have increased the demand on management of experimental data due to the thousands of molecular moieties that may be found in a biological

sample. Though there are several emerging lipid-based mass spectrum databases and software solutions such as LipidBlast (Kind et al., 2013) LipidSearch (Peake et al., 2013) and LipidView (Simons and Arendt, 2010) that are well suited for identifying lipids, significant efforts need to be made to develop a comprehensive mass spectrometric method that generates data files which meet all of the criteria required by these programs (i.e. MS/MS spectra with sufficiently intense fragment ions; this may be an issue with fragmentation of phosphatidylcholine species following positive ESI: Lee et a., 2011).

Accurate quantitation of all the lipids in a lipidomic profile is another considerable if not more daunting challenge. Although the use of stable isotopes is widely accepted as the gold standard in quantitative MS (Snyder et al., 2015), this approach is not feasible in screening lipidomics applications since every analyte would have to have its own stable isotope. Stable isotopes for each and every specific lipid are not available, and those that do exist can be costly. Surrogate internal standards that share similar physical and chemical characteristics to several of the compounds of interest may be used instead. Specifically for lipidomics, exogenous lipids may be used as internal standards if factors such as the carbon length and degree of unsaturation of fatty acyl constituents, and phospholipid head group (if applicable) are taken into account (Koivusalo et al., 2001). Standardizing results to a single standard or standard curve is often employed. Although, this should be considered semi-quantitative analysis as the behaviour of lipids from multiple lipid classes after ESI cannot be normalized using a single lipid standard.

2.5 *Omega-3 Highly Unsaturated Fatty Acid Supplementation and Lipidomic Research*

Over the past decades, the relationship between blood lipids and omega-3 highly unsaturated fatty acid (HUFA) intake has been examined extensively. This has been greatly

influenced by early associations between the consumption of fish and positive health outcomes, such as reducing the risk of developing heart disease (Dyerberg and Band, 1979; Chowdhury et al., 2014). Most of this research has used fatty acid compositional data derived from gas chromatography analyses, resulting in specific parent acyl lipid species information being lost and limited to the fatty acid composition of lipid classes through separation techniques such as thin layer chromatography (Xu et al., 2007). Lipidomics can allow us to identify relationships between lipids, diet and health at the level of individual acyl species of complex lipids. Therefore, the metabolism of these very specific lipid molecules can be better characterized. The emerging literature on analysis of native lipids containing omega-3 HUFA in biological samples include the analysis of single lipid classes of cell cultures (Ramanadham et al., 2000; Rucker et al., 2013), isolated tissues (Lamaziere et al., 2011; Murthy et al., 2002; Sjövall et al., 2015), plasma, erythrocytes and other circulating blood cells (Ottestad et al., 2012; Pacetti et al., 2004; Stanke-Labesque et al., 2008; Uhl et al., 2013). Currently, there is no research available encompassing omega-3 HUFA supplementation and lipidomic profiling of acyl species in multiple lipid families in whole blood.

Chapter 3

Rationale, Objectives and Hypotheses

Fatty acid profiling techniques such as gas GC-FID, which form the basis for the lipid analyses of most of the available nutrition and health research, looks at the total fatty acid composition of biological tissues, and not the existing acyl species of the lipids. Moreover, the effects of fish oil supplementation has been examined extensively in the past decades, revealing possible cardioprotective effects (Harris et al., 2013) and the important role of DHA in neurological function and fetal development (Larque et al., 2012) but changes in tissue lipids have been limited to GC-FID analyses. Due to sample processing, significant information that may be of physiological relevance is lost. This information could provide a more thorough understanding of biological membrane remodeling events, and metabolism of fatty acids and lipids. Notably, fatty acid compositional research has examined the different rates of incorporation of different HUFAs into cellular membranes (Holub et al., 2011). However, the parent acyl-containing species information that is lost could provide insights with regards to recent versus long-term intake of omega-3 HUFA, or about their preferential incorporation into acyl-specific lipids. For instance, preliminary investigations in our laboratory have indicated that 16:0/DHA phosphatidylcholine (PC) increases dramatically in the latter stages of pregnancy in the rat, with only modest increases in other DHA-containing acyl-specific lipids (such as 18:0/DHA PC, 18:1/DHA PC; *unpublished observations*). Additionally, a shift towards the use of whole blood in lipid research seems to be prevalent in recent literature. This has been accompanied by investigations that have established associations between the lipid profiles of blood fractions (Metherel et al., 2012; Stark et al., 2015 (*unpublished observations*)). The use of whole blood may provide a more comprehensive examination of an individual's lipid profile.

Information from the analysis of whole blood can be used to draw conclusions about cellular bilayers and plasma lipoproteins, which can reveal important details about metabolism. In addition, there is less sample processing involved with the use of whole blood. Although recent developments in MS have highlighted the quantitative potential of MS methods (Serna et al., 2015), many applications of traditional fatty acid compositional research have used qualitative approaches for practical purposes, such as the Omega-3 Index (percent weight of EPA + DHA in erythrocytes; Harris et al., 2004). This also highlights the distinction between quality vs. quantity of fat. As such, not all of the emerging lipidomic profiling methods are fully quantitative, but have qualitative characteristics (Bird et al., 2015).

This thesis, therefore, aims to establish conditions for semi-quantitative lipidomic analysis of whole blood samples through HPLC-MS/MS that are fast, accurate and repeatable, and can be applied to whole blood stored in cryovials or on dried blood spot matrices. In addition, the molecular changes occurring in the human blood lipidome following fish oil supplementation at three different doses will be examined. Techniques to manage and interpret the lipidomic data will also be explored at the preliminary level (e.g. different ways of normalizing mass spectrometric data, and the potential of various spectral libraries and/or software solutions). Additionally, given the complexity of whole blood lipids, the methods from the proposed research have the potential to be readily adapted for the analysis of various biological samples if appropriate lipid volumes can be obtained.

3.2 *Objectives*

The present thesis involves the development and application of a novel lipidomic method employing UHPLC-MS/MS (see flow diagram: Figure 1). The initial objective was to establish

an untargeted lipidomic method for the characterization of lipids in human whole blood using a UHPLC-MS/MS method on the front-end of a Quadrupole-Orbitrap hybrid mass spectrometer. This involved preliminary work using commercially-available lipid standards and the application of the method using lipid extracts from human whole blood that included serial dilution analyses to determine appropriate volumes of blood to be used in sample preparations. Fine-tuning of chromatographic (ex. UHPLC column selection) and mass-spectrometric settings (ex. positive vs. negative mode) was also completed and the method was assessed in terms of its ability to detect, measure and report the most abundant lipids in human whole blood.

Upon the development of a whole blood lipidomic method, two applications were examined. The first application examined was the use of the method to determine the lipidomic profiles of liquid whole blood and dried blood spots (DBS) across individuals reporting low, medium and high levels of omega-3 fatty acid intake (n=3; 1F, 2M). This involved examining the extraction efficiency of both matrices, and comparing the results against traditional fatty acid composition data as determined by GC-FID. The second application and final objective was to characterize the changes that occur in the human whole blood lipidome with very specific dietary intakes of EPA+DHA using samples from a previous intervention trial. Specific acyl specific lipids that incorporate EPA and DHA as well as the lipids that they displace in the lipidome were identified. These changes were also tracked using neutral-lipid and polar-lipid thin-layer chromatography coupled to GC-FID in order to quantify total EPA and DHA content of specific lipid classes.

3.3 *Hypotheses*

1. An HPLC-MS/MS method will be developed that can detect native PC, PE, PI, PS, cardiolipin (CL), CE, free fatty acid (FFA), and TAG acyl species in positive ESI mode.
2. The relationship between increasing concentrations of lipids from blood lipid extracts and the observed instrument response will be positive and linear (data from serial dilutions of lipid extracts normalized to a single internal standard).
3. Lipidomic analysis of lipid extracts from dried blood spots and whole blood will give comparable results in terms of normalized lipid abundances for all lipids, independent of the extraction time and omega-3 HUFA status.
4. Increasing intake of EPA and DHA will increase EPA and DHA acyl species across all lipid classes.
5. Palmitoyldocosahexaenoyl phosphatidylcholine (16:0/DHA PC) will be the most responsive acyl-specific lipid to supplementation of DHA, and will increase the most compared to other DHA-containing lipids with increasing doses of the supplement.

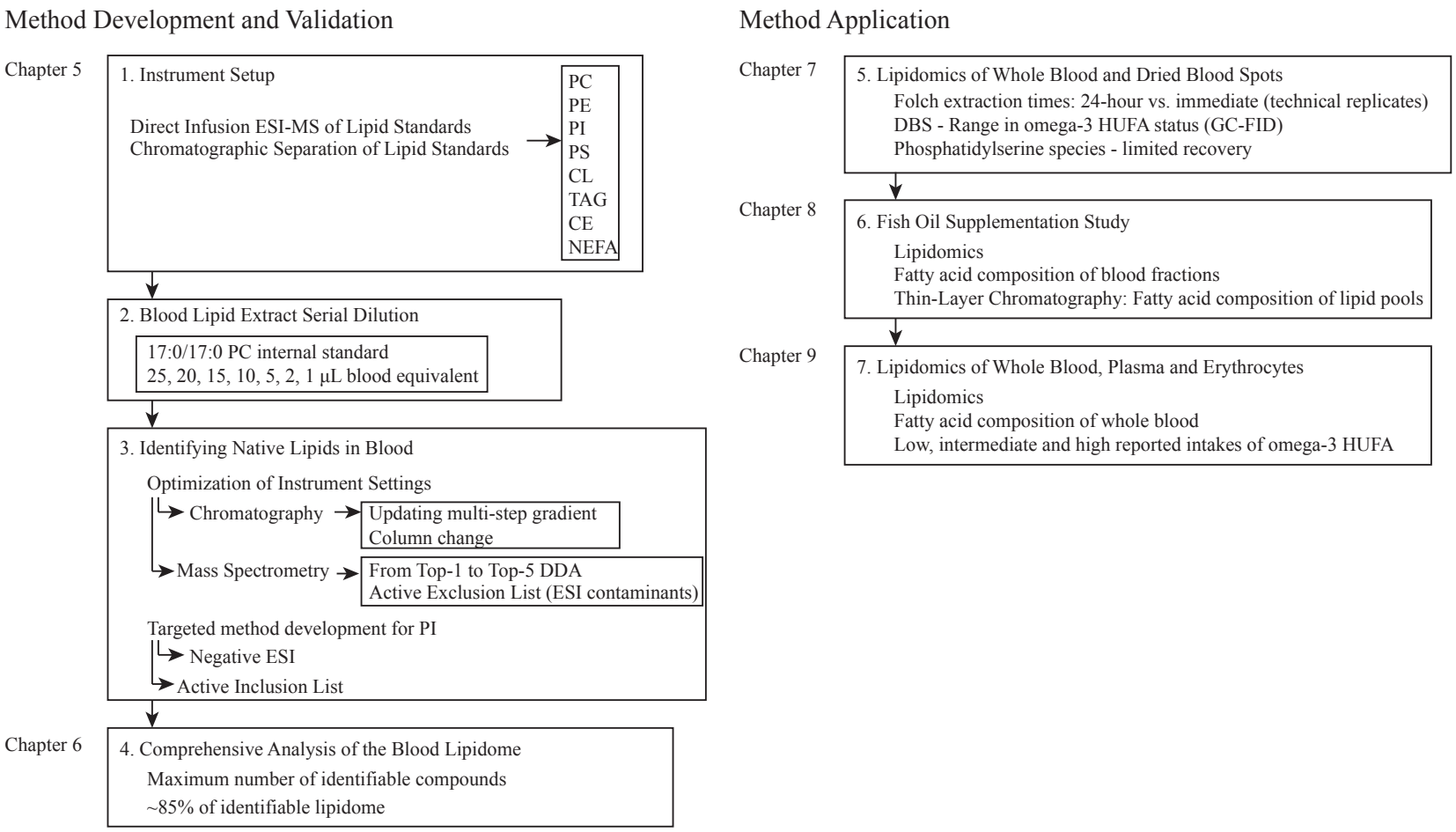

Figure 1. Flow chart highlighting the main experiments in this thesis. The steps for the development of the lipidomic profiling method are highlighted in Chapter 5, method validation in Chapter 6, application for profiling of dried blood spots in Chapter 7, whole blood lipidomics following omega-3 HUFA supplementation in Chapter 8, and blood fraction lipidomics in Chapter 9. Electrospray ionization mass-spectrometry (ESI-MS); phosphatidylcholine (PC); phosphatidylethanolamine (PE); phosphatidylinositol (PI); phosphatidylserine (PS); cardiolipin (CL); triacylglycerol (TAG); cholesteryl ester (CE); non-esterified fatty acid (NEFA); data-dependent acquisition (DDA); dried blood spot (DBS); highly unsaturated fatty acid (HUFA); gas chromatography-flame ionization detection (GC-FID).

Chapter 4

Methodological Foundations

4.1 *Blood Collection, Separation and Preparation Procedures*

Venous blood was collected and stored as described previously (Metherel et al., 2013). Briefly, blood was collected from the antecubital vein by a trained technician into sterile vacutainers to which 200 µL 0.2M ethylenediaminetetraacetic acid (EDTA, Sigma-Aldrich) were added. Aliquots of whole blood (500 µL) were collected in duplicate. One of the aliquots was separated into plasma and erythrocyte fractions by centrifugation at 1734 *rcf* (Patterson, 2013). In addition, 50 µL of blood were applied to pre-washed (1:1 chloroform:methanol) chromatography paper strips (Analtech Inc., Neward, DE) onto an area of ~ 1-2 cm^2 for dried blood spots. Strips were allowed to air-dry and were then placed in separate test tubes and sealed. All samples were then stored at -80°C until analysis.

4.2 *Lipid Extraction*

Total lipid extracts were obtained from whole blood, plasma and dried blood spots using a method according to Folch et al., 1957. In brief, 50 µL of thawed blood or plasma, or a single dried blood spot were mixed with a solution of chilled 2:1 chloroform:methanol (v/v), and left at 4°C for 24 hours. Samples were vortexed, and 500 µL of 0.2M sodium-phosphate buffer were added to induce layer separation. After inversion, samples were centrifuged for 5 minutes at 1734 *rcf*. The organic layer, which contains all of the lipids, was collected. An additional 2 mL of chloroform were added to the aqueous layer. Samples were re-vortexed, re-centrifuged, and the organic layer was collected and combined with the one obtained in the first extraction. The methanol/water layer was discarded. Samples were stored in chloroform at 4°C until further

analysis. Lipids were extracted from erythrocytes using the method of Reed et al., 1960. Briefly, 200 µL of thawed, weighed erythrocytes were added to chilled methanol and vortexed immediately. One mL of chilled chloroform was added, and the samples were stored overnight at -80ºC to prevent 'sticky pellet'. Samples were then vortexed, centrifuged at 1734 *rcf* for 5 minutes and the supernatant was collected in a separate test tube. 2 mL of chilled 1:1 chloroform:methanol (v/v) were added to the pellet, samples were vortexed and centrifuged again at 1734 *g*. The supernatant was combined with the one obtained from the first extraction, and 1.8 mL sodium phosphate buffer were added. Samples were inverted twice and centrifuged at 1734 *g* for five minutes. The chloroform layer, which contains all the lipids, was collected and the methanol/water layer was discarded. Samples were stored in chloroform at 4ºC until analysis.

4.3 *High- and Ultra-High Performance Liquid Chromatography*

HPLC and UHPLC settings were used on the front end of the mass spectrometer using a Dionex UPLC system. Two reversed-phase columns were used during method development. Initially, a C18 Ascentis Express, 15cm x 2.1 mm x 2.7 µm (Sigma-Aldrich, St. Louis, MO) was used for the initial development of the method and was replaced by a similar column with smaller particle size (C18 Ascentis Express, 15cm x 2.1 mm x 2.0 µm) (Sigma-Aldrich, St. Louis, MO) to improve chromatographic resolution. A binary solvent system was used (Bird et al., 2010; Hu et al., 2008; Peake et al., 2013) that consisted of mobile phase A: 60:40 acetonitrile:water (v/v), 10 mM ammonium formate, and 0.1% formic acid; and mobile phase B: 90:10 isopropanol:acetonitrile (v/v), 10 mM ammonium formate and 0.1% formic acid. Depending on the desired lipid amount, aliquots of samples were dried and re-suspended in 100

μL 65:35:5 acetonitrile:isopropanol:water (v/v/v) with 0.1% formic acid (hereafter referred to as HPLC sample solvent). The autosampler used 5 μL aliquots for sample analysis. A multi-step gradient was utilized (Hu et al., 2008), where from 0 – 1.5 minutes it was 32% B, from 1.5 – 4 min 45% B, from 4 – 5 min 52% B, from 5 – 8 min 58% B, from 8 – 11 min 66% B, from 11 – 14 min70% B, from 14 – 18 min 75% B, from 18 – 21 min 97% B, from 21 – 25 min 95% B was maintained, from 25 – 25.1 min B was decreased to 32%, and allowed to equilibrate until the 30 min mark. The flow was set to 260 μL/min, column temperature at 45°C, and tray temperature at 4°C.

4.4 *Positive Electrospray Ionization-Mass Spectrometry and Tandem Mass Spectrometry*

The mass spectrometer was a Thermo Q-Exactive Quadrupole-Orbitrap (hereafter referred to as Q-Orbitrap) (Thermo-Fisher Scientific, Waltham, MA). MS parameters were set as follows: Scan range: 200-2000 *m/z*; sheath gas flow rate: 35; spray voltage: +3.0 kV; capillary temperature: 300°C. Full scan MS experiments used di-isooctyl phthalate, *m/*z ratio 391.28429, as a lock mass for mass shift corrections. This is a common ESI contaminant, and was present in the sample solvent and in the mobile phase. Untargeted, data-dependent acquisition methods were used for tandem MS experiments (Top1 and Top5, later specified depending on the experiment) unless otherwise stated. An exclusion list of the *m/z* ratios of 25 common positive ESI contaminants was created and specified on the method. The Q-Orbitrap's quadrupole mass filter can use that information to remove the specified ions from the spectra, reducing the signal-to-noise ratio. The Thermo Xcalibur QualBrowser (Version 2.1; Thermo-Fisher Scientific, Waltham, MA) was used for extracting ion chromatograms using saved layouts, exporting tandem MS spectra, and integrating peak areas. Chromeleon Xpress (Version 7.2; Thermo-

Fisher Scientific, Waltham, MA) was used to monitor and control the Dionex UPLC settings. The tandem MS spectra for compounds of interest were exported from Xcalibur as .RAW files, converted to .MGF using ProteoWizard, and loaded into the NIST 2.0 program for identification with the LipidBlast (Kind, 2013) and LipidMAPS (Fahy et al., 2009) databases.

Due to the thousands of lipids that may be identified within a single biological sample (Han and Gross, 2003), all MS experiments were untargeted in nature unless otherwise stated. Specifically, tandem mass spectrometry was performed in a data-dependent manner, where either the top 1 or top 5 most intense ions in the full MS spectrum at any given point in time were re-directed for fragmentation. While increasing the number of top ions to fragment is an effective tool in the analysis of a complex sample, as the number of top N ions is increased in the MS method, the resulting full scan MS chromatograms decrease in peak resolution since the scanning frequency is inevitably reduced (Michalski et al., 2011).

4.5 *Thin Layer Chromatography to Separate Lipid Classes*

Thin layer chromatography was used to separate total lipid extracts into specific lipid classes prior to fatty acid composition analysis by GC-FID. Both neutral and polar lipid separation techniques were used. Total lipid extracts from plasma, erythrocytes and whole blood were dried and reconstituted into 50 µL of chloroform, loaded on to a thin layer chromatography plate (Silica Gel G, 20 x 20 cm, 250 um, Analtech Inc., Newark, DE) using a Hamilton syringe, and resolved in a mixture of 60:40:2 heptane:diethyl ether:glacial acetic acid (v/v/v) (Armstrong, 2008). FFA, TAG, and CE bands were scraped after spraying with 0.1% 2,7-dichlorofluorescin in methanol (w/v), visualizing under UV light, and comparing to external lipid standards. Lipids were extracted from the scrapings twice with 2:1 chloroform:methanol (Folch, 1957) containing

1 μg/mL C 22:3n-3 ethyl ester standard (Nu-Check Prep, Elysian, MN, USA) and 50 μg/mL butyl-hydroxytoluene (BHT).

Polar lipid thin layer chromatography plates (Silica Gel H, 20 x 20 cm, 250 um, Analtech Inc., Newardk, DE) were loaded with total lipid extracts reconstituted into 50 μL chloroform and applied to each plate using a Hamilton syringe. A mobile phase consisting of 30:9:25:6:18 chloroform:methanol:isopropanol:0.25% potassium chloride in water (w/v):triethylamine was used. Phospholipids resolved in the following order: SM, PC, PS, PI, and PE from bottom to top. Bands were scraped after visualizing with 0.1% 2,7-dichlorofluorescin in methanol (w/v) and comparing to external standards, lipids were extracted, derivatized to make fatty acid methyl esters and ran on the GC-FID using the protocol described in Section 4.6.

4.6 *Gas Chromatography – Flame Ionization Detection*

The lipid extracts in chloroform were dried under a stream of nitrogen gas. One mL of 14% BF_3 in methanol and 300 μL of hexane were added, and samples were then placed on a heating block at 100°C for 1 hour to yield fatty acid methyl esters (Armstrong et al., 2008). Fatty acid methyl esters were collected, dried under a stream of nitrogen gas, and re-constituted into 50 μL hexane. Samples were analyzed on a Varian 3900 gas chromatograph equipped with a DB-FFAP 15 m x 0.1 mm i.d. x 0.1 μm film thickness, nitroterephthalic acid modified, polyethylene glycol, capillary column (J and W Scientific from Agilent Technologies, Mississauga, ON) and used hydrogen as the carrier gas. One-μL aliquots were introduced by a Varian CP-8400 autosampler into the injector, which was heated to 250ºC and used a 25:1 split ratio. The initial temperature was 150ºC with a 0.25-minute hold, followed by a 35ºC/min ramp to 200ºC. An 8ºC/min ramp followed until 245ºC were reached, where the temperature was held

for 15 minutes. The flame ionization detector temperature was set to 300ºC, air and nitrogen make-up gas flows were 300 mL/min and 45 mL/min, respectively, and the sampling frequency was 50 Hz. Peaks were identified by retention time using an external standard mix (GLC-462, Nu-Check Prep, Elysian, MN, USA).

4.7 *Statistical Analyses*

Concentrations of fatty acids in GC-FID experiments were determined using the C22:3n-3 internal standard (to yield μg fatty acid/100 μL blood or plasma). Erythrocyte fatty acid concentrations are expressed as μg fatty acid/200 mg erythrocytes. The percent weight of each fatty acid in total fatty acid pools is also expressed. In HPLC-MS and UHPLC-MS experiments, peak areas were normalized by dividing the area under the curve for each extracted ion chromatogram by the area under the curve for the di-17:0 PC internal standard and multiplying by 100. Units for lipidomic data are expressed as arbitrary units (A.U.) and the data are therefore considered semi-quantitative, a method to express MS data (Lazaro et al., 1999). Comparisons of whole blood and dried blood spot lipidomics, and the whole blood lipidomics at different intakes of omega-3 HUFA were assessed by one-way ANOVA and/or two-tailed Student's t-tests. Post hoc tests were performed using Tukey's Honestly Significant Difference test and statistical significance was inferred as $p < 0.05$ after a significant F-value as determined by the one-way ANOVA. SPSS for Windows statistical software (release 11.5.1; SPSS Inc., Chicago, IL, USA) was used. Data are presented as the mean ± standard deviation as indicated.

Chapter 5

Development of an Untargeted Lipidomic Method for the Analysis of Human Whole Blood

5.1 *Introduction*

Traditional fatty acid profiling techniques have provided insights with regards to lipid metabolism *in vivo* and *in vitro*, and have been used to support relationships between dietary fat intakes and disease risk (Mozaffarian et al., 2013, de Oliveira et al., 2014). These techniques are generally gas chromatography-based, which require fatty acyl chains to be isolated from their parent lipids and be chemically derivatized for analysis (Metherel et al., 2013). As a result, whether fatty acids come from glycerophospholipids, CE, TAG, or are part of other lipid pools, becomes unknown. Techniques such as thin-layer chromatography can isolate specific lipid classes prior to fatty acid determination, but the specific acyl species of the original lipids remains unidentifiable. More recently, the development of mass spectrometric and liquid chromatographic techniques have allowed for the identification of acyl specific species of complex lipids, but untargeted lipidomic analyses are typically limited to semi-quantitative if the appropriate precautions are taken. Absolute quantitation using MS is widely known to be problematic (Pitt, 2009) and is usually restricted to targeted measurements with appropriate internal standards. This chapter addresses the issues associated with the development of a semi-quantitative lipidomic profiling method, and provides the foundation for the application of this method for the analysis of biological tissues. For method validation, human whole blood was chosen over erythrocytes or plasma due to the fact that it is a more comprehensive sample. It contains TAG and CE, which are predominant in plasma; and PE and PS, which are abundant in the erythrocyte bilayer.

5.2 *Method Development*

5.2.1 *Mass Spectrometry - Setting Instrument Conditions for Lipid Standards*

In ESI-MS, compounds can ionize to form various molecular adducts with compounds such as ammonium, lithium, sodium, and potassium (Koivusalo et al., 2001). The formation of these ions is largely dependent on two factors: the nature of the solvent in which the compounds are dissolved and the concentration of the solute. As a result, a series of initial experiments were carried out in the Q-Orbitrap instrument to examine the molecular behavior of commercially-available lipid standards with the ESI process. Specifically, the standards tested were: 16:0 FFA, di-17:0 PC, di-17:0 PE, di-16:0 PI, di-16:0 PS, 17:0 CE, tri-17:0 TAG, tetra-18:2 CL, and free cholesterol at equivalent concentrations of 50 μg/100 μL in 1:1 methanol:water + 0.1% formic acid + 10mM ammonium formate. These solutions were introduced into the mass spectrometer with a 10 μL Hamilton syringe (Hamilton Company, NV, USA) connected directly to the ESI source via fused-silica tubing, at a flow rate of 0.5 μL/min. Since glycerolipids and cholesteryl esters are known to form stable cations (Weir et al., 2013; Murphy et al., 2011), the instrument was operated in positive ESI-mode with a spray voltage of +3.0 kV. The spectra generated were visualized on real-time, mass-shift corrected using a lock mass, and saved over 1-minute acquisition periods. By comparing blank runs against lipid standard runs, the most abundant molecular ions for the compounds tested were determined. Based on the results from the Q-Orbitrap, it was concluded that the most abundant molecular ion configuration using our solvent system for PC, PE, PI and PS is $[M+H]^+$, while that for TAG, CE, and CL is $[M+NH_4]^+$ and free cholesterol $[M+H-H_2O]^+$. The FFA standard was the only one that could not be detected in positive ESI mode. This can be attributed to the chemical properties of this compound; the deprotonated form of a carboxylic acid ($R\text{-}COO^-$) is more abundant than the protonated form (R-

COOH) when in solution due to resonance stabilization of the negative charge by the oxygen atoms around the alpha-carbon. However, by switching the spray voltage to -3.0kV to ionize the sample, an ion was observed at *m/z* 255.2324 (Figure 2, Spectrum A). It was concluded that this represented the deprotonated form of 16:0 FFA, since its predicted *m/z* ratio is 255.2330 (delta 0.583 ppm, lock mass correction with di-isooctyl phthalate was not applied). As a result, samples need to be analyzed under negative ESI conditions in order to detect FFA. Subsequent experiments were performed in positive ESI mode at the expense of not reporting FFA, which only make up approximately 6% of human blood acyl-containing lipids under normal conditions (Supporting data in Figure A.1, Appendix A).

5.2.2 High Performance Liquid Chromatography – Resolving Lipid Standards

After having examined the molecular behavior of lipid standards with positive ESI in section 5.2.1, the next step was to use HPLC to separate the lipids prior to ionization. This was necessary as whole blood is a complex matrix that contains a wide array of lipids of which many are isobaric compounds (i.e. share the same molecular formula and *m/z* ratio, but are different lipids; for example 16:0/20:4 PC and 18:2/18:2 PC are both 36:4 PC, $C_{44}H_{81}NO_8P$ if $[M+H]^+$, *m/z* ratio 782.5694). Chromatographic separation prior to ESI enables resolution of such compounds, enabling their characterization. Previous reports (Bird et al., 2011; Hu et al., 2008; Peake et al., 2013) have used comparable HPLC techniques in order to achieve separation of lipids across all lipid classes. These studies used a binary solvent system, multi-step HPLC gradient protocol, and a reversed-phased C18 column (method described in detail in Section 4.4). Moreover, in these studies lipids were also ionized and successfully detected in positive ESI mode. The nine compounds that were tested in Section 5.2.1 were prepared again at a

concentration of 50 µg/100 µL in 65:35:5 acetonitrile:isopropanol:water (v/v/v) + 0.1% formic acid. The mild acidity (pH ~ 4.7) of this solvent supports the protonation of lipids. The samples were run with the 30-minute chromatographic protocol by Bird et al (Figure 4 A). The mass spectrometer was operated in positive ESI mode (except for 16:0 FFA, this sample was run in negative ESI), used a lock mass, and Top1 data-dependent acquisition for tandem MS. Figure 3 shows the combined extracted ion chromatograms for the precursor ion *m/z* ratios with a ±0.01 Da scan window of each of the nine lipids tested. The individual extracted ion chromatograms were overlaid into a single chromatogram, hence each lipid was 100% abundant in their individual runs. The overlay indicated all nine compounds were chromatographically unique with none of the peaks being wide or tailing, which indicates adequate selectivity by the stationary phase. Tandem MS spectra were used to confirm the identities of the lipid standards. Moving forward, the behaviour of blood lipids was examined with the current chromatographic and mass spectrometric method over a range of native lipid concentrations.

5.2.3 *Untargeted HPLC-MS/MS and Serial Dilutions of Human Whole Blood*

After the successful detection of lipid standards and an indication that chromatographic separation was likely, the behavior of native lipids in human whole blood was examined. A previous report (Koivusalo et al., 2001) has suggested that, for quantitative purposes, diluting lipids to an appropriate range is necessary in order to maintain a linear relationship between increasing sample concentration and the observed spectrum absolute intensity. Specifically, the literature suggests that concentrations of up to 5 pmol/µL of phospholipid standards show a linear response. At higher concentrations, however, a logarithmic relationship begins to be observed, losing the linear response needed for quantitation using internal standards. A possible

explanation for the linear then logarithmic relationship with increasing lipid concentration involves lipid aggregation and micelle formation when using polar solvents. The more concentrated lipid droplets may result in short chain acyl containing-molecules that are concentrated at the surface of the droplet, preventing ionization of long chain acyl-containing lipids that gather inside (Han et al., 2006). Therefore, a series of dilutions from blood lipid extracts were assessed in order to determine an appropriate working concentration to minimize sequestering of lipids with the droplet. Lipids were extracted from the blood of one participant in 100 µL aliquots, and diluted in chloroform to represent 25.0 µL, 20.0 µL, 15.0 µL, 10.0 µL, 5.0 µL, 2.0 µL and 1.0 µL of blood. Samples were dried, re-suspended in 100 µL 65:35:5 acetonitrile:isopropanol:water (v/v/v) + 0.1% formic acid, and spiked with a 5.0 nmol/µL solution of di-17:0 PC. Samples were run for Top5 data-dependent tandem MS acquisition. The chromatogram obtained from the 10 µL dilution with the estimated elution times for the main lipid classes in blood and the full-scan MS summed ion spectrum from the chromatogram indicated the most abundant lipids in blood (Figure 5A and 5B). The importance of chromatography when analyzing the lipidome of a complex biological sample are shown in this figure – isobaric species cannot be resolved due to the complexity of tandem MS spectra and algorithms would need to be developed in order to interpret this type of data. The three most abundant ions, *m/z* 758.5698, 874.7851 and 666.6183 (identified as 16:0/18:2 PC $[M+H]^+$, 16:0/18:1/18:2 TAG $[M+NH_4]^+$, and 18:2 CE $[M+NH_4]^+$, respectively using tandem MS spectra), were used to compare the 7 dilutions from whole blood total lipids. The areas for the chromatographic peaks of those three compounds were calculated across all of the dilutions, normalized to the area of the 17:0/17:0 PC standard, and plotted as shown in Figure 6. Interestingly, the dilution curves show a positive linear relationship between lipid concentration

and instrument response up to 5 nmol/μL (internal standard concentration; $0.983 \leq R^2 \leq 0.992$). These results contradict the logarithmic relationship of lipid standards at concentrations higher than 5 pmol/uL observed by Koivusalo et al., 2001. This may be explained by the fact that this response was observed using triple-quadrupole and ion trap mass spectrometers, which may have limited dynamic ranges as compared with the Q-Orbitrap that was used presently.

From these experiments, the 10 μL dilution was chosen as the most appropriate working concentration for future experiments. Choosing a greater dilution factor may limit the detection and quantitation of lipids that are natively found in low abundance in blood while less diluted samples may result in co-elution of isobaric compounds and/or ion suppression. In order to determine if the current method could characterize native lipids across all lipid classes, the tandem MS spectra generated for all compounds in the 10 μL dilution were examined. Approximately 4500 tandem MS spectra were generated from the analysis of a single lipid extract. Upon examining approximately 250 of the spectra that had precursor ion masses in the range of what was expected for glycerolipids and cholesteryl esters (Tables A.1 through A.6, Appendix A), acyl-specific information was generated for PC, TAG and CE only. Extracting ion profiles for the accurate masses of some known PE, PI and PS species revealed chromatographic peaks, but confirmation of actual acyl species could not be made as tandem MS spectrum were not available. This was due to precursor ion intensities of these molecules being much lower than PC species, therefore the Top5 data-dependent setting did not select for PE, PI and PS ions. Without this selection, tandem MS analyses were not performed and the specific fatty acyls species could not be identified. An inherent characteristic of PC that likely contributed to these results is its high native abundance in whole blood compared with other phospholipids. While PC is a key structural component of chylomicron monolayers and erythrocyte bilayers, PE, PI

and PS are primarily found in erythrocytes in the inner part of the bilayer and in much smaller proportions (Leidl et al., 2008). Furthermore, PC is well known to have ion-suppressing properties in positive ESI-MS, as it is highly ionizable (i.e. it 'hogs' the charge) and prevents other compounds from being ionized (Kim et al., 2008). Therefore, additional measures were required in order to improve chromatographic separation and further resolve lipids.

5.2.4 *Development of the Chromatographic Method*

In order to address the issues identified with the preliminary method, which included ion suppression and lipid co-elution, the multi-step gradient was examined and modified. There was significant co-elution of peaks during minutes 12 to 17 (phospholipids) and between 22-24 (TAG and CE) (Figure 5A). Therefore, the transition from Solvent A (more polar) to Solvent B (more non-polar) was modified to be slower throughout these times and shifted the original 30-minute gradient (Figure 4A, Bird et al., 2011) to a 47-minute protocol (Figure 4B) with reduced solvent ramps for phospholipids and TAG/CE. New lipid extracts were prepared from whole blood samples using the 10 μL dilution that was determined in Section 5.2.3, and then run using the new chromatography gradient with the Top5 data-dependent setting. The results from this experiment revealed tandem MS spectra for 16002 ions. The fact that the number of tandem MS spectra generated here increased by over 3.5 fold compared with the ~4500 originally generated, tends to confirm that there was considerable ion suppression with the initial chromatographic settings. Of the 16002 tandem MS spectra, approximately 450 were examined based on pre-determined precursor accurate masses (Tables A.1 through A.7, Appendix A). Remarkably, the fatty acyls of several PE and lyso-PC were identified in addition to the previously observed PC, TAG and CE. Free cholesterol was also detected. However, characterizing species of PS and PI

was still not possible. Rather than making further alterations to the chromatographic gradient, switching to a UHPLC method was examined. A column with similar phase, length and internal diameter, but with smaller particle sizes was used (15 cm x 2.1 mm x **2.7 µm** vs. 15 cm x 2.1 mm x **2.0 µm**; Sigma Aldrich, C18 Ascentis Express). Pressures of up to 550 bar were reached under the same 260 µL/min flow and gradient system, achieving UHLPC conditions (Varma et al., 2011). This resulted in increased resolution through visibly narrower peaks (Figure A.2 C, Appendix A), and more than 18600 tandem MS spectra successfully identified. From these, approximately 600 were checked, and confirmed the acyl species of more PC, TAG, CE, PE, Plasmenyl PE, lyso-PC, and several new PS and SM. Unfortunately, PI species could still not be resolved even under these conditions.

5.2.5 *Method Optimization for the Targeted Characterization of Phosphatidylinositol Acyl Species*

In an attempt to characterize PI acyl species in a human blood sample, a modification was made to the tandem MS settings. Instead of selecting untargeted Top5 data-dependent ions for fragmentation, the quadrupole mass filter capabilities of the Q-Orbitrap were used by specifying the *m/z* ratios of 5 compounds in a targeted inclusion list. These selected-ion monitoring experiments only enable precursor ions with the desired *m/z* ratios to enter the higher-energy collisional dissociation (HCD) cell and be fragmented. PI species that have been previously identified in human erythrocytes (Leidl et al., 2008) were targeted ($[M+H]^+$ for all). These included: 16:0/20:4 PI, *m/z* 859.5331; 18:0/18:2 PI, *m/z* 863.5644; 18:0/18:1 PI, *m/z* 865.5801; 18:0/20:4 PI, *m/z* 887.5644; and 18:0/20:3 PI, *m/z* 889.5801. Three technical replicates of one blood sample were prepared and diluted and ran with the UHPLC method in positive ESI with

the *m/z* inclusion list above. The results from this experiment were ineffective even with the implementation of the *m/z* inclusion list as no tandem MS spectra were generated. This suggests that PI ion suppression by highly-abundant co-eluting compounds such as PC occurred. In addition to this, the detection of PI in positive ESI mode can be problematic due to its chemical structure, and a poor ability to hold a positive charge (Enriquez-Algeciras et al., 2013). Although the pure 16:0/16:0 PI standard tested in Sections 5.2.1 and 5.2.2 showed that it could be detected in positive ESI, previous reports have had success in detecting it using negative ESI (Koivusalo et al. 2001; Uhl et al., 2013). To run these samples in negative ESI experiments, the spray voltage was set to -3.0kV and as flows and temperatures were kept the same as in positive ESI. A new negative $[M-H]^-$ parent ion inclusion list was generated for the same 5 PI that were targeted before: 16:0/20:4 PI, *m/z* 857.5175; 18:0/18:2 PI, *m/z* 861.5488; 18:0/18:1 PI, *m/z* 863.5645; 18:0/20:4 PI, *m/z* 885.5488; and 18:0/20:3 PI, *m/z* 887.5645. A formic acid doublet with the formula $C_2H_3O_4$ for the $[2M-H]^-$ molecular ion gave a strong signal at *m/*z 91.0031 and was chosen as the lock mass since the positive ESI lock mass (di-isooctyl phthalate, *m/z* 391.28429) was not seen in full scan negative ESI MS. Upon running the technical replicates, only one out the 5 compounds gave tandem MS spectra that allowed identification (18:0/20:4 PI). Although tandem MS spectra for compounds with the parent masses specified in the inclusion list were generated, fragmentation was not successful in creating daughter ions that were sufficiently intense, and left the precursor ion virtually intact. For this reason, the normalized collision energy (NCE, the amount of energy applied in the HCD cell to fragment compounds) was increased from 17.5 to 40. The three samples were run again, tandem MS spectra were generated at 5 time points throughout the chromatogram, and all 5 PI were confirmed. The chromatograms obtained from the same sample when run with either positive

(Figure 7A) or negative ESI (Figure 7B), and the tandem MS spectra obtained for *m/z* 857.5186 (Figure 7C) that was used to identify it as 16:0/20:4 PI ($[M-H]^-$). Interestingly, it appears that phospholipids can be detected in both positive and negative ESI with the current methods, confirming previous reports on the zwitterionic nature of phospholipids (Koivusalo et al. 2001). Conversely, TAG and CE show poor ionization efficiencies in negative ESI based on the intensity of the peaks generated (Figure 7B). These observations have been reported elsewhere (Sandra et al., 2010).

5.2.6 *Summary of Method, Limitations and Future Directions*

In conclusion, the positive ESI-UHPLC-MS/MS method developed enabled the acyl-specific characterization of PC, PE, PS, TAG, CE, and SM in whole blood by taking a data-dependent untargeted approach. Together, these lipids constitute approximately 80% of human whole blood acyl-containing lipids (supporting data in Figure A.1, Appendix A). Although the analysis of FFA and PI species requires negative ESI and a targeted inclusion list, this chapter has proven that these lipid classes can also be reported. Further development of the mass spectrometric method may enable the analysis of all lipids from a single analytical run. Specifically, the Q-Orbitrap has the ability to alternate between positive and negative ESI within a single sample run. However, it takes the instrument significantly more time to perform scans since the action of switching from positive to negative ESI or vice versa is not instantaneous. The decreased scanning frequency decreases the sharpness of the resulting chromatographic peaks, limiting the reliability of quantitation. In addition, PI analyses are not well suited for untargeted or global analyses, as additional extraction steps are typically required to improve

recovery as they can have strong interactions with proteins and may require denaturation using acid treatment (Homeyman et al., 1983).

One of the primary limitations of the current method is the inability to distinguish between omega-3, -6, -7, and -9 fatty acids. Furthermore, *cis*- and *trans*- isomers cannot be discriminated, and the location of fatty acyls within the glycerol backbones of phospholipids and TAG cannot be reported at this point. Further work is necessary in order to address these issues. Specifically, new methods have been developed for locating double bonds within fatty acids (Háková et al., 2015), their stereochemistry (Kuksis et al., 2005), and *sn*-1, *sn*-2, or *sn*-3 arrangement in glycerolipids (Byrdwell, 2015). Adaptations may be made to the current method in order to accommodate such modifications.

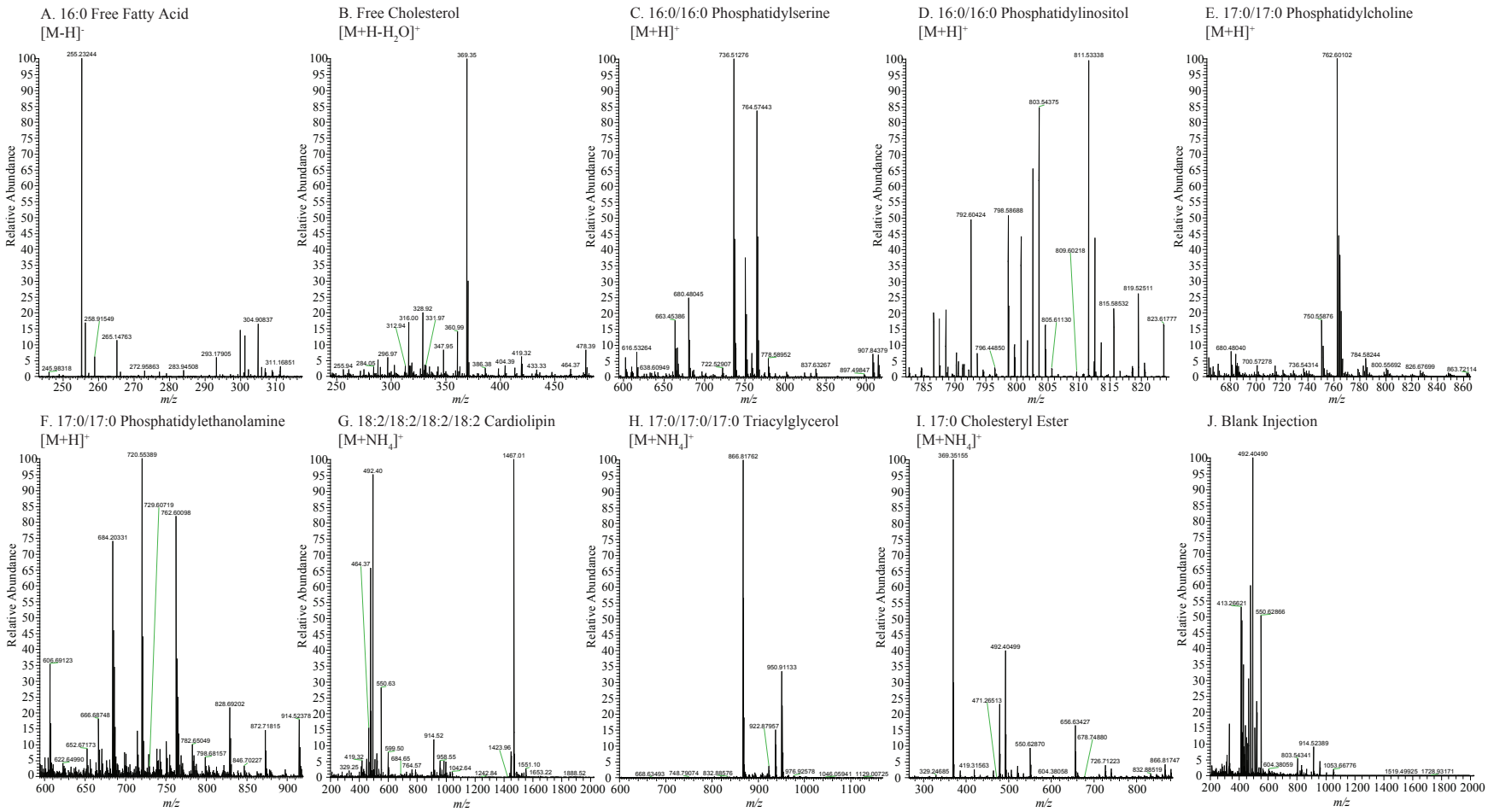

Figure 2. Full-scan MS spectra for A. 16:0 free fatty acid; B. Free Cholesterol; C. di-16:0 phosphatidylserine; D. di-16:0 phosphatidylinositol; E. di-17:0 phosphatidylcholine; F. di-17:0 phosphatidylethanolamine; G. tetra-18:2 cardiolipin; H. tri-17:0 triacylglycerol; I. 17:0 cholesteryl ester; J. Blank injection. Each spectrum highlights the molecular adducts observed for each lipid species. The most abundant ion in each spectrum is represented by the configuration underneath the name of the compound.

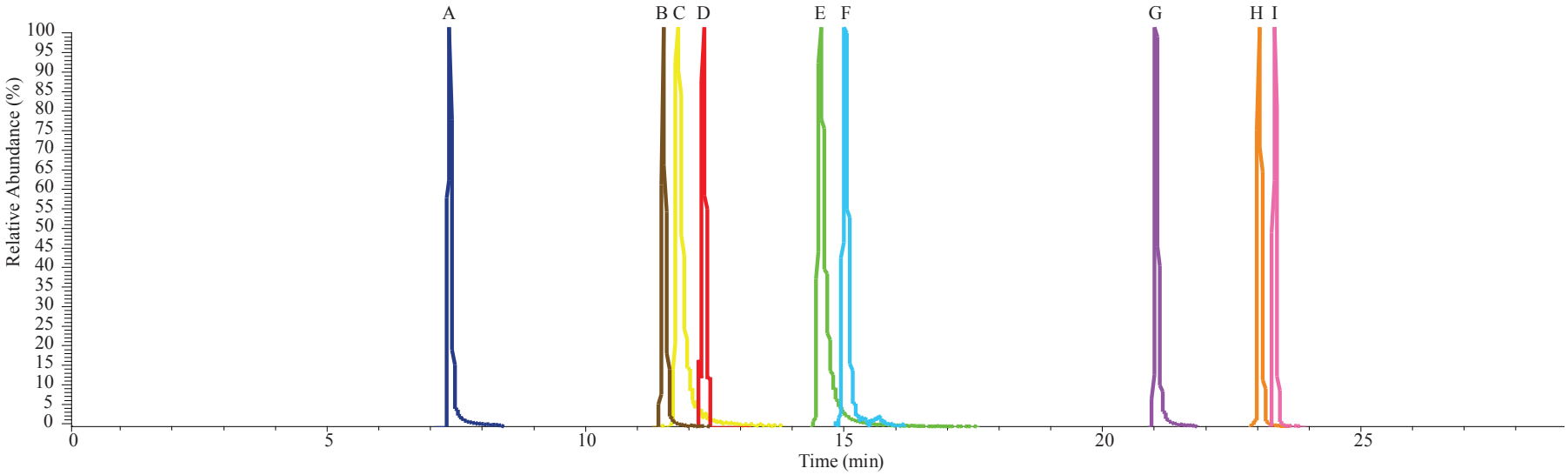

Figure 3. Extracted ion chromatograms for lipid standards. A. FFA; B. FC; C. PS; D. PI; E. PC; F. PE; G. CL; H. TAG; I. CE. Ion profiles were extracted by scanning for the most abundant molecular adducts for each lipid class as determined from Figure 2, within ± 0.01 Da. All of the lipid standards analyzed produced well-shaped chromatographic peaks, and are able to be extracted based on precursor ion accurate masses.

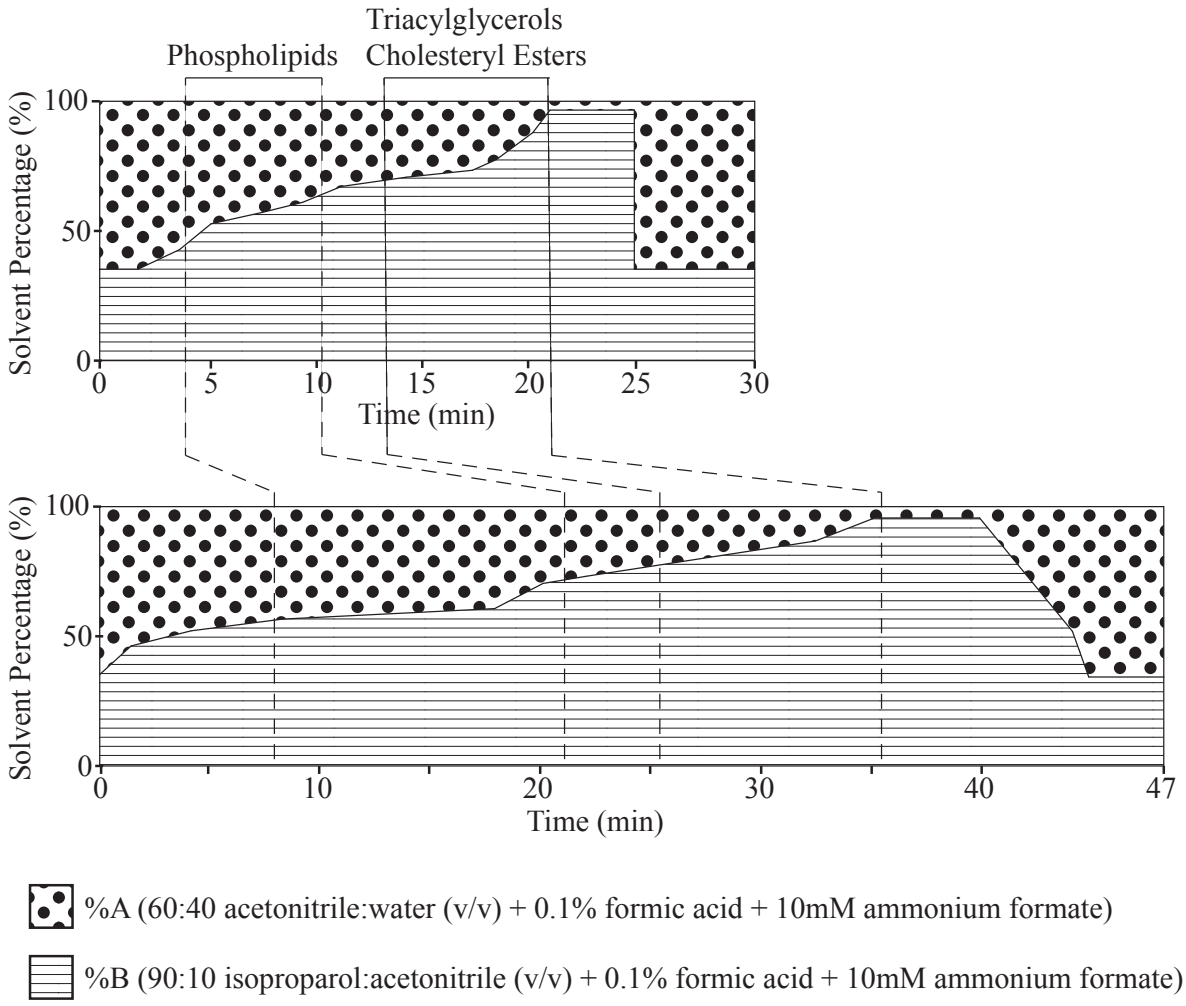

Figure 4. A. Chromatographic protocol by Bird et al., 2011. **B.** Updated chromatographic protocol optimized for lipidomic analysis of human whole blood. Elution time ranges for phospholipids and triacylglycerols/cholesteryl esters are specified, highlighting the slower shift towards Solvent B in the updated protocol in order to resolve co-eluting lipids. Solvent flow was set constant at 260 μL/min.

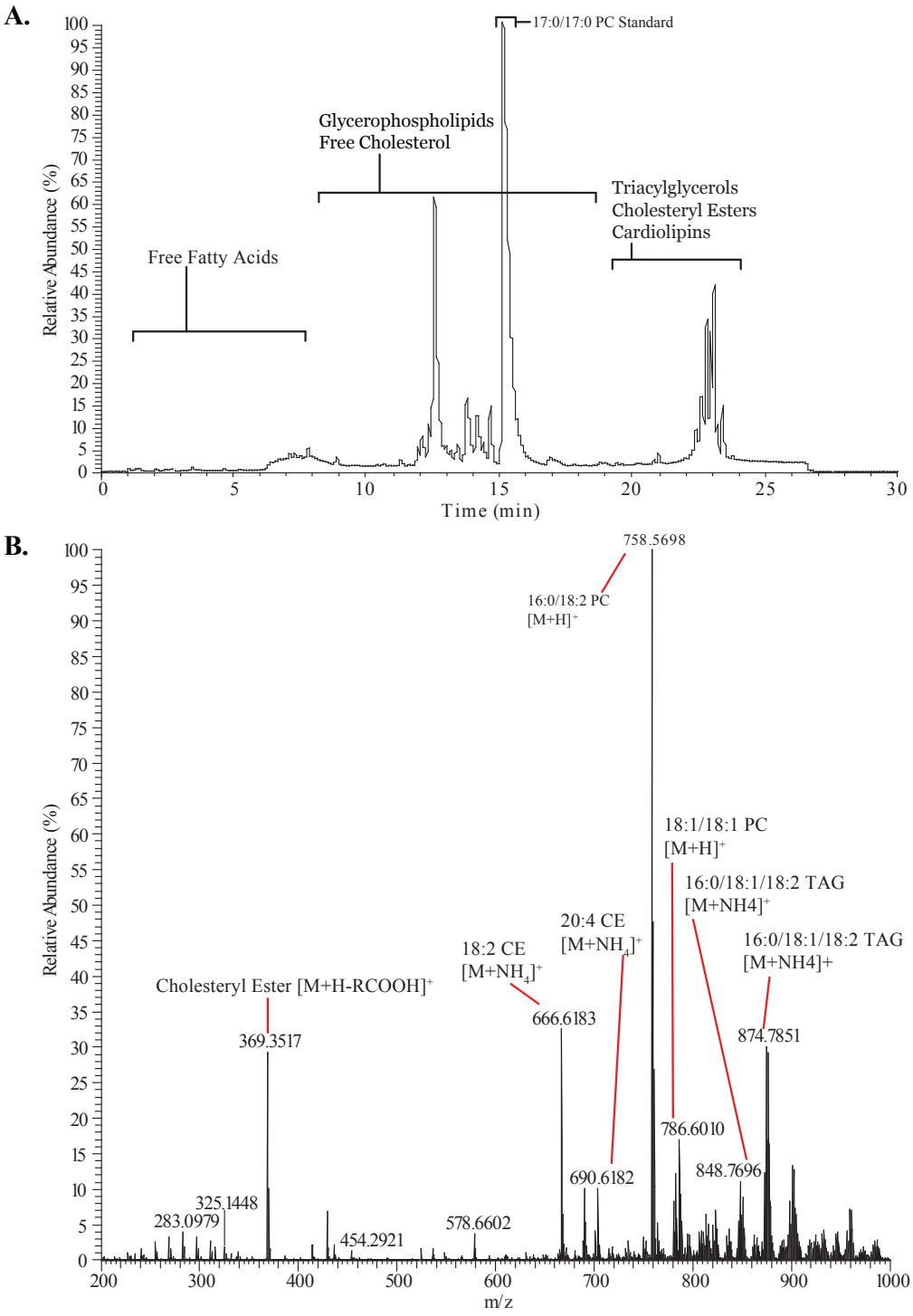

Figure 5. A. Full-scan MS chromatogram from 10 µL blood, using the multi-step protocol established by Bird et al., 2011. The elution times for several confirmed lipids in blood are highlighted, and their relative abundances compared to a spiked di-17:0 PC standard. **B.** Summed ion spectrum for the chromatogram in Figure 5 A, highlighting the most abundant lipids in human whole blood.

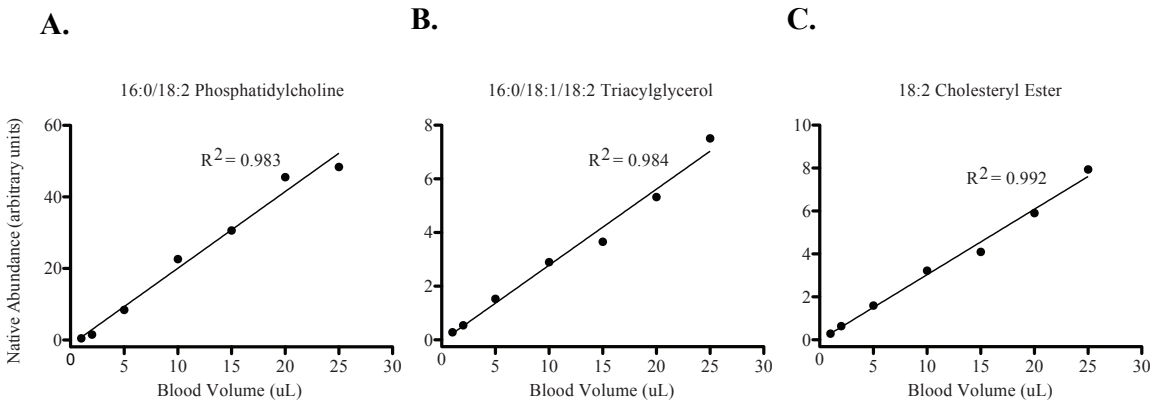

Figure 6. Examination of instrument response with increasing concentration of lipids **A.** 16:0/18:2 phosphatidylcholine (PC); **B.** 16:0/18:1/18:2 triacylglycerol (TAG); C. 18:2 cholesteryl ester (CE). Blood volumes were created by extracting from 100 µL using 2:1 chloroform:methanol (v/v), and diluting with chloroform.

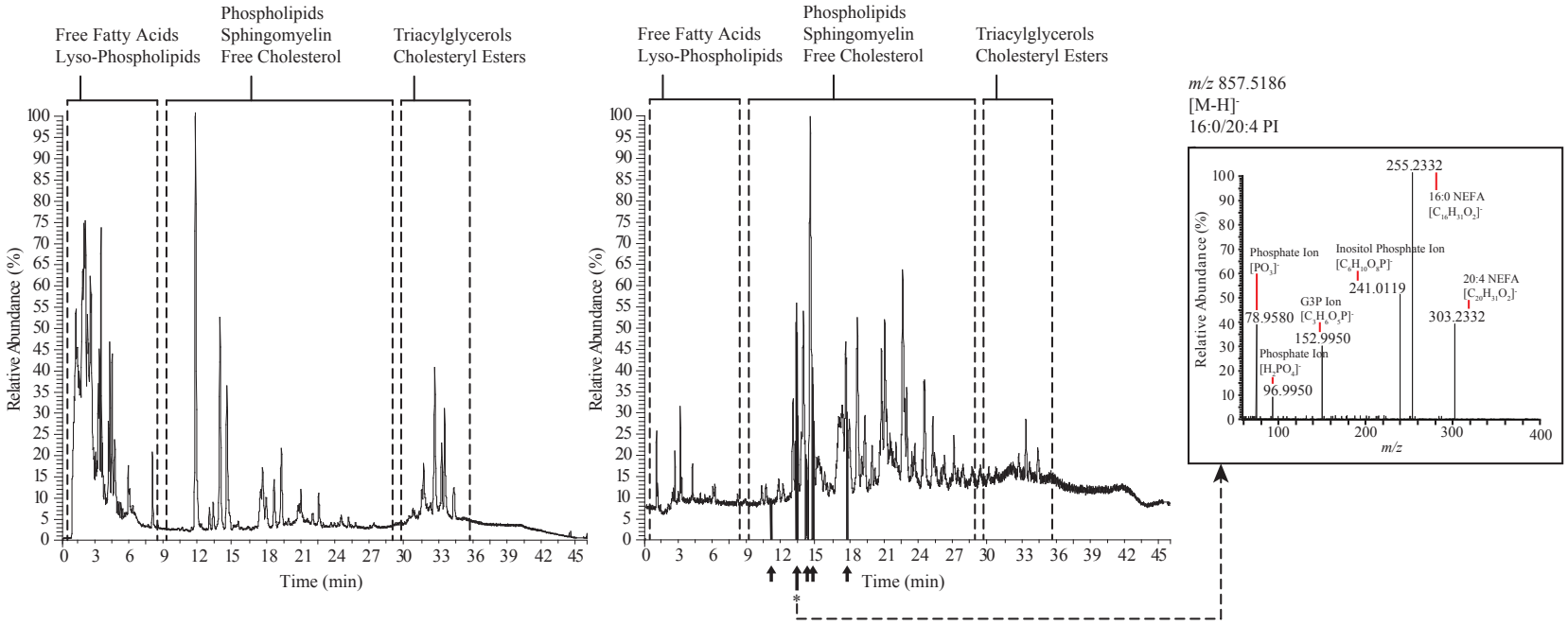

Figure 7. Full-scan MS chromatograms for 10 µL blood lipid extract in **A.** positive ESI and **B.** negative ESI. The time intervals for elution of blood lipids are indicated, and highlights how different lipids have different ionization efficiencies e.g., TAG and CE are more efficiently ionized in positive ESI compared to negative ESI. The arrows indicate the five instances where tandem MS was performed based on the specified inclusion list. **C.** Tandem MS spectrum for *m/z* 857.5186, this ion's accurate mass was included in the MS method's inclusion list to ensure its fragmentation. The resulting fragments were used to confirm the identity of this molecule as 16:0/20:4 phosphatidylinositol (PI).

Chapter 6

Validation of an Untargeted Lipidomic Method for the Analysis of Human Whole Blood

6.1 *Introduction*

The development and refinement of an untargeted method capable of identifying over 18000 spectra in the whole blood lipidome was based largely on chromatographic and MS settings. In order validate the method, the tandem MS spectra generated needed to be qualitatively characterized. This characterization is dependent on searches of mass spectra databases such as those developed and maintained by NIST. However, lipidomic data in the NIST databases is limited therefore alternative databases must be accessed such as LipidBlast database (Kind et al., 2013) and LipidMAPS Mass Spectrometry tools (Fahy et al., 2008).

6.2 *Comprehensive Lipidomics of Human Whole Blood*

A comprehensive characterization of all detectable acyl-containing lipids in a single blood sample was performed on a single 10 μL blood lipid extract equivalent run under Top5 data-dependent conditions, positive ESI, and with the UHPLC gradient developed in Section 5.2. From this sample, approximately 400 tandem MS spectra were examined in detail from 18635 tandem MS spectra generated. Each spectrum was individually extracted, exported, and analyzed using the NIST2.0 program with the LipidBlast database (Kind et al., 2013) and LipidMAPS Mass Spectrometry tools (Fahy et al., 1008). From this experiment, 219 lipids were identified in terms of their lipid group (i.e. total carbon atoms and C-C double bonds in acyl chains; e.g. PC 34:2 and TAG 52:3) based on accurate masses and chromatographic retention times by single MS. Out of these 219 lipids, acyl specific data was generated for 163 lipids

across cholesteryl esters, PC, PE, PS, and TAG using tandem MS. A list of 548 compounds was generated (full list in Tables B.1 through B.6, Appendix B) and includes the observed *m/z* ratio, identity, and area under the curve for each lipid. Notably, only combinations of even-chained fatty acids were analyzed in this process. While odd-chained fatty acids such as heptadecanoic acid (C17:0) and tricosanoic acid (C23:0) are present in blood, and more specifically in erythrocyte bilayers, they constitute less than 0.5% of total erythrocyte fatty acids by percent weight (Patterson et al., 2014). The exclusion of odd-chained fatty acids from the analysis of tandem MS spectra made searches significantly less burdensome.

The application of a lipidomic method for the analysis of biological samples generates complex and extensive amounts of data. Though the current UHPLC-MS/MS method has demonstrated the capacity to provide data for hundreds of compounds, it can provide more accurate results if it is tailored to target specific lipids. Traditional techniques such as thin-layer chromatography coupled with GC-FID or GC-MS may be better alternatives if the interest is in examining quantitative changes in total lipid pools. Glycerophospholipids are discussed in Section 6.2.1, TAG in Section 6.2.2 and CE in Section 6.2.3.

6.2.1 *Glycerophospholipids*

Lipid group identification was possible for 49 PC, 33 PE, and 20 PS. In order to detect these lipids, a list of all of the possible combinations of fatty acyls between di-12:0 to di-24:1 of lipid group molecular ion accurate masses was generated for PC, PE and PS (Table A.6, Appendix 6). There were 91 lipid group accurate mass combinations for each of the three phospholipids (total of 273) that were extracted and integrated. Many of these ion extractions, however, resulted in flat chromatograms below the limits of detection (LOD), shown as "<LOD"

for area under the curve (AUC) in Appendix B. This indicates that phospholipids with fatty acyl configurations resulting in those lipid groups (i.e. di-24:1 PC → 48:2 PC) are either below the limit of detection of the current method, or are truly not present in the sample. Furthermore, tandem MS spectral analyses confirmed 23 acyl species of PC, 3 lyso-PC, 17 PE and plasmenyl-PE, and 5 PS. The extracted ion profiles for the precursor ions of all of these lipids were integrated, and are shown in Appendix B organized by phospholipid class and ascending molecular weight. By comparing the AUC of acyl-specific and non-acyl specific data, it can be concluded that this method can provide acyl-specific information for approximately 81% of PC, 62% of PE and 70% of PS actually present in whole blood.

6.2.2 *Triacylglycerols*

As in Section 6.2.1, the sum of the peak areas for total confirmed TAG was calculated. In terms of total identifiable TAG by lipid group, the current method enabled the detection of 94 TAG species out of 105 compounds that were searched for ($[M+NH_4]^+$ accurate masses, Table A.7, Appendix A). Additionally, analysis of tandem MS spectra generated for this sample enabled the confirmation of 35 TAG acyl species, which constitute approximately 48% of total blood TAG. This low proportion of TAG acyl species reported can be attributed to the structural complexity of TAG, and all of the fatty acyl combinations that may exist in a biological sample (*sn*-1, *sn*-2, *sn*-3 location; acyl chain length, unsaturation). The accurate mass and molecular formula for a single TAG lipid group may be composed of at least 30 isobaric species (Figure 8). Since the ions that are generated from TAG fragmentation are direct indications of the molecular weights of the fatty acyls that constitute it, tandem MS spectra that were generated for co-eluting TAG revealed fragments for multiple species (Figure 9). Although it was not possible to provide

the specific acyl composition for many TAG lipid groups, the fragments that were observed were analyzed and are shown in Table B.6, Appendix B. This limits the number of fatty acyl combinations that make up that lipid group to 5 or less. By doing this, the proportion of acyl-specific data generated in terms of the total TAG pool increased from 48% to 90%.

6.2.3 *Cholesteryl Esters*

In contrast to glycerophospholipids and TAG, CE species analysis is relatively straightforward due to the fact that there is only one fatty acyl chain per CE molecule. Here, the accurate masses of 20 cholesteryl esters were calculated and used to extract ion chromatograms. Interpreting CE spectra to confirm the identity of CE species relied primarily on full-scan MS and not tandem MS spectra. Precisely, the spray voltage that was used to ionize the lipids as they eluted from the UHPLC column appears to have fragmented a large proportion of the ester bonds that held fatty acyls to their parent CE. As a result, a large *m/z* 369.3516 ion, representing a cholesterol cation ($[M+H-RCOOH]^+$) with molecular formula $C_{27}H_{45}$, was observed when each of the 20 CE ion profiles was extracted. Fragmentation was accompanied by the neutral loss of fatty acyls. For highly abundant CE species such as 18:2 CE, the precursor ion was fragmented both at the spray source and at the HCD cell, producing the cholesterol cation in both MS and tandem MS. For less abundant CE species like 20:5 CE, fragmentation occurred only at the ion source, and the cholesterol fragment was only observed in MS since no tandem MS was generated. As a result, the presence of *m/*z 369.3516 in full-scan MS was used as a diagnostic fragment when extracting ion profiles for all CE in order to confirm their identity. Following identification, all 20 CE species were integrated and the absolute proportions of each are given in Table B.1, Appendix B.

6.3 *Discussion and Conclusion*

Overall, the current UHPLC-MS/MS method is capable of detecting acyl species of PC, PE, PS, TAG and CE by taking a data-dependent untargeted approach. Further development of the mass spectrometric method may enable the characterization of more than the 163 acyl-specific lipids identified presently. Specifically, some mass spectrometers have the ability to do fast polarity switching, which allows positive and negative ESI within the same analytical run (Yuan et al., 2012). Fast polarity switching would allow PI and FFA species to be reported in our untargeted lipidomic method. Although the current UHPLC-MS/MS method is unable to determine the localization and stereochemistry of acyl-double bonds in native lipids or identify the *sn*-1, *sn*-2, *sn*-3 fatty acyl positions, difficulty resolving isobaric TAG species should be addressed first. several isobaric TAG species co-elute and limits the number of specific compounds that can be identified. While the current method used a single reversed-phase C18 column, two-dimensional UHPLC (Byrdwell, 2011; Stoll et al., 2007) and/or nano-flow liquid chromatography (Gama et al., 2013) would likely improve chromatographic separation and decrease co-elution. Also, ionization of TAG via atmospheric pressure chemical ionization often yields better results than ESI (Byrdwell, 2011; Byrdwell et al., 2001). Finally, the implementation of inclusion lists for the analysis of targeted lipids may improve peak resolution compared to the current Top5 data-dependent acquisition conditions.

Despite the lipid identification challenges, the greatest challenge with the current lipidomic profiling method is data extraction and processing. Although the LipidBlast database (Kind et al., 2013) and LipidMAPS consortium (Fahy et al., 2005, 2008) were used exhaustively for the identification of lipid acyl species, they are designed for targeted lipid profiling and do not have automatic experimental data processing tools. As a result, each tandem MS spectrum

that was analyzed had to be individually extracted, converted to the appropriate file format, and imported into the NIST 2.0 software. After the identification of each acyl species, peak areas had to be individually integrated, and the raw area under the curve values were manually typed in a blank spreadsheet. Data-handling software solutions are beginning to emerge. LipidSearch (Version 4.0; Thermo-Fisher Scientific, Waltham, MA, USA) offers lipid identification tools with an extensive library of more than 1.5 million lipid ions and predicted fragment ions, as well as peak alignment and integration options. However, these software applications appear to rely on relatively crude search parameters and their ability to identify acyl species of specific lipids is limited. For example, a preliminary use of a trial version of LipidSearch revealed that PC acyl species could not be discriminated because the relative abundances of fragment ions with acyl specific information were below the threshold specified in the search parameters. The software was only able to detect the precursor $[M+H]^+$ ion and the phosphocholine ion (*m/z* 184.0735; $C_5H_{15}O_4NP$) and could only generate lipid group-specific data (i.e. total number of carbon atoms and C-C double bonds; e.g. PC 34:2). The fragment ions that would be used to determine the acyl composition of PC species were less than 0.05% of the most abundant ion (the phosphocholine head fragment). This phenomenon has been reported elsewhere (Lee et al., 2011). In the future, increasing the normalized collision energy (energy used to cause fragmentation), or operating the instrument in negative ESI mode may result in more abundant fragment ions, and potential enabling the detection of acyl species specific lipids by LipidSearch (Peake et al., 2015). In spite of the limitations of the current method, the proportion of acyl species that were characterized is relatively comprehensive of the lipidome. The examination of native lipids in dried blood spots, and then in whole blood following fish oil supplementation promises to be highly informative and novel to the field.

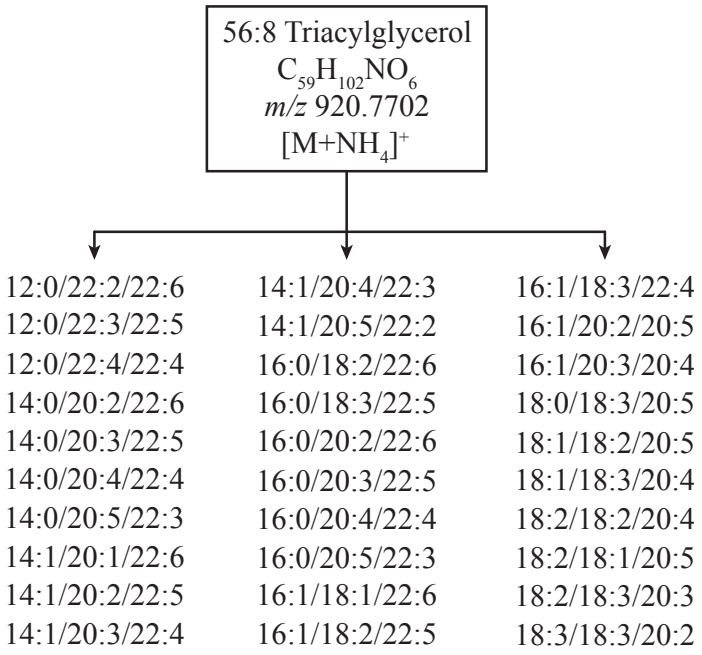

Figure 8. Thirty of the acyl species of specific configurations of 56:8 triacylglycerol (TAG) lipid group (56 acyl-chain carbons, 8 C-C double bonds) with the same molecular weight. The isobaric compounds shown here do not take into account configurations with odd-chain fatty acyls, *sn*-1, *sn*-2 or *sn*-3 localization, C-C double bond locations, or *cis*- and *trans*- conformation.

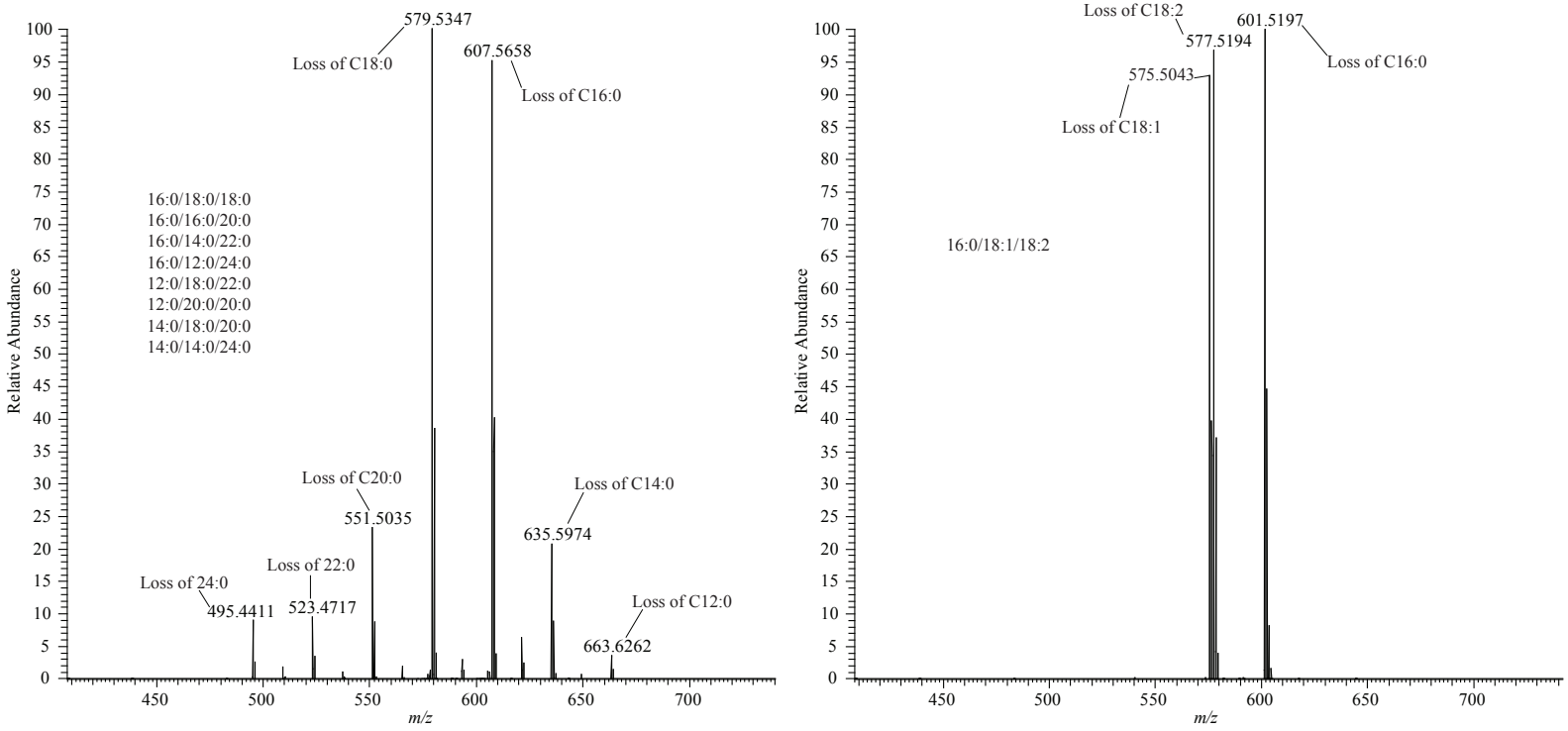

Figure 9. A. Tandem MS spectrum for the extracted ion profile of 52:0 triacylglycerol (TAG), *m/z* 880.8328. This spectra reveals diacylglycerol (DAG) fragments corresponding to the losses of several fatty acids. Eight combinations that give rise to isobaric TAG are shown **B.** Tandem MS spectrum for the extracted ion profile of 52:3 TAG, *m/z* 874.7858. In contrast to spectrum A., only three fragments are shown, meaning that there is one predominant species of TAG for 52:3 TAG which has fatty acids 16:0/18:1/18:2.

Chapter 7

Semi-Quantitative Lipidomic Profiling of Human Whole Blood and Dried Blood Spots

7.1 *Introduction*

Over the past years, there has been an increase in the use of whole blood in lipid literature and in clinical settings (Baylin et al., 2005; Doull et al., 2001). While most of the research focuses on plasma, erythrocytes, and/or other circulating blood cells, the use of whole blood has several advantages (Risé et al., 2007). Firstly, whole blood is a more complex sample and, as such, may be more informative. Moreover, the isolation of erythrocytes and plasma requires blood to be collected via venipuncture, while applications such as the neonatal heel prick and fingertip prick dried-blood spotting are minimally invasive and require little training. These techniques are regularly used to test for congenital diseases such as phenylketonuria, cystic fibrosis and sickle cell disease (Green et al., 1998; Health Quality Ontario, 2003). Notably, whole blood has been used for the development of biomarkers that strongly correlate with the omega-3 fatty acid content of various mammalian tissues (Stark, 2008), which may be used to determine omega-3 fatty acid status using popular guidelines such as the Omega-3 Index (Harris et al., 2004). These biomarkers have been validated in dried blood spots previously (Metherel et al., 2009). Furthermore, the stability of fatty acids in dried blood spots has been examined in detail under optimal laboratory conditions (Metherel et al., 2013) and in fieldwork with limited resources (Nurhasan et al., 2015). Currently, there are two reports from the same research group on lipidomic profiling of dried blood spots (Koulman et al., 2014; Prentice et al., 2015). Although no significant differences were observed between the lipidomic profiles of whole blood and dried blood spots in the validation work, these papers have several limitations. Firstly, the

comparisons between dried blood spots and whole blood are qualitative. The values given represent the proportion that specific lipids constitute in the sum of lipid intensities measured (i.e. the relative percent of lipids in the measured lipid pool). Although this drawback does not limit the use of dried blood spots in applications where, for example, the ratio of one lipid to another is examined, it may conceal the possibility that the total sums for whole blood and dried blood spot ion intensities are different. Moreover, both reports only present data for limited numbers of PC, SM, CE and TAG. Though some PE data is presented in the electronic supplementary material, it is not discussed. There may be a specific effect of spotting and drying blood on paper, or in the extraction of other lipid classes that are also present in blood, such as PS and PI. These were not measured. Lastly, lipidomic data is only reported in terms of lipid class and lipid grouping (i.e. PC 34:2). While some assumptions are made with regards to what the fatty acyl constituents are, the researchers did not take advantage of the tandem MS spectra generated to examine possible effects that fatty acyl length and degree of unsaturation may have on dried blood spot lipidomic profiles.

In this chapter, the lipidomic profiles of dried blood spots and whole blood will be contrasted using the novel method that was developed. Specifically, the lipidomic profiling method is employed to examine the use of dried blood spot technical replicates qualitatively and semi-quantitatively. The extraction efficiency of lipids from dried blood spots is also examined. Finally, the use of dried blood spots for lipidomic profiling is validated using a small sample of adults (n=3) that reported frequent, sporadic, and no consumption of omega-3 highly unsaturated fatty acid-rich sources, such as fish or nutraceuticals.

7.2 *Lipidomics of Whole Blood and Dried Blood Spot Technical Replicates*

The blood of one, 23 year-old male participant was collected from the antecubital vein into an EDTA-lined vacutainer. Ten whole blood technical replicates were aliquoted (500 µL each) stored in at -80ºC until analysis. Additionally, ten dried blood spot technical replicates were prepared by pipetting 50 µL of fresh, unfrozen whole blood into pre-washed (1:1 chloroform:methanol, v/v) chromatography paper strips, onto an area of approximately 1 cm^2. The blood was allowed to air-dry for approximately one hour, and then stored in capped test tubes at -80ºC (Metherel et al., 2013). Prior to analysis, whole blood samples were allowed to thaw at room temperature for 30 minutes. Six 50 µL aliquots were transferred to 12 x 75 disposable culture tubes, then 3 mL of 2:1 chloroform:methanol (v/v) were added in order to extract lipids as described in Chapter 4. Similarly, six dried blood spots were taken out of storage, placed on 12 x 75 disposable culture tubes, and 3 mL of 2:1 chloroform:methanol (v/v) were added. To examine the effect of extraction time, three out of the six whole blood samples and three dried blood spots were left in solvents for 24 hours (hereafter referred to as WB_{24} and DBS_{24}, respectively). The remaining three whole blood samples and dried blood spots were vortexed vigorously for 1 minute, then 500 µL of 0.2 M Na_2PO_4 in ddH_2O were added in order to induce phase separation. Samples were inverted twice and centrifuged at 1734 *rcf* for 5 minutes. The bottom chloroform layer containing the lipids was extracted, and 2 mL of fresh chloroform were added to the aqueous portion of the 6 samples. All were vortexed and centrifuged again. The resulting organic phases were taken and combined with the first extracts. These total lipid extracts for these whole blood and dried blood spot samples are hereafter referred to as WB_i and DBS_i, indicating that the lipids were extracted immediately following the addition of chloroform/methanol. Total lipid extracts were dried fully under a stream of N_2 gas, and

reconstituted into 1 mL of chloroform. Based on the results from the blood dilution experiments performed in Chapter 5, a 100 µL aliquot was taken from the total lipid extracts, representing 10 µL of blood. The 100 µL samples were spiked with 500 pmol of a concentrated di-17:0 PC standard solution to allow semi-quantitative analyses and account for sample-to-sample variability. Samples were then added to HPLC vials, dried fully under N_2 gas, and re-suspended in 100 µL of the HPLC sample solvent. The samples were then stored at 4ºC until analysis. On the following day, lipids were extracted from WB_{24} and DBS_{24}, aliquoted, and spiked with di-17:0 PC as described above. All samples were run with the chromatographic protocol developed in Chapter 5, and using Top5 data-dependent acquisition with positive ESI. From the list of identifiable lipids reported in Appendix B, 11 acyl specific lipids were selected for the validation of dried blood spots (Table 1). This list includes several PC with a range of acyl-chain lengths and levels of unsaturation, as well as a lyso- PC, two PE, a PS, a TAG, and a CE. The dried blood spot samples that were extracted immediately following the addition of chloroform/methanol (DBS_i) resulted in significantly lower recoveries compared with WB_i, DBS_{24}, and WB_{24} ($p < 0.05$ for all; Table 1). The fact that there are no significant differences between the lipid recoveries of WB_i and WB_{24} may be explained by the larger contact area of WB with the extraction solvents compared to DBS. Since chloroform/methanol is added to whole blood while it is liquid, the resulting sample is a homogeneous mixture. On the other hand, dried blood spots have a much smaller surface area since the lipids are contained within a ~1 cm^2 piece of chromatography paper, and do not solubilize as easily in the extraction solvents. It appears, however, that leaving the DBS samples in chloroform/methanol for 24 hours reverses this effect as no significant differences were observed between recoveries from DBS_{24}, WB_i or WB_{24}. Since these results are based on technical replicates of one volunteer's blood, the next

step was to examine the lipidomic profiles of whole blood and dried blood spots from different individuals.

6.3 *Whole Blood and Dried Blood Spot Lipidomic Analysis of Humans with Low, Intermediate, and High Omega-3 Status*

In order to confirm the validity of the results from the technical replicate experiments, a small sample of participants was recruited (n =3; 2M, 1F; aged 18 - 25). These participants were asked about their regular diets; Participant 1 (P1) indicated consuming fish frequently (4-5 times per week), Participant 2 (P2) indicated taking a fish oil supplement containing 300 mg of EPA+DHA per capsule once per week and consumption of fish approximately once monthly, and Participant 3 (P3) reported no consumption of fish, fish oil, or omega-3 enriched foods. Venous blood was taken from the three participants from the antecubital vein into EDTA-lined vacutainers. Blood was aliquoted and prepared into dried blood spots as explained in Section 6.2. Lipids were extracted from WB and DBS samples for each of the three participants 24 hours after the addition of 2:1 chloroform:methanol (v/v). Lipid extracts were diluted appropriately, spiked with 17:0/17:0 PC as an internal standard, and reconstituted in the HPLC sample solvent. The samples were run with the UHPLC method developed in Chapter 5, using positive ESI and Top5 data-dependent acquisition for tandem MS. In order to contrast and express the lipidomic data in terms of whole blood omega-3 highly unsaturated fatty acid status, a single 50 µL aliquot from the original whole blood samples was used to determine the fatty acid composition for the three participants. This was done as described previously (Metherel et al., 2013). In short, fatty acids were derivatized to fatty acid methyl esters using 1 mL 14% BF_3 in methanol and analyzed via GC-FID. C 22:3n-3 was used as the internal standard (Nu-Check

Prep, Elysian, MN, USA). Fatty acid composition data is presented in Table 4 as concentration and Table C.1, Appendix C as weight percent in total fatty acids. The blood biomarker levels such as the % n-3 HUFA in total HUFA and the sum of the % of EPA+DHA reflected the high, medium, and low omega-3 HUFA intakes reported verbally by participants P1, P2, and P3, respectively. After confirming the range in omega-3 HUFA status via GC-FID, lipidomic data was extracted for the 11 lipids examined in Section 6.2 as well as 11 HUFA-containing lipids for a total of 22 specific lipids (Table 2). From the lipids examined, only 18:0/22:6 PS was significantly lower in DBS compared to WB (two-tailed Student's t-test, $p = 0.02$), suggesting that PS species may not be extracted from DBS as efficiently as other lipids. To explore this further, data for five additional PS species were extracted from the existing chromatograms (Table 3). All PS species measured were significantly lower in DBS compared to WB samples ($p < 0.05$ for all comparisons). This confirmed limited recoveries of PS species from dried blood spots. Interestingly, all phospholipids have one acidic group (-OH) around the phosphorus atom, while PS residues have an additional carboxylic acid residue that makes PS species acidic compounds at physiological pH (Folch, 1948). Hydrogen bonding between acidic compounds and the cellulose fibers within the chromatography paper used to collect DBS is known to occur (Sahin et al., 2008), and may explain the limited recoveries of PS observed.

7.4 *Conclusions, Limitations and Future Directions*

Lipidomic profiling of dried blood spots can provide a reliable representation of the whole blood lipidome for PC, PE, TAG, and CE. However it appears that lipid extraction from DBS requires extended periods of time. Moreover, the recovery of PS appears to be limited even with the 24-hour extraction period. The homogenization or sonication of DBS in the

chloroform/methanol may aid in increasing PS recoveries by increasing the surface area of the blood with the extraction solvents (Metherel et al., 2009). Lipid extraction techniques employing different solvent systems (Koulman et al., 2014) or manipulating the pH of the extraction solvents may also result in higher PS recoveries from DBS. Interestingly, the relationships between omega-3 HUFA in lipidomic profiles and fatty acid profiles may provide additional insights. Specifically, the blood of P1 has the highest concentration of EPA (Table 4; 2.50 µg/100µL whole blood) compared to P2 (2.19 µg/100 µL whole blood) and P3 (0.56 µg/100 µL whole blood), but 16:0/20:5 PC is highest in P2 (Table 2, 41.76 A.U.; P1 and P3 are 35.99 A.U. and 8.80 A.U., respectively). EPA has been demonstrated to increase rapidly in response to recent intake (Metherel et al., 2009). As such, certain acyl species of blood lipids such as 16:0/20:5 PC may be an indicator of very recent omega-3 HUFA intake. Other acyl species of blood lipids, such as erythrocyte membrane-associated phospholipids, may be better indicators for habitual, long-term intake; these take significantly longer periods of time to be remodeled compared to plasma lipids (Patterson et al., 2013). Levels of 16:0/22:6 PC were considerably higher in P1 (106.03 A.U.) as compared with P2 (62.10 A.U.) and P3 (34.88 A.U.) suggesting it may be a marker of long term omega-3 HUFA intake. To explore the relationship between dietary intake of omega-3 HUFA and acyl specific lipids, the lipidomic profiles of whole blood from humans with very defined dose intakes of EPA + DHA as part of a previous intervention trial (Patterson, 2012) were examined.

Table 1. ***Lipidomic profiles of whole blood and dried blood spot technical replicates.***

			Lipid Abundance (*Arbitrary Units*, Average ± SD)			
Observed *m/z*	**Lipid**	**Adduct**	**DBS_i**	**WB_i**	**DBS_{24}**	**WB_{24}**
496.3398	Lyso-16:0 PC	$[M+H]^+$	42.9 ± 4.9^a	96.5 ± 6.0^b	103.0 ± 4.6^b	92.4 ± 1.6^b
758.5694	16:0/18:2 PC	$[M+H]^+$	381.6 ± 57.2^a	1033.6 ± 95.7^b	1110.7 ± 28.4^b	1033.8 ± 36.0^b
782.5692	16:0/20:4 PC	$[M+H]^+$	749.5 ± 97.5^a	1319.0 ± 80.6^b	1379.1 ± 42.5^b	1232.8 ± 26.5^b
834.6006	18:0/22:6 PC	$[M+H]^+$	13.5 ± 4.1^a	28.0 ± 2.4^b	30.0 ± 1.4^b	28.1 ± 0.6^b
780.5534	16:0/20:5 PC	$[M+H]^+$	29.2 ± 4.1^a	58.0 ± 3.0^b	61.1 ± 2.0^b	53.0 ± 2.7^b
806.5691	16:0/22:6 PC	$[M+H]^+$	51.7 ± 8.5^a	130.5 ± 12.6^b	137.5 ± 4.9^b	131.3 ± 5.6^b
716.5221	16:0/18:2 PE	$[M+H]^+$	6.3 ± 0.8^a	11.9 ± 0.7^b	13.0 ± 0.5^b	12.0 ± 0.1^b
764.5221	16:0/22:6 PE	$[M+H]^+$	11.7 ± 1.6^a	20.8 ± 1.5^b	22.7 ± 1.0^b	21.0 ± 0.4^b
836.5432	18:0/22:6 PS	$[M+H]^+$	37.1 ± 4.4^a	54.9 ± 0.9^b	48.6 ± 6.5^b	57.5 ± 2.8^b
876.8011	16:0/18:1/18:1 TAG	$[M+NH_4]^+$	96.9 ± 28.9^a	212.9 ± 14.3^b	240.2 ± 9.7^b	215.8 ± 9.0^b
666.6181	18:2 CE	$[M+NH_4]^+$	62.8 ± 11.4^a	110.4 ± 7.4^b	119.2 ± 11.2^b	108.3 ± 3.1^b

m/z = mass to charge ratio. DBS_i = immediate lipid extraction from dried blood spots. DBS_{24} = lipid extraction from dried blood spots 24 hours after the addition of extraction solvents. WB_i = immediate lipid extraction from whole blood. WB_{24} = lipid extraction from whole blood 24 hours after the addition of extraction solvents. Phosphatidylcholine (PC); phosphatidylethanolamine (PE); phosphatidylserine (PS); triacylglycerol (TAG); cholesteryl ester (CE). $p \leq 0.001$ for all differences shown (except 18:0/22:6 PS, $p < 0.05$) after one-way ANOVA with Tukey post-hoc test.

Table 2. ***Lipidomic profiles of whole blood and dried blood spots for high, intermediate, and low omega-3 HUFA status***

			Lipid Abundance (*Arbitrary Units*)						Average ± SD	
Observed *m/z*	**Lipid**	**Adduct**	**HighWB**	**MedWB**	**LowWB**	**HighDBS**	**MedDBS**	**LowDBS**	**WBave**	**DBSave**
496.3398	Lyso-16:0 PC	$[M+H]^+$	90.89	78.77	100.31	88.77	62.79	91.43	90.0 ± 10.8	81.0 ± 15.8
758.5694	16:0/18:2 PC	$[M+H]^+$	1458.29	941.76	1045.18	1436.38	829.27	997.77	1148.4 ± 273.3	1087.8 ± 313.4
780.5534	16:0/20:5 PC	$[M+H]^+$	35.99	41.76	8.80	41.23	40.31	8.65	28.7 ± 17.8	30.0 ± 19.0
782.5692	16:0/20:4 PC	$[M+H]^+$	562.51	828.97	676.50	628.52	796.71	688.97	689.3 ± 133.7	704.7 ± 85.2
806.5691	16:0/22:6 PC	$[M+H]^+$	106.03	62.10	34.88	84.73	57.39	34.36	68.2 ± 36.3	60.1 ± 26.2
808.5862	18:0/20:5 PC	$[M+H]^+$	18.98	16.06	6.86	16.63	14.58	6.77	14.0 ± 6.3	12.7 ± 5.2
832.5694	18:1/22:6 PC	$[M+H]^+$	3.04	3.14	1.54	2.48	2.78	1.33	2.6 ± 0.9	2.2 ± 0.8
834.6006	18:0/22:6 PC	$[M+H]^+$	29.55	18.09	10.51	21.65	17.04	10.42	19.6 ± 9.9	16.5 ± 5.9
716.5221	16:0/18:2 PE	$[M+H]^+$	9.04	8.30	7.86	7.76	6.34	6.81	8.4 ± 0.6	7.0 ± 0.7
764.5221	16:0/22:6 PE	$[M+H]^+$	22.38	19.15	12.32	23.59	17.51	11.34	17.9 ± 5.2	17.4 ± 6.1
722.5120	Plasmenyl-PE P16:0/20:5	$[M+H]^+$	3.20	2.14	0.58	2.62	1.74	0.58	2.0 ± 1.3	1.6 ± 1.0
748.5277	Plasmenyl-PE P16:0/22:6	$[M+H]^+$	7.99	3.51	3.16	6.42	4.46	2.86	4.9 ± 2.7	4.6 ± 1.8
752.5590	Plasmenyl-PE P18:0/20:4	$[M+H]^+$	27.86	32.95	33.54	25.33	27.22	29.88	31.5 ± 3.1	27.5 ± 2.3
836.5432	18:0/22:6 PS	$[M+H]^+$	43.23	40.20	28.58	23.66	13.38	11.36	37.3 ± 8.1[a]	16.2 ± 6.6[b]
876.8011	16:0/18:1/18:1 TAG	$[M+NH_4]^+$	242.01	213.57	240.78	237.85	233.99	266.02	232.1 ± 16.1	246.0 ± 17.5
894.7542	16:0/18:2/20:5 TAG	$[M+NH_4]^+$	1.41	2.31	0.50	1.21	2.58	0.57	1.4 ± 0.9	1.5 ± 1.0
918.7036	16:0/18:2/22:6 TAG	$[M+NH_4]^+$	6.85	5.34	0.84	6.12	5.68	0.88	4.3 ± 3.1	4.2 ± 2.9
920.7699	18:1/18:2/20:5 TAG	$[M+NH_4]^+$	6.88	5.41	0.85	6.10	5.74	0.89	4.4 ± 3.1	4.2 ± 2.9
922.7859	16:0/18:1/22:6 TAG	$[M+NH_4]^+$	10.11	10.00	1.25	9.18	10.62	1.35	7.1 ± 5.1	7.1 ± 5.0
666.6181	18:2 CE	$[M+NH_4]^+$	128.95	109.19	103.03	151.25	121.72	114.45	113.7 ± 13.5	129.1 ± 19.5
688.6029	20:5 CE	$[M+NH_4]^+$	6.77	2.55	0.69	5.77	2.65	0.75	3.3 ± 3.1	3.1 ± 2.5
714.6182	22:6 CE	$[M+NH_4]^+$	7.20	4.04	2.28	5.89	4.49	2.48	4.5 ± 2.5	4.3 ± 1.7

High (P1), Med (P2) and Low (P3) represent omega-3 HUFA status, from fatty acid composition data generated with GC-FID. Full fatty acid profiles found in Appendix C. Whole Blood (WB); Dried Blood Spot (DBS); Phosphatidylcholine (PC); phosphatidylethanolamine (PE); phosphatidylserine (PS); triacylglycerol (TAG); cholesteryl ester (CE). [a] is significantly from [b] with $p = 0.02$ after a two-tailed Student's t-test.

Table 3. ***Lipidomic profiles of phosphatidylserine species in whole blood and dried blood spot for high, intermediate, and low omega-3 HUFA status***

			Lipid Abundance (*Arbitrary Units*)						Average ± SD	
Observed *m/z*	**Lipid**	**Adduct**	**HighWB**	**MedWB**	**LowWB**	**HighDBS**	**MedDBS**	**LowDBS**	**WBave**	**DBSave**
790.5592	18:0/18:1 PS	$[M+H]^+$	7.26	5.00	5.45	3.15	1.36	1.80	5.9 ± 1.2^a	2.1 ± 0.9^b
814.5593	18:0/20:3 PS	$[M+H]^+$	3.29	2.11	3.47	1.50	0.55	1.16	3.0 ± 0.7^a	1.1 ± 0.5^b
812.5433	18:0/20:4 PS	$[M+H]^+$	49.47	54.25	63.27	23.83	15.12	21.65	55.7 ± 7.0^a	20.2 ± 4.5^b
837.5436	18:0/22:5 PS	$[M+H]^+$	0.28	0.18	0.32	0.13	0.02	0.09	0.3 ± 0.1^a	0.1 ± 0.1^b
836.5435	18:0/22:6 PS	$[M+H]^+$	43.71	40.07	28.19	23.64	13.59	11.33	37.3 ± 8.1^a	16.2 ± 6.6^b

m/z = mass to charge ratio. Whole Blood (WB); Dried Blood Spot (DBS); Phosphatidylserine (PS). High, Med and Low represent omega-3 highly unsaturated status (HUFA), from fatty acid composition data generated with gas chromatography-flame ionization detection (GC-FID). Full fatty acid profiles found in Appendix C. ^{a} is significantly from ^{b} with $p < 0.05$ after a two-tailed Student's t-test.

Table 4. ***Fatty Acid Composition – Concentrations in Whole Blood***

Whole Blood Total Lipids *(µg fatty acid per 100 µL whole blood)*					
Name	**P1**	**P2**	**P3**	**Average**	**SD**
C 12:0	0.17	0.13	0.10	0.14	0.04
C 14:0	1.76	2.15	1.55	1.82	0.30
C 16:0	54.23	52.26	47.97	51.49	3.20
C 17:0	0.81	0.75	0.63	0.73	0.09
C 18:0	30.09	32.20	29.31	30.53	1.49
C 20:0	0.78	0.93	0.82	0.84	0.08
C 22:0	1.82	2.19	1.88	1.96	0.20
C 23:0	0.46	0.52	0.41	0.46	0.05
C 24:0	3.11	4.23	3.60	3.65	0.56
SFAs	**96.96**	**98.96**	**89.32**	**95.08**	**5.09**
C 12:1	0.01	0.01	0.01	0.01	<0.00
C 14:1	0.07	0.07	0.03	0.06	0.03
C 16:1	2.01	2.01	1.48	1.83	0.31
C 18:1n-7	4.02	3.95	4.09	4.02	0.07
C 18:1n-9	39.26	41.78	36.11	39.05	2.84
C 20:1n-9	0.56	0.68	0.56	0.60	0.07
C 22:1n-9	0.10	0.19	0.18	0.16	0.05
C 24:1n-9	4.37	4.99	3.92	4.43	0.54
MUFAs	**51.16**	**54.27**	**46.81**	**50.75**	**3.75**
C 18:2n-6	63.34	47.80	45.05	52.06	9.86
C 18:3n-6	0.14	0.83	0.25	0.41	0.37
C 20:2n-6	0.65	0.52	0.51	0.56	0.08
C 20:3n-6	2.56	3.15	2.54	2.75	0.35
C 20:4n-6	20.30	26.20	23.00	23.17	2.95
C 22:2n-6	0.20	0.22	0.21	0.21	0.01
C 22:4n-6	1.72	2.59	3.31	2.54	0.80
C 22:5n-6	0.62	0.92	0.99	0.84	0.19
N-6	**89.54**	**82.24**	**75.87**	**82.55**	**6.84**
C 18:3n-3	1.82	1.21	0.87	1.30	0.48
C 20:3n-3	0.13	0.10	0.08	0.11	0.02
C 20:5n-3	2.50	2.19	0.56	1.75	1.04
C 22:5n-3	2.62	3.18	2.54	2.78	0.35
C 22:6n-3	7.79	6.97	3.71	6.16	2.16
N-3	**14.87**	**13.66**	**7.77**	**12.10**	**3.80**
C 20:3n-9	0.17	0.31	0.18	0.22	0.08
PUFAs	**104.58**	**96.21**	**83.82**	**94.87**	**10.45**
HUFAs	**38.42**	**45.63**	**36.93**	**40.32**	**4.65**
EPA+DHA	**10.30**	**9.16**	**4.27**	**7.91**	**3.20**
Total	**252.71**	**249.44**	**219.96**	**240.70**	**18.04**

Saturated fatty acids (SFAs); Mono-unsaturated fatty acids (MUFAs); Omega-6 fatty acids (N-6); Omega-3 fatty acids (N-3); Polyunsaturated fatty acids (PUFAs); Highly unsaturated fatty acids (HUFAs); Eicosapentaenoic acid (EPA); Docosahexaenoic acid (DHA).

Chapter 8

Lipidomic Profiling of Human Whole Blood Following Omega-3 Highly Unsaturated Fatty Acid Supplementation

8.1 *Introduction*

The fatty acid composition of blood before and after omega-3 HUFA supplementation has been examined extensively in the literature, although data on whole blood is relatively limited. Previously, with acute supplementation and washout is has been observed that EPA increases and decreases rapidly in blood, while DHA changes appear to be more gradual (Metherel et al., 2009). Others have supported these observations, where the slow turnover of DHA in erythrocytes reflects long-term intake of omega-3 HUFA (Patterson et al., 2013). Though significant work has been done on the development of blood biomarkers that reflect short-term and long-term omega-3 HUFA intake using fatty acid compositional data (Browning et al., 2012) little work has been done examining the effect of omega-3 HUFA supplementation on acyl-specific blood lipids. Therefore, the location of omega-3 HUFA in complex blood lipids with different levels of fish oil intake was examined. To do so, blood samples from a previous intervention trial with tight dietary intakes of EPA and DHA (Patterson, 2012) were analyzed using the UHPLC-MS/MS method developed throughout Chapters 5 and 6 of this thesis.

8.2 *Methods*

8.2.1 *Participants and Blood Samples*

Participants were recruited from the University of Waterloo area through flyers and emails. A screening fingertip prick sample was collected, and participants completed a semi-quantitative food frequency questionnaire to assess EPA and DHA intakes. Individuals were

excluded if they were currently consuming supplements with EPA and DHA, or if fingertip prick whole blood revealed that EPA and DHA were greater than 3% of total fatty acids by weight percent. At baseline, anthropometric measures were collected along with a fasting venous blood sample from twenty individuals, and they were instructed to not consume any nutraceuticals or EPA/DHA-containing foods (anthropometric measures can be found in Patterson, 2012 Doctoral Thesis). The participants were provided with fish oil capsules and were instructed to take one capsule per day for four weeks (providing ~250 mg/day EPA+DHA), and then two capsules per day for the next four weeks (providing ~500 mg/day EPA+DHA). After the eight-week period, a subset of five participants was asked to take four capsules per day for an additional four weeks (providing ~1000 mg/day EPA+DHA). Fasting venous blood samples were collected again after 4 and 8 weeks for the 20 participants, and at week 12 for the subset of five. Blood samples were aliquoted in triplicates of 500 uL and stored at -80ºC until analysis.

8.2.2 *Fatty Acid Composition and Lipidomic Analyses*

The fatty acid composition of whole blood, plasma phospholipids and erythrocytes was determined as described in Chapter 4 using in GC-FID in 2012 (Patterson, 2012). The samples that were used for lipidomic profiling remained frozen at -80ºC from the time of collection until preparation for UHPLC-MS/MS analysis. To test the quality and state of the samples after more than 2 years in storage, quantitative and qualitative fatty acid compositional data was generated for the whole blood of a subset of 3 participants from each of the four time points. There were no significant differences in the fatty acid profiles of the blood samples compared to the data from 2012, suggesting that whole blood fatty acids may be stable in -80ºC storage for longer than 6 months (Metherel et al., 2013).

Due to the complexity and extensiveness of the lipidomic data that can be generated with the current UHPLC-MS/MS method, and the issues associated with data processing, a list of 46 target lipids was generated. These were used to profile whole blood samples throughout the experiments in this chapter. Overall, the UHPLC-MS/MS method for lipidomic profiling of human whole blood developed in Chapter 5 identified 163 acyl specific lipids. Individual acyl species of lipids were examined for individual lipids that made up the top 85% of the lipidome. The top 85% all of the detectable lipids (Appendix B) were determined by sorting in descending order the area under the curve (AUC). This was done until the sum of these AUC constituted at least 85% of the total sum for all lipids within the lipid class to which they belong. The specific lipids falling outside of the 85% made limited contributions to the overall lipidome (<0.01% to 0.13% of total lipid AUC). Providing acyl-specific data for the top 85% of lipids within a lipid class can provide information about specific molecules, yet still giving insights with regards to what may be happening to the entire lipid pool (Byrdwell, 2015b). While data can be generated for hundreds of lipids and minor lipids can be highly bioactive (Ji et al., 2011), the targeted list of 46 provides a parsimonious but highly informative snapshot of the lipidome for screening purposes.

The sixty-five whole blood samples (20 baseline, 20 week 4, 20 week 8, and 5 week 12) were prepared for UHPLC-MS/MS analysis as described in Chapter 4. Briefly, samples were removed from -80ºC storage, thawed, extracted twice using 2:1 chloroform:methanol (v/v), and spiked with di-17:0 PC in the HPLC sample solvent. The 47-minute multi-step gradient was used with positive ESI and Top5 data-dependent acquisition. The ion profiles for the 46 lipids that constituted the top 85% of total lipids were extracted and the peaks were integrated. As in

previous chapters, the raw integrated data (area under the curve) were standardized by dividing them by the area under the curve for the internal standard (di-17:0 PC) and multiplying by 100.

8.2.3 *Thin Layer Chromatography and Adjustment of the Lipidomic Data*

The fatty acid composition of total PC, PE, PS, PI, SM, TAG, FFA and CE was determined by GC-FID after thin layer chromatography isolation as described in Chapter 4 for a subset of 3 participants at baseline, week 4, week 8 and week 12 of the supplementation period. Initially, this was done in order to contrast the acyl-specific lipidomic data derived from UHPLC-MS/MS analyses to fatty acid compositional data, as thin layer chromatography/GC-FID fatty acid determinations are quantitatively robust (Firl et al., 2013). However, this fatty acid compositional data served a second purpose for standardization when the raw lipidomics data was inconsistent. While all of the semi-quantitative data generated in this thesis was standardized to a di-17:0 PC internal standard, there were significant differences in the responses that were observed for the standard peak in the lipidomic analyses that were completed. Due to instrument availability, the samples were run in three different sequences over the span of two weeks. Day-to-day variation of absolute instrument responses are widely known for quantitative and semi-quantitative MS methods in general, and may result from several factors such as instrument cleanliness, ion source flow rates, and state of the mass spectrometer's vacuum (Pitt, 2009). Therefore, in order to analyze the lipidomic data and examine the effect of EPA and DHA supplementation over time, the data was normalized systematically to reflect the changes in specific lipid pool total concentrations generated through thin layer chromatography and GC-FID. As an example, the ratios between total PE between the four time points as determined by thin layer chromatography and GC-FID were applied to the lipidomic data from the UHPLC-

MS/MS method. Granted that using thin layer chromatography/ GC-FID data was effective for normalizing lipidomic data, generating it entails a considerable additional amount of analytical work that is not practical for routine analyses.

8.3 *Results*

Native lipid abundances of the top 85% abundant lipids are reported as A.U., were examined for the 20 participants over 8 weeks at intakes of 250 mg/day and 500 mg/day (Table 5), and intakes of 250 mg/day, 500 mg/day and 1000 mg/day were examined in a subset of 5 participants over 12 weeks (Table 6). Due to the nature of the semi-quantitative method, it is only possible to examine and compare specific lipid acyl species within lipid classes, but not between them. At baseline, the most abundant PC with DHA acyl species is 16:0/DHA PC, and that for EPA-containing species is 16:0/EPA PC. Notably, these same species appear to be the most responsive to increasing doses of EPA+DHA within the PC pool. While there is some incorporation of dietary EPA and DHA into other lipids (like 18:0/DHA PC, 18:1/DHA PC, 18:0/EPA PC), it appears that the bulk of these two fatty acids are going into palmitate-containing PC. On average, 16:0/DHA PC and 16:0/EPA PC increase by 16.22 A.U. and 21.14 A.U. respectively by week 8 compared to baseline in the group of 20 (Table 5; $p < 0.001$); and by 33.58 A.U. and 41.78 A.U. respectively by week 12 compared to baseline in the group of 5 (Table 6; $p < 0.05$). Interestingly, these two lipids appear to change in a dose-response manner. The supplemented dose of EPA+DHA between weeks 4 and 8 was 500 mg/day, and between weeks 8 and 12 it was 1000 mg/day. This is reflected by the absolute increases in 16:0/DHA PC and 16:0/EPA PC at the end of weeks 8 and 12 compared to baseline values. While some incorporation of EPA and DHA does take place over time in PE acyl species, significantly higher

plasmenyl-PE P-16:0 EPA (most abundant species at baseline; $p < 0.001$) is only observed at week 12 compared to baseline. This lipid, like 16:0/DHA PC and 16:0/EPA PC appears to increase proportionally to the dose of EPA+DHA supplemented; there is an increase of 0.41 A.U. at week 8 compared to baseline, and a further increase of 1.01 A.U. at week 12 compared to baseline in the subset of 5 participants (Table 6). In the contrary, 16:0/DHA PE, which is the most abundant DHA-containing acyl species in the PE pool at baseline is not different at any of the time points. Finally, there appears to be some incorporation of EPA and DHA into other lipid pools such as CE, TAG. No differences are observed in 18:0/DHA PS at any of the time points. Remarkably, the lipidomic data for PE species reveals flux of omega-6 HUFAs. Specifically, PE species such as 16:0/20:4, 18:0/20:4 and Plasmenyl PE P-18:0/20:4 are significantly lower at week 12 compared to baseline. Furthermore, there is an increase in the proportion of 18:1/20:4 PC species in the group of 20 participants at week 12.

8.4 *Discussion*

This study suggests that the PC pool is a major site for omega-3 HUFA incorporation in blood. Notably, PC is a substantial component of both plasma lipoproteins and erythrocyte bilayers, but PE and PS are found primarily in the erythrocyte fraction (Figure 10; Table E.1, Appendix E). In addition to previous reports (Metherel et al., 2009; Patterson et al., 2013), this supports that the plasma fraction is more responsive to changes in EPA and DHA dietary intake compared to erythrocytes. Interestingly, these findings are further supported by the plasma phospholipid and erythrocyte total fatty acid composition data (Tables 7 and 8), and the whole blood lipid pool fatty acid composition data (Table 9; Tables D.1 through D.7, Appendix D). While plasma phospholipid EPA is significantly higher after four weeks of supplementation and

DHA after 8 weeks compared to baseline in the group of 20 and ($p < 0.05$ for both), erythrocyte EPA appears to only be significantly higher than baseline at week 8 and erythrocyte DHA is only different at week 12. Finally, the fatty acid composition data for total PE (Table 9) shows that there is no difference in total DHA in PE even after 12 weeks of supplementation, but total EPA in PE is over 3-fold higher at week 12 compared to baseline ($p < 0.05$).

In addition to these observations that suggest slower turnover of omega-3 HUFA in erythrocytes membrane lipids compared to plasma phospholipids, three potential acyl-specific lipids were identified that reflect the doses of EPA and DHA being consumed through fish oil supplementation. These lipids are 16:0/DHA PC, 16:0/EPA PC, and plasmenyl-PE P-16:0/EPA. The difference in the absolute increase of these lipids to baseline was nearly a factor of 2 from week 8 to week 12, which is the factor by which the dose increased. Since PC is a major structural component of erythrocyte bilayers but also plasma lipoproteins, it was therefore expected that some acyl-specific PC molecule would reflect rapid changes in EPA+DHA intake. Although, it was interesting to see that plasmenyl-PE P-16:0/EPA, which is primarily associated with the erythrocyte bilayer (Nagan and Zoeller, 2001) also reflects recent intake. This finding supports previous reports (Patterson et al., 2014) on the faster flux of EPA in and out of erythrocyte membranes compared to DHA. However, it appears that EPA mobilization is fast in the PE pool as well which has not been reported previously.

8.4 *Conclusions, Limitations, and Future Directions*

In conclusion, the lipidomic data supports previous findings of fast turnover of EPA and DHA in plasma, but slower in erythrocyte phospholipids (Metherel et al., 2009; Patterson et al., 2014). Through the acyl-specific characterization of whole blood lipids from a previous

supplementation study with tight dietary control (Patterson, 2012), 16:0/DHA PC, 16:0/EPA PC, and plasmenyl-PE P-16:0/EPA were found to be very responsive to increasing intakes of EPA+DHA. Specifically, these lipids increased in a dose-dependent manner, and may be adequate indicators of frequent or habitual intake of EPA+DHA. Interestingly, the reduction that was observed in some omega-6 HUFA acyl specific PE like 16:0/20:4 PE, 18:0/20:4 PE and plasmenyl-PE P-18:0/20:4 suggests that phospholipid remodeling may be taking place possibly through the Lands Cycle (Lands, 1958). One of the main limitations of this study is that the current UHPLC-MS/MS analyses did not allow for direct comparisons to be made between lipid pools containing EPA and DHA acyl-specific lipids. This was due to the fact that only one internal standard (di-17:0 PC) was used to normalize the data. Since different lipids exhibit different electrical properties in ESI-MS that are intrinsic of their molecular configurations, they generate different absolute instrument responses that may only be normalized through the use of internal standards that share those same electrical properties (Koivusalo et al., 2001). Therefore, an internal standard for each lipid class is likely required. If the use of stable isotope standards for quantitation is not feasible or possible, multiple lipid standards may be used if factors such as the phospholipid head group, and fatty acyl length and degree of unsaturation are taken into account. Furthermore, the analyses performed in this study were only in whole blood. While some conclusions were made regarding PE acyl species and changes in erythrocyte membranes, erythrocyte PC cannot be distinguished from plasma PC at this point. This could provide more insights with regards to lipid bilayer remodeling with omega-3 HUFA supplementation. Future work should examine lipidomic changes of acyl-specific lipids across blood fractions. Additionally, it remains unknown whether specific enzymes that are involved in phospholipid remodeling processes such as phospholipase-A2 (Tanaka et al., 2010) and lyso-phospholipid

acyltransferases (Shindou et al., 2013) are upregulated. Finally, though the participants that were part of this study consumed very tightly-controlled amounts of EPA+DHA, the supplementation period was only 8 weeks for the group of 20, and 12 weeks for the subgroup of 5. Lipidomic discrimination of complex lipids in a long-term supplementation study could reveal acyl-specific lipids that are remodeled slowly over the span of several months, and could therefore be validated as indicators of long-term omega-3 HUFA intake. Some of the DHA-containing PS and PE species that did not change in this study could be appropriate biomarkers but longer supplement intervention times are required.

Table 5. ***Lipidomic Examination of Human Whole Blood Following Fish Oil Supplementation for 8 weeks.***

			Lipid Abundance, n = 20 (*Arbitrary Units*, Average ± SD)		
Observed *m/z*	**Lipid**	**Adduct**	**Baseline**	**Week 4**	**Week 8**
760.5843	PC 16:0/18:1	$[M+H]^+$	284.60 ± 66.08	268.98 ± 55.75	303.04 ± 55.89
758.5704	PC 16:0/18:2	$[M+H]^+$	560.84 ± 100.02	532.74 ± 113.35	550.66 ± 84.17
782.5699	PC 16:0/20:4	$[M+H]^+$	414.37 ± 68.83	370.16 ± 94.38	381.85 ± 81.23
780.5536	PC 16:0/20:5	$[M+H]^+$	12.47 ± 5.83^a	19.53 ± 6.45^b	33.61 ± 11.52^c
806.5693	PC 16:0/22:6	$[M+H]^+$	42.70 ± 9.57^a	44.65 ± 14.94^a	58.92 ± 14.30^b
788.6178	PC 18:0/18:1	$[M+H]^+$	64.09 ± 11.59	64.05 ± 14.12	73.15 ± 12.91
786.6022	PC 18:0/18:2	$[M+H]^+$	223.78 ± 51.85	222.93 ± 55.13	207.94 ± 33.78
810.6002	PC 18:0/20:4	$[M+H]^+$	89.19 ± 23.49	77.99 ± 24.94	73.32 ± 21.67
808.5851	PC 18:0/20:5	$[M+H]^+$	3.93 ± 1.96^a	6.90 ± 2.49^b	12.45 ± 3.23^c
834.6009	PC 18:0/22:6	$[M+H]^+$	12.12 ± 3.12^a	13.01 ± 3.83^a	17.34 ± 3.67^b
808.5872	PC 18:1/20:4	$[M+H]^+$	24.69 ± 5.51^a	22.91 ± 6.98^a	31.66 ± 7.83^b
832.5853	PC 18:1/22:6	$[M+H]^+$	2.35 ± 0.69	2.34 ± 0.77	2.88 ± 0.91
Total PC measured			**1735.14 ± 206.07**	**1646.19 ± 299.48**	**1746.82 ± 218.10**
718.5380	PE 16:0/18:1	$[M+H]^+$	11.48 ± 1.72	11.16 ± 1.74	11.44 ± 1.87
716.5227	PE 16:0/18:2	$[M+H]^+$	4.66 ± 1.20	4.38 ± 1.05	4.45 ± 1.18
740.5227	PE 16:0/20:4	$[M+H]^+$	9.36 ± 1.64	8.46 ± 1.58	8.49 ± 1.17
738.5069	PE 16:0/20:5	$[M+H]^+$	0.40 ± 0.16^a	0.46 ± 0.15^a	0.68 ± 0.14^b
764.5225	PE 16:0/22:6	$[M+H]^+$	5.83 ± 1.76	5.65 ± 1.65	6.63 ± 1.74
768.5512	PE 18:0/20:4	$[M+H]^+$	8.73 ± 1.70	7.81 ± 1.65	7.78 ± 1.49
742.5383	PE 18:1/18:2	$[M+H]^+$	5.42 ± 1.20	4.88 ± 1.19	5.05 ± 1.28
766.5370	PE 18:1/20:4	$[M+H]^+$	6.49 ± 0.68	6.04 ± 1.15	6.14 ± 1.12
724.5284	Plasmenyl-PE P-16:0/20:4	$[M+H]^+$	8.32 ± 2.33^a	6.86 ± 1.44^b	6.92 ± 1.22^b
722.5114	Plasmenyl-PE P-16:0/20:5	$[M+H]^+$	0.53 ± 0.20^a	0.64 ± 0.16^a	0.93 ± 0.17^b
750.5428	Plasmenyl-PE P-16:0/22:5	$[M+H]^+$	8.27 ± 1.94^a	7.01 ± 1.44^b	7.22 ± 1.20^{ab}
748.5273	Plasmenyl-PE P-16:0/22:6	$[M+H]^+$	1.94 ± 0.43	1.77 ± 0.41	2.01 ± 0.30
752.5598	Plasmenyl-PE P-18:0/20:4	$[M+H]^+$	16.39 ± 3.23^a	13.91 ± 2.94^b	13.94 ± 2.84^b
Total PE measured			**87.82 ± 13.05**	**79.02 ± 11.59**	**81.68 ± 10.74**

790.5589	PS 18:0/18:1	$[M+H]^+$	1.26 ± 0.40	1.12 ± 0.31	1.37 ± 0.37
812.5437	PS 18:0/20:4	$[M+H]^+$	11.46 ± 4.60	8.76 ± 3.11	15.40 ± 24.50
836.5434	PS 18:0/22:6	$[M+H]^+$	6.33 ± 2.56	5.22 ± 1.55	6.07 ± 1.42
Total PS measured			**19.05 ± 6.45**	**15.10 ± 4.51**	**22.83 ± 25.06**
822.2553	TAG 14:0/16:0/18:1	$[M+NH_4]^+$	17.81 ± 21.88	18.47 ± 19.21	22.72 ± 21.48
852.8020	TAG 16:0/16:0/18:0	$[M+NH_4]^+$	3.93 ± 2.79	3.85 ± 2.44	4.30 ± 4.23
850.7812	TAG 16:0/16:0/18:1	$[M+NH_4]^+$	37.85 ± 36.03	39.43 ± 40.30	49.05 ± 48.07
876.7986	TAG 16:0/18:1/18:1	$[M+NH_4]^+$	136.29 ± 70.90	133.32 ± 54.64	174.28 ± 98.11
874.7862	TAG 16:0/18:1/18:2	$[M+NH_4]^+$	151.41 ± 52.49	147.75 ± 37.68	174.16 ± 85.72
872.7674	TAG 16:0/18:1/18:3	$[M+NH_4]^+$	6.48 ± 4.37	6.51 ± 3.33	9.08 ± 6.14
896.7700	TAG 16:0/18:1/20:5	$[M+NH_4]^+$	1.31 ± 0.53	1.54 ± 0.69	1.72 ± 0.89
922.7840	TAG 16:0/18:1/22:6	$[M+NH_4]^+$	1.28 ± 0.73^{a}	2.06 ± 1.02^{a}	4.00 ± 2.25^{b}
872.7674	TAG 16:0/18:2/18:2	$[M+NH_4]^+$	24.00 ± 10.31	25.70 ± 10.96	29.25 ± 15.49
902.8143	TAG 18:0/18:1/18:2	$[M+NH_4]^+$	11.56 ± 5.63	11.71 ± 3.78	15.97 ± 10.65
902.8143	TAG 18:1/18:1/18:1	$[M+NH_4]^+$	37.09 ± 16.34^{ab}	35.88 ± 13.23^{a}	48.78 ± 19.33^{b}
900.7988	TAG 18:1/18:1/18:2	$[M+NH_4]^+$	49.64 ± 22.87	50.05 ± 20.63	58.51 ± 25.53
898.7857	TAG 18:1/18:2/18:2	$[M+NH_4]^+$	10.99 ± 7.95	12.30 ± 7.41	13.37 ± 8.64
Total TAG measured			**489.63 ± 205.52**	**488.57 ± 145.22**	**605.18 ± 293.02**
668.6340	CE 18:1	$[M+NH_4]^+$	3.38 ± 0.78	3.62 ± 1.18	4.03 ± 0.90
666.6185	CE 18:2	$[M+NH_4]^+$	24.12 ± 4.23^{a}	25.40 ± 4.72^{ab}	28.51 ± 4.77^{b}
690.6186	CE 20:4	$[M+NH_4]^+$	3.81 ± 1.98	3.04 ± 1.45	3.35 ± 1.52
688.6029	CE 20:5	$[M+NH_4]^+$	0.12 ± 0.15^{a}	0.21 ± 0.13^{a}	0.56 ± 0.29^{b}
714.6175	CE 22:6	$[M+NH_4]^+$	0.28 ± 0.12^{a}	0.36 ± 0.19^{a}	0.58 ± 0.24^{b}
Total CE measured			**31.72 ± 5.44^{a}**	**32.64 ± 6.44^{ab}**	**37.03 ± 6.44^{b}**

Mass-to-charge ratio (*m/z*); Phosphatidylcholine (PC); Phosphatidylethanolamine (PE); Phosphatidylserine (PS); Triacylglycerol (TAG); Cholesteryl ester (CE); Highly unsaturated fatty acid (HUFA). Superscript differences highlight significantly different values after one-way ANOVA + Tukey HSD post-hoc test with $p < 0.05$.

Table 6. ***Lipidomic Examination of Human Whole Blood Following Omega-3 HUFA Supplementation for 12 weeks.***

			Lipid Abundance, n = 5 (*Arbitrary Units*, Average ± SD)			
Observed *m/z*	**Lipid**	**Adduct**	**Baseline**	**Week 4**	**Week 8**	**Week 12**
760.5843	PC 16:0/18:1	$[M+H]^+$	289.01 ± 92.38	261.43 ± 82.16	280.19 ± 68.53	226.57 ± 53.66
758.5704	PC 16:0/18:2	$[M+H]^+$	502.44 ± 71.94	458.79 ± 83.41	503.39 ± 103.27	511.50 ± 134.15
782.56994	PC 16:0/20:4	$[M+H]^+$	478.52 ± 22.61	425.96 ± 75.56	419.09 ± 45.96	392.48 ± 70.54
780.5536	PC 16:0/20:5	$[M+H]^+$	11.23 ± 5.37^{a}	16.33 ± 5.76^{a}	31.19 ± 11.66^{a}	53.01 ± 18.69^{b}
806.5693	PC 16:0/22:6	$[M+H]^+$	38.57 ± 9.31^{a}	45.02 ± 16.37^{ab}	51.53 ± 11.20^{ab}	72.15 ± 22.81^{b}
788.6178	PC 18:0/18:1	$[M+H]^+$	70.42 ± 12.18	71.32 ± 16.98	76.02 ± 14.06	68.59 ± 16.17
786.6022	PC 18:0/18:2	$[M+H]^+$	198.57 ± 44.16	202.80 ± 56.03	210.20 ± 54.40	220.51 ± 78.42
810.6002	PC 18:0/20:4	$[M+H]^+$	106.56 ± 19.28	94.15 ± 25.70	88.72 ± 17.33	77.15 ± 22.70
808.5851	PC 18:0/20:5	$[M+H]^+$	4.10 ± 1.69^{a}	7.45 ± 3.03^{ab}	13.07 ± 4.35^{bc}	17.37 ± 6.57^{c}
834.6009	PC 18:0/22:6	$[M+H]^+$	10.97 ± 3.00^{a}	14.38 ± 4.71^{ab}	16.38 ± 4.22^{ab}	19.84 ± 4.93^{b}
808.5872	PC 18:1/20:4	$[M+H]^+$	26.01 ± 4.41	27.34 ± 6.91	33.86 ± 5.15	31.35 ± 11.58
832.5853	PC 18:1/22:6	$[M+H]^+$	1.99 ± 0.89	2.41 ± 1.03	2.43 ± 0.88	3.38 ± 1.53
Total PC measured			**1738.40 ± 203.36**	**1627.39 ± 349.09**	**1726.07 ± 294.73**	**1693.89 ± 415.26**
718.5380	PE 16:0/18:1	$[M+H]^+$	11.05 ± 1.24	10.89 ± 1.24	11.37 ± 1.08	12.27 ± 0.97
716.5227	PE 16:0/18:2	$[M+H]^+$	4.08 ± 0.54	3.86 ± 0.47	3.85 ± 0.35	4.37 ± 0.24
740.5227	PE 16:0/20:4	$[M+H]^+$	10.13 ± 0.83^{a}	9.44 ± 0.77^{ab}	9.41 ± 0.75^{ab}	8.22 ± 0.92^{b}
738.5069	PE 16:0/20:5	$[M+H]^+$	0.40 ± 0.14^{a}	0.47 ± 0.11^{a}	0.67 ± 0.11^{a}	1.22 ± 0.27^{b}
764.5225	PE 16:0/22:6	$[M+H]^+$	5.44 ± 1.49	5.53 ± 1.03	6.55 ± 1.07	5.97 ± 1.68
768.5512	PE 18:0/20:4	$[M+H]^+$	9.70 ± 1.28^{a}	8.93 ± 1.03^{a}	8.80 ± 1.10^{a}	6.72 ± 0.69^{b}
742.5383	PE 18:1/18:2	$[M+H]^+$	5.01 ± 0.61	4.16 ± 0.74	4.58 ± 0.58	5.32 ± 0.74
766.5370	PE 18:1/20:4	$[M+H]^+$	6.77 ± 0.60	6.24 ± 0.53	6.30 ± 0.89	5.73 ± 0.65
724.5284	Plasmenyl-PE P-16:0/20:4	$[M+H]^+$	8.30 ± 1.12	7.56 ± 1.47	7.15 ± 1.01	8.01 ± 0.80
722.5114	Plasmenyl-PE P-16:0/20:5	$[M+H]^+$	0.48 ± 0.12^{a}	0.61 ± 0.11^{ab}	0.89 ± 0.15^{b}	1.49 ± 0.22^{c}
750.5428	Plasmenyl-PE P-16:0/22:5	$[M+H]^+$	8.29 ± 1.04	7.69 ± 1.57	7.49 ± 0.86	8.19 ± 0.60
748.5273	Plasmenyl-PE P-16:0/22:6	$[M+H]^+$	1.75 ± 0.29^{ab}	1.69 ± 0.26^{a}	1.90 ± 0.23^{ab}	2.19 ± 0.20^{b}
752.5598	Plasmenyl-PE P-18:0/20:4	$[M+H]^+$	16.96 ± 0.54^{a}	15.23 ± 0.81^{a}	15.28 ± 1.91^{a}	12.45 ± 0.98^{b}
Total PE measured			**88.36 ± 7.28**	**82.30 ± 6.95**	**84.24 ± 7.70**	**82.15 ± 6.69**

790.5589	PS 18:0/18:1	$[M+H]^+$	1.21 ± 0.45	0.99 ± 0.36	1.21 ± 0.49	1.60 ± 0.34
812.5437	PS 18:0/20:4	$[M+H]^+$	10.82 ± 6.15	8.82 ± 1.82	10.45 ± 2.82	5.55 ± 2.87
836.5434	PS 18:0/22:6	$[M+H]^+$	5.16 ± 2.72	5.44 ± 1.18	5.99 ± 1.42	5.06 ± 0.84
Total PS measured			**17.19 ± 6.90**	**15.26 ± 2.70**	**17.65 ± 4.51**	**12.21 ± 3.39**
822.2553	TAG 14:0/16:0/18:1	$[M+NH_4]^+$	24.35 ± 36.74	22.91 ± 20.87	23.06 ± 16.66	10.73 ± 6.26
852.8020	TAG 16:0/16:0/18:0	$[M+NH_4]^+$	3.90 ± 3.81	4.98 ± 2.91	4.68 ± 3.49	2.46 ± 0.86
850.7812	TAG 16:0/16:0/18:1	$[M+NH_4]^+$	42.86 ± 58.06	44.40 ± 39.84	49.05 ± 39.09	22.20 ± 11.01
876.7986	TAG 16:0/18:1/18:1	$[M+NH_4]^+$	124.72 ± 95.30	138.93 ± 75.44	160.77 ± 76.83	106.05 ± 52.03
874.7862	TAG 16:0/18:1/18:2	$[M+NH_4]^+$	127.24 ± 35.68	145.20 ± 42.38	158.65 ± 45.95	138.78 ± 33.33
872.7674	TAG 16:0/18:1/18:3	$[M+NH_4]^+$	5.12 ± 2.23^{ab}	5.86 ± 1.15^{ab}	7.46 ± 2.04^{b}	3.38 ± 1.38^{a}
896.7700	TAG 16:0/18:1/20:5	$[M+NH_4]^+$	1.18 ± 0.49^{a}	1.87 ± 0.80^{ab}	1.92 ± 0.32^{ab}	0.91 ± 0.20^{a}
922.7840	TAG 16:0/18:1/22:6	$[M+NH_4]^+$	1.08 ± 0.75^{a}	2.00 ± 0.98^{ab}	3.09 ± 1.12^{b}	2.21 ± 1.46^{ab}
872.7674	TAG 16:0/18:2/18:2	$[M+NH_4]^+$	16.28 ± 2.52	23.78 ± 9.95	23.76 ± 10.19	22.19 ± 6.67
902.8143	TAG 18:0/18:1/18:2	$[M+NH_4]^+$	8.49 ± 4.77	10.98 ± 3.28	13.68 ± 5.59	5.64 ± 4.50
902.8143	TAG 18:1/18:1/18:1	$[M+NH_4]^+$	30.96 ± 10.20	33.26 ± 9.98	39.34 ± 14.90	34.55 ± 28.91
900.7988	TAG 18:1/18:1/18:2	$[M+NH_4]^+$	38.39 ± 11.01	46.12 ± 16.80	48.56 ± 15.67	51.98 ± 25.75
898.7857	TAG 18:1/18:2/18:2	$[M+NH_4]^+$	6.72 ± 2.60	11.58 ± 7.08	10.37 ± 5.19	12.61 ± 6.30
Total TAG measured			**431.28 ± 240.72**	**491.87 ± 164.07**	**544.40 ± 187.52**	**413.68 ± 136.89**
668.6340	CE 18:1	$[M+NH_4]^+$	3.18 ± 0.73	3.30 ± 1.16	3.49 ± 1.22	4.97 ± 1.64
666.6185	CE 18:2	$[M+NH_4]^+$	22.76 ± 3.29	23.47 ± 5.12	26.27 ± 7.52	30.09 ± 8.45
690.6186	CE 20:4	$[M+NH_4]^+$	5.57 ± 2.60	4.08 ± 1.61	3.90 ± 1.10	4.30 ± 1.13
688.6029	CE 20:5	$[M+NH_4]^+$	0.11 ± 0.06^{a}	0.28 ± 0.20^{ab}	0.65 ± 0.38^{ab}	0.84 ± 0.57^{b}
714.6175	CE 22:6	$[M+NH_4]^+$	0.30 ± 0.12	0.47 ± 0.19	0.58 ± 0.20	0.33 ± 0.12
Total CE measured			**31.93 ± 5.77**	**31.61 ± 8.02**	**34.89 ± 9.90**	**40.53 ± 11.73**

Mass-to-charge ratio (*m/z*); Phosphatidylcholine (PC); Phosphatidylethanolamine (PE); Phosphatidylserine (PS); Triacylglycerol (TAG); Cholesteryl ester (CE); Highly unsaturated fatty acid (HUFA). Superscript differences highlight significantly different values after one-way ANOVA + Tukey HSD post-hoc test with $p < 0.05$.

Table 7. Concentration of EPA and DHA in Whole Blood, Plasma Phospholipids and Erythrocytes over 8 weeks of Omega-3 HUFA Supplementation (n = 20)

Blood Fraction	Fatty Acid	Baseline	Week 4	Week 8
Whole Blood	EPA	0.80 ± 0.36^{a}	1.64 ± 0.43^{b}	2.68 ± 0.58^{c}
(*μg fatty acid/100μL blood*)	DHA	3.95 ± 0.75^{a}	5.39 ± 1.05^{b}	6.88 ± 1.26^{c}
Plasma Phospholipids	EPA	0.72 ± 0.41^{a}	1.22 ± 0.27^{b}	2.09 ± 0.68^{c}
(*μg fatty acid/100μL plasma*)	DHA	3.37 ± 0.70^{a}	3.75 ± 0.75^{ab}	4.28 ± 0.86^{b}
Erythrocytes	EPA	1.89 ± 0.65^{a}	2.46 ± 0.59^{a}	3.98 ± 1.00^{b}
(*μg fatty acid/200mg cells*)	DHA	13.61 ± 2.76	13.58 ± 3.35	15.08 ± 2.73

Eicosapentaenoic acid (EPA); Docosahexaenoic acid (DHA); Highly Unsaturated Fatty Acid (HUFA).

Table 8. Concentration of EPA and DHA in Whole Blood, Plasma Phospholipids and Erythrocytes over 12 weeks of Omega-3 HUFA Supplementation (n = 5)

Blood Fraction	Fatty Acid	Baseline	Week 4	Week 8	Week 12
Whole Blood	EPA	0.89 ± 0.31^{a}	1.74 ± 0.48^{ab}	2.71 ± 0.87^{bc}	4.11 ± 1.21^{c}
(*μg fatty acid/100μL blood*)	DHA	4.25 ± 0.90^{a}	5.37 ± 0.73^{ab}	6.16 ± 1.52^{ab}	7.33 ± 1.11^{b}
Plasma Phospholipids	EPA	0.77 ± 0.42^{a}	1.19 ± 0.40^{ab}	2.51 ± 1.17^{bc}	2.81 ± 1.03^{c}
(*μg fatty acid/100μL plasma*)	DHA	3.21 ± 1.07	3.83 ± 1.02	4.28 ± 1.59	5.37 ± 1.39
Erythrocytes	EPA	1.72 ± 0.40^{a}	2.21 ± 0.32^{ab}	3.35 ± 0.87^{b}	5.21 ± 0.84^{c}
(*μg fatty acid/200mg cells*)	DHA	11.86 ± 2.34^{ab}	11.20 ± 1.82^{a}	13.12 ± 2.29^{ab}	15.29 ± 1.44^{b}

Eicosapentaenoic acid (EPA); Docosahexaenoic acid (DHA); Highly Unsaturated Fatty Acid (HUFA).

Table 9. ***Fatty Acid Composition of Blood Phosphatidylethanolamines (n = 3)***

	Concentration (*μg fatty acid/100 μL whole blood*)			
Fatty Acid	**Baseline**	**Wk4**	**Wk8**	**Wk12**
C 14:0	0.44 ± 0.16	0.40 ± 0.09	0.23 ± 0.08	0.56 ± 0.37
C 16:0	5.55 ± 0.92	5.32 ± 0.81	4.81 ± 0.37	4.97 ± 0.70
C 18:0	5.95 ± 0.91	5.67 ± 1.42	5.71 ± 0.26	4.74 ± 0.99
C 20:0	0.10 ± 0.01	0.11 ± 0.01	0.09 ± 0.01	0.19 ± 0.22
C 22:0	0.06 ± 0.01	0.06 ± 0.01	0.06 ± <0.01	0.12 ± 0.11
C 24:0	0.07 ± 0.02	0.08 ± 0.01	0.07 ± 0.02	0.17 ± 0.11
SFAs	**12.26 ± 1.93**	**11.87 ± 2.02**	**11.02 ± 0.20**	**10.89 ± 1.49**
C 12:1	<0.01 ± <0.01	0.03 ± 0.03	0.01 ± 0.01	0.03 ± 0.02
C 14:1	0.02 ± 0.01	0.03 ± 0.01	0.02 ± 0.02	0.09 ± 0.05
C 16:1	0.13 ± 0.06	0.19 ± 0.11	0.11 ± 0.06	0.34 ± 0.34
C 18:1n-7	0.38 ± 0.09	0.37 ± 0.09	0.29 ± 0.04	0.41 ± 0.15
C 18:1n-9	5.30 ± 1.62	4.63 ± 0.37	3.47 ± 0.49	3.79 ± 0.71
C 20:1n-9	0.13 ± 0.02	0.13 ± 0.02	0.11 ± 0.01	0.18 ± 0.09
C 22:1n-9	0.61 ± 0.06	0.59 ± 0.08	0.58 ± 0.03	0.82 ± 0.54
C 24:1n-9	0.06 ± 0.02	0.05 ± 0.02	0.06 ± 0.02	0.06 ± 0.02
MUFAs	**6.63 ± 1.67**	**6.01 ± 0.40**	**4.64 ± 0.52**	**5.70 ± 1.76**
C 18:2n-6	1.46 ± 0.35	1.24 ± 0.10	1.20 ± 0.18	1.71 ± 0.95
C 18:3n-6	0.03 ± <0.01	0.02 ± 0.01	0.02 ± <0.01	0.04 ± 0.03
C 20:2n-6	0.07 ± 0.02	0.08 ± 0.01	0.07 ± <0.01	0.10 ± 0.03
C 20:3n-6	0.26 ± 0.10	0.25 ± 0.04	0.26 ± 0.07	0.26 ± 0.07
C 20:4n-6	4.18 ± 0.75	4.23 ± 0.73	4.25 ± 0.65	4.02 ± 0.28
C 22:2n-6	0.05 ± <0.01	0.06 ± 0.02	0.04 ± <0.01	0.08 ± 0.04
C 22:4n-6	1.20 ± 0.11	1.20 ± 0.21	1.12 ± 0.07	1.04 ± 0.14
C 22:5n-6	0.17 ± 0.07	0.18 ± 0.03	0.16 ± 0.05	0.14 ± 0.02
N-6	**7.43 ± 1.24**	**7.26 ± 0.95**	**7.12 ± 0.87**	**7.38 ± 1.02**
C 18:3n-3	0.14 ± 0.04	0.15 ± 0.04	0.15 ± 0.01	0.17 ± 0.09
C 20:3n-3	0.01 ± 0.01	0.03 ± 0.01	0.03 ± 0.01	0.05 ± 0.03
C 20:5n-3	0.12 ± 0.07[a]	0.18 ± 0.05[a]	0.27 ± 0.05[a]	0.45 ± 0.08[b]
C 22:5n-3	0.62 ± 0.15[a]	0.68 ± 0.05[ab]	0.74 ± 0.05[ab]	0.84 ± 0.04[b]
C 22:6n-3	0.82 ± 0.30	0.89 ± 0.19	1.02 ± 0.24	1.24 ± 0.20
N-3	**1.71 ± 0.54[a]**	**1.93 ± 0.31[ab]**	**2.20 ± 0.35[ab]**	**2.75 ± 0.31[b]**
C 20:3n-9	0.03 ± 0.01	0.03 ± 0.01	0.02 ± 0.01	0.03 ± 0.01
PUFAs	**9.17 ± 1.79**	**9.21 ± 1.22**	**9.35 ± 1.21**	**10.17 ± 1.28**
HUFAs	**7.42 ± 1.40**	**7.66 ± 1.08**	**7.87 ± 1.03**	**8.08 ± 0.53**
EPA+DHA	**0.94 ± 0.36**	**1.07 ± 0.24**	**1.29 ± 0.30**	**1.69 ± 0.27**
Total	**28.06 ± 3.31**	**27.09 ± 2.81**	**25.01 ± 1.62**	**26.76 ± 4.01**

Saturated fatty acids (SFAs); Mono-unsaturated fatty acids (MUFAs); Omega-6 fatty acids (N-6); Omega-3 fatty acids (N-3); Polyunsaturated fatty acids (PUFAs); Highly unsaturated fatty acids (HUFAs); Eicosapentaenoic acid (EPA); Docosahexaenoic acid (DHA). Superscript differences represent significantly different values after one-way ANOVA + Tukey HSD ($p < 0.05$).

Chapter 9

Lipidomic Discrimination of Complex Lipids in Whole Blood, Plasma and Erythrocytes of Individuals with Low, Intermediate and High Levels of Omega-3 HUFA Intake

9.1 *Introduction*

Lipidomic analyses of blood lipids and the response to omega-3 PUFA intervention have been examined (Patterson et al., 2014; Uhl et al., 2013), but a comprehensive assessment of plasma, erythrocyte and whole blood across individuals with different omega-3 HUFA status is needed. This is required as changes in response to dietary EPA and DHA are more rapid in plasma compared with erythrocytes, and DHA is slower to change than EPA (Metherel et al., 2009; Patterson et al., 2012). The experiments in this chapter will expand on the examination of whole blood complex lipids that was carried out in Chapter 8, using the UHPLC-MS/MS acyl-specific lipidomic profiling method developed in Chapter 5 to profile the whole blood, plasma and erythrocyte fractions of individuals across a range of omega-3 HUFA intakes.

9.2 *Methods*

9.2.1 *Participants and Blood Samples*

Volunteer participants were recruited from the University of Waterloo. An initial screening visit was performed where participants were asked about their consumption of fish, nutraceuticals containing EPA/DHA, or EPA/DHA-enriched foods. Initially, approximately 15 volunteers attended this screening visit, and nine of them were asked to participate in the study based on their verbally reported consumption of EPA/DHA. Specifically, three of these

participants reported consuming either very little or no EPA/DHA-containing foods or supplements; three reported sporadic consumption of fish once or twice every two weeks; and three reported either high consumption of fish (more than twice per week) or regular consumption of EPA/DHA supplements. Five males and four females were recruited for this study; their anthropometric measures were assessed (Table 10). A single fasting venous blood sample was collected into one-10 mL EDTA-lined vacutainer by a phlebotomist at the volunteer's convenience and all samples were collected within one week. After collection, three 500 µL whole blood aliquots were separated and stored in cryovials at -80ºC until analysis. The remainder of the blood was separated into plasma and erythrocyte fractions by centrifugation at 1734 *rcf* as described earlier (Patterson et al., 2013). Plasma and erythrocytes were separated into three 500 µL aliquots in cryovials and also stored at -80ºC until analysis. All participants provided informed written consent and the University of Waterloo Human Ethics Committee approved all protocols and procedures.

9.2.2 *Lipidomic and Fatty Acid Profiling Methods*

Briefly, samples were removed from -80ºC storage, thawed, extracted twice using 2:1 chloroform:methanol (v/v), and aliquoted for UHPLC-MS/MS or for derivatization to fatty acid methyl esters followed by GC-FID (only whole blood was used for fatty acid composition determinations). The lipidomic sample lipid extracts were spiked with di-17:0 PC in the HPLC sample solvent. The 47-minute multi-step gradient as described in Chapter 5 was used with positive ESI and Top5 data-dependent acquisition. Only the ion profiles for complex lipids containing either omega-3 or omega-6 HUFAs were extracted and the peaks were integrated. As in previous chapters, the raw integrated data (area under the curve) were standardized by

dividing them by the area under the curve for the internal standard (di-17:0 PC) and multiplying by 100. The whole blood lipid extract aliquot that was separated for fatty acid composition was dried under a stream of N_2 gas, and fatty acid methyl esters were generated after methylation in 1 mL 14% BF_3 in methanol at 100ºC (Metherel et al., 2009). Samples were then analyzed via GC-FID. C 22:3n-3 was used as the internal standard (Nu-Check Prep, Elysian, MN, USA).

9.2.3 *Statistical Analyses*

The normalized lipidomic data (A.U.) for the lipids examined (complete list in Table E.1, Appendix E) was correlated with whole blood total DHA concentration and whole blood total EPA concentration using Pearson's correlation. The resulting correlation coefficients were sorted in decreasing order, and the correlations with the top 5 *r*-values (that ranged from 0.76 to 0.99 and *p* value of < 0.01) were used to create scatterplots.

9.3 *Results*

The lipidomic examination of complex lipids in whole blood, plasma and erythrocytes revealed that the plasma fraction is rich in PC, CE and TAG; the erythrocyte fraction is rich in PC, PE, plasmenyl-PE and PS; and whole blood is comprehensive of all these lipids (Figure 10). The correlation analyses that were performed and the resulting scatterplots of the top 5 most strongly correlated complex lipids with total DHA and EPA in whole blood are shown in Figure 11. In each of the scatterplots, the slopes of the lines of best fit have been included to highlight the complex lipids where EPA and DHA appear to be localized with increasing EPA and DHA status. The slopes of the lines for lipids that were previously identified as highly responsive to EPA+DHA intake in Chapter 8 are less steep in the erythrocyte lipidomics vs. DHA and EPA

scatterplots compared to the plasma lipidomics vs. DHA and EPA scatterplots. The best fit lines for scatterplots of total DHA concentration in whole blood against 16:0/DHA PC and 16:0/EPA PC in blood fractions have the steepest slopes across whole blood (15.51, 17.77; respectively), plasma (24.66, 15.68; respectively) and erythrocytes (2.97, 4.03; respectively) compared to all other PC species. Interestingly, some of the complex lipids that correlated the most strongly with total DHA in whole blood did not have DHA in them, but rather EPA or in one case, a negative association with docosatetraenoic acid (C22:4n-6; erythrocyte lipidomics scatterplot). Likewise, some DHA-containing complex lipids like 18:0/DHA PC were found to be strongly correlated with total EPA in whole blood. These relationships highlight the close interplay between EPA and DHA in metabolism and incorporation into complex lipids.

9.4 *Discussion and Conclusion*

Three acyl-specific lipids, 16:0/DHA PC, 16:0/EPA PC and plasmenyl-PE P-16:0/EPA were identified as being highly responsive to the dietary manipulation in a dose-response manner in Chapter 8. In addition, previous findings in our laboratory suggest a slower turnover of omega-3 HUFA in erythrocytes as compared with plasma (Metherel et al., 2009; Patterson et al., 2012). , The present study examined the lipidomic profiles of HUFA-containing complex lipids in whole blood, plasma and erythrocytes from nine individuals that reported consuming various levels of fish, EPA/DHA-enriched foods, or EPA/DHA-containing supplements. Rather than rely on dietary records or food frequency questionnaires, which is subject to error (Patterson et al., 2012), the absolute concentrations of EPA and DHA in whole blood were determined to indicate omega-3 status and correlated with lipidomic data. This was done to examine acyl-specific complex lipids where EPA and DHA may be localized when total concentrations of EPA and

DHA are increased in blood. Notably, the experiments performed here revealed that 16:0/DHA PC and 16:0/EPA PC appear to preferentially incorporate and retain DHA and EPA compared to other PC species in both plasma and erythrocyte fractions, as total DHA and EPA concentrations increase in whole blood.

To our knowledge, this study is the first to examine a range of intakes of EPA and DHA through fatty acid compositional data (derived from GC-FID) and examinations of acyl-containing complex lipids (through UHPLC-MS/MS) at the same time to identify the specific acyl-specific complex lipids across blood fractions that were the most responsive to increasing concentrations of DHA and EPA in whole blood. Although whole blood biomarkers have been previously identified and reflect dietary intake of EPA+DHA (Patterson et al., 2012) no direct associations can be made at this point regarding specific amounts of EPA and DHA that were consumed by the participants and the lipidomic responses in blood fractions. One of the limitations of this study is that the data is cross sectional and insights on incorporation are limited to static time points and *rate of change* and *kinetic turnover* cannot be discussed. Additionally, the use of a single PC internal standard (di-17:0 PC) prevents direct comparisons to be made between different lipid pools (i.e. comparing the slopes of the lines for 16:0/DHA PC vs. 16:0/DHA PE in a given blood fraction). Future research should examine the effect of tightly-controlled intakes of EPA+DHA in acyl-specific lipids in blood fractions, as well as examining dose-responsive lipids over an extended period of time. Further work is also necessary to shift this semi-quantitative method to a quantitative lipidomics method, possibly through the use of multiple internal standards.

In conclusion, it appears that 16:0/DHA PC and 16:0/EPA PC are the most abundant DHA- and EPA-containing PC species (respectively) across all blood fractions. It also appears

16:0/DHA PC and 16:0/EPA PC to be very responsive in plasma compared to erythrocytes, and seem to increase the most as DHA and EPA increase in the diet as determined by levels of DHA and EPA in whole blood. This work provides the foundation for the potential use of acyl-specific complex lipids as biomarkers for omega-3 HUFA status.

Table 10. ***Anthropometric Measures for the Nine Participants of the Blood Fraction Lipidomics Study***

	Males (n = 5)	Females (n = 4)
Anthropometric Measures	**Average ± Standard Deviation**	
Age (years)	22.75 ± 1.53	23.47 ± 6.07
Height (cm)	177.88 ± 5.57	167.93 ± 7.04
Mass (kg)	80.58 ± 16.17	63.08 ± 7.04

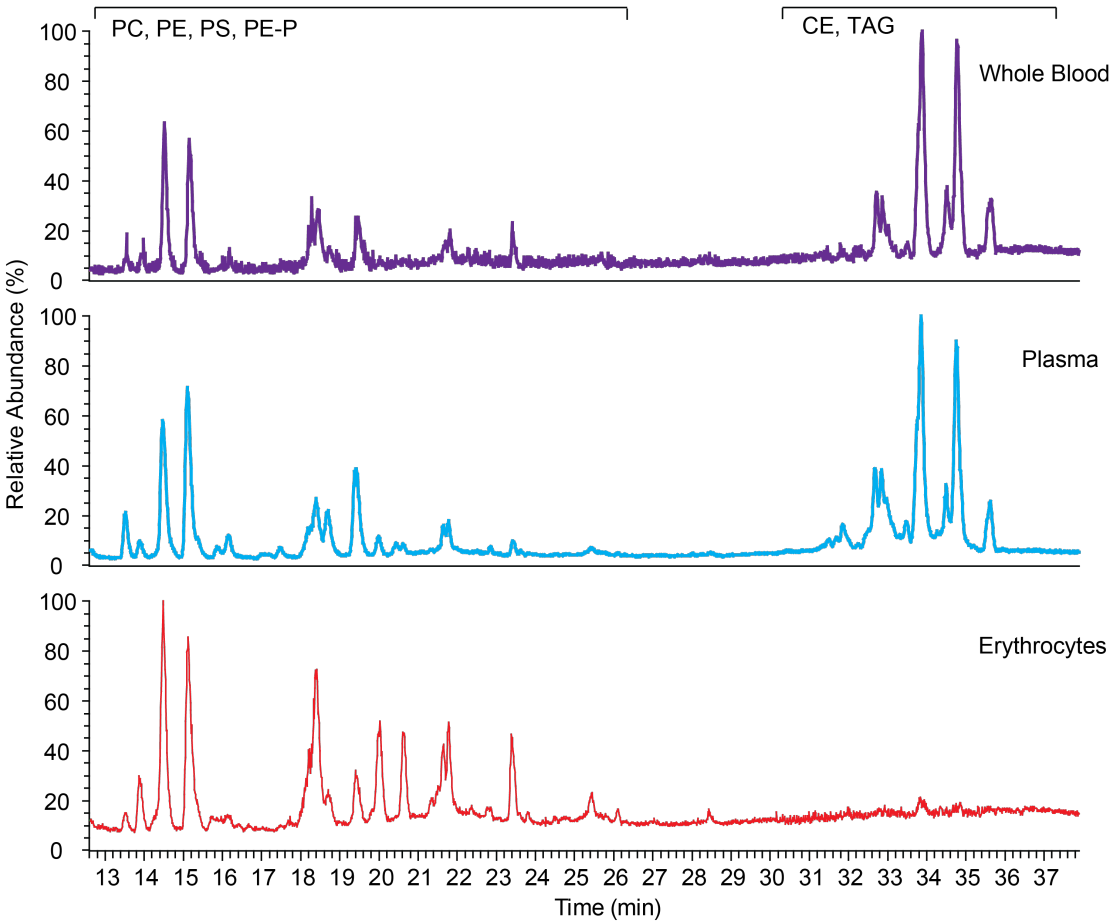

Figure 10. Whole blood, plasma and erythrocyte total ion current (TIC) full-scan MS chromatograms. Phosphatidylcholine (PC); Phosphatidylethanolamine (PE); Phosphatidylserine (PS); Plasmenyl-Phosphatidylethanolamine (PE-P); Cholesteryl ester (CE); Triacylglycerol (TAG).

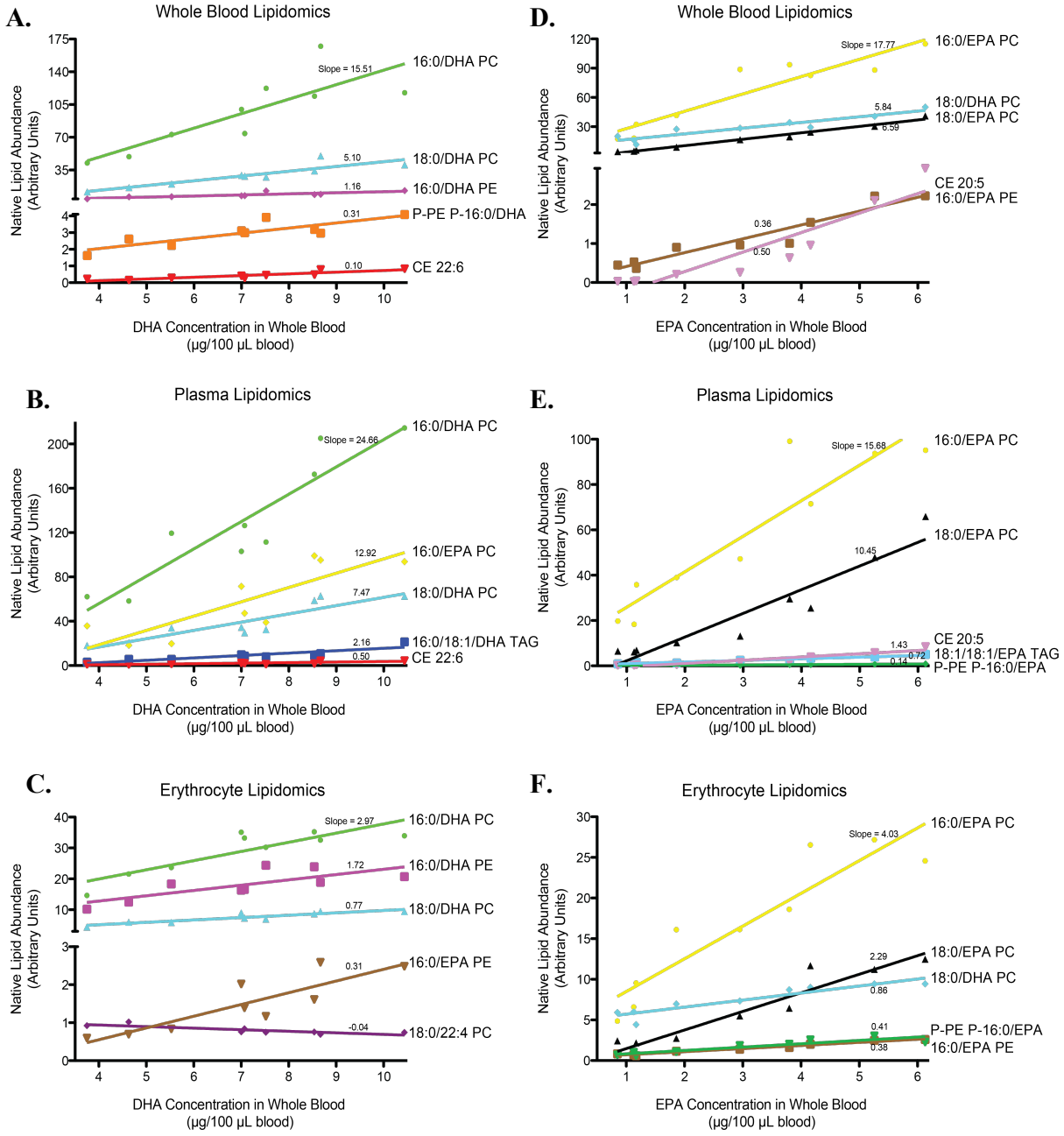

Figure 11. Scatterplots of the acyl-specific HUFA-containing lipids that were correlated the most strongly with either total DHA (left) or EPA (right) concentrations in whole blood determined by GC-FID. **A.** Whole lipidomics vs. DHA concentration in whole blood **B.** Plasma lipidomics vs. DHA concentration in whole blood **C.** Erythrocyte lipidomics vs. DHA concentration in whole blood **D.** Whole lipidomics vs. EPA concentration in whole blood **E.** Plasma lipidomics vs. EPA concentration in whole blood **F.** Erythrocyte lipidomics vs. EPA concentration in whole blood. Phosphatidylcholine (PC); Phosphatidylethanolamine (PE); Phosphatidylserine (PS); Plasmenyl-Phosphatidylethanolamine (PE-P); Cholesteryl ester (CE); Triacylglycerol (TAG).

Chapter 10

Discussion and Conclusion

10.1 *General Discussion*

Previous studies have characterized the lipidomes of cellular systems (Bird et al., 2011; Hermansson et al., 2005; Ramanadham et al., 2000) and mammalian tissues (Lamaziere et al., 2011; Murthy et al., 2002; Sandra et al., 2010; Sjövall et al., 2015). Though some of this work has examined the lipid remodeling effects of omega-3 highly unsaturated fatty acid supplementation, little work has been done on blood. This thesis presents a thorough examination of human blood native lipids following omega-3 HUFA supplementation, while outlining all of the steps and limitations associated with the development of a UHPLC-MS/MS lipidomic profiling method.

In line with the stated hypotheses (Chapter 4), a method was developed to detect acyl species of PC, PE, PS, CE, and TAG in positive ESI mode. The method ended up being UHPLC-MS/MS rather than HPLC-MS/MS, and determination of PI, FFA, and CL were not possible. The relationship between increasing concentrations of lipids from blood lipid extracts and the observed instrument response was confirmed to be positive and linear at the sample dilutions tested. The lipidomic profiles of whole and dried blood spots provided comparable lipid abundances when dried blood spot lipid extraction was extended to a 24-hour protocol, with the exception of persistent low PS recoveries. Increasing EPA and DHA intakes were positively associated with increasing EPA and DHA in several but not all acyl species of lipids, as changes in PS were not observed. Finally, 16:0/DHA PC was highly responsive to DHA supplementation, however, other acyl specific species responsive to fish oil intervention were also identified.

Although there are several limitations associated with the current lipidomic profiling method that are highlighted in Chapters 5 and 6, its use enabled the validation of dried blood spots for lipidomic profiling, and the characterization of lipid remodeling events in acyl-specific complex lipids following supplementation of EPA and DHA. While some work is necessary in order to fully validate the use of dried blood spots for lipidomic profiling, the present observations show that the analysis of PC, PE, TAG and CE species in a single analytical run is possible. In dried blood spots, the significantly decreased recoveries of PS species needs to be examined further, and modifications to the mass spectrometric method are needed in order to examine PI and FFA species. Using blood samples that were collected under tight dietary control of EPA+DHA intake, three specific whole blood lipids (16:0/DHA PC, 16:0/EPA PC and plasmenyl-PE P-16:0/EPA) that are very responsive to supplementation in a dose-dependent manner were identified. Additionally, 16:0/DHA PC and 16:0/EPA PC were shown to have the steepest slopes when correlated against omega-3 HUFA status across the whole blood, erythrocytes, and plasma fractions. Therefore, 16:0/DHA PC and 16:0/EPA PC have potential to be developed into biomarkers of omega-3 HUFA intake. However further work with short term and long term omega-3 HUFA interventions are needed to confirm the 16:0/DHA PC and 16:0/EPA PC response, but also screen for other informative acyl specific lipids. Biomarkers for recent vs. long term omega-3 HUFA would be useful in observational studies, as well as determining adherence and compliance to omega-3 HUFA intervention in clinical trials. Also, by identifying specific acyl lipids and their unique chemistry, alternative methodology could be developed that provide rapid and cost efficient results required for clinical screening.

Due to the tens of thousands of lipids that can be detected in a biological system using MS (Han and Gross, 2003), and the painstaking steps of the current workflow for lipid

identification and integration, it was neither practical nor productive to characterize the entire lipidome of the samples that were examined in this thesis. The focus on the characterization of the top 85% of lipids in whole blood (Chapter 8) may serve as the basis for future untargeted lipidomic analyses of other whole blood samples. This approach could be automated into software and greatly increase the analytical throughput by minimizing the current challenge of data processing. In particular, using a top 85% approach to identify lipids combined with a set of internal standards that enabled comprehensive quantitation would be a breakthrough in lipidomic data processing. Further work is necessary to establish quantitative lipidomic profiling methods (i.e. internal standards) and comprehensive lipid class determinations in a single analytical run (i.e. challenge of detecting PI and FFA in positive ESI) using UHPLC-MS/MS. The use of thin layer chromatography/ GC-FID data to control for day-to-day UHPLC-MS/MS variation may have potential in the development and assessment of a quantitative lipidomic method as lipidomic data could be expressed relative to quantified lipid classes. Additional work is also required to ensure lipid extraction techniques are comprehensive across lipid classes (i.e. low PS recovery from dried blood spot sampling matrix).

10.2 *Conclusion*

A comprehensive lipidomic profiling method was developed for the analysis of acyl-specific complex lipids in human whole blood. Over 500 lipids were identified based on accurate masses of parent lipid species, and confirming acyl-specific species was achieved for 163 of these lipids. Through this method, the use of dried blood spots was validated for lipidomic profiling of PC, PE, CE and TAG. Additionally, the current UHPLC-MS/MS method was used to examine the lipidomic changes that occur in human whole blood following very specific

intakes of EPA+DHA from samples of a previous intervention trial (Patterson, 2012). 16:0/DHA PC and 16:0/EPA PC appear to have potential as omega-3 HUFA biomarkers. In addition, novel techniques in quantitation and data processing were explored at the preliminary level that included GC-FID quantitative corrections and a top 85% lipid identification approach. The extrapolation of the current lipidomic profiling method for analysis of other biological samples is possible; additional work is needed to establish appropriate instrument conditions, as these would be tailored specifically for the sample of interest.

References

Albert CM, Campos H, Stampfer MJ, Ridker PM, Manson JE, Willett WC, Ma J. Blood levels of long-chain n-3 fatty acids and the risk of sudden death. N Engl J Med. 2002 Apr 11;346(15):1113-8. PubMed PMID: 11948270.

Arita M. Mediator lipidomics in acute inflammation and resolution. J Biochem. 2012 Oct;152(4):313-9. Epub 2012 Aug 24. Review. PubMed PMID: 22923733.

Armstrong JM, Metherel AH, Stark KD. Direct microwave transesterification of fingertip prick blood samples for fatty acid determinations. Lipids. 2008 Feb;43(2):187-96. Epub 2007 Dec 15. PubMed PMID: 18084783.

Ausloos P, Clifton CL, Lias SG, Mikaya AI, Stein SE, Tchekhovskoi DV, Sparkman OD, Zaikin V, Zhu D. The critical evaluation of a comprehensive mass spectral library. J Am Soc Mass Spectrom. 1999 Apr;10(4):287-99. Erratum in: J Am Soc Mass Spectrom 1999 Jun;10(6):565. PubMed PMID: 10197350.

Banerjee S, Mazumdar S. Electrospray ionization mass spectrometry: a technique to access the information beyond the molecular weight of the analyte. Int J Anal Chem. 2012;2012:282574. doi: 10.1155/2012/282574. Epub 2011 Dec 15. PubMed PMID: 22611397; PubMed Central PMCID: PMC3348530.

Baylin A, Kim MK, Donovan-Palmer A, Siles X, Dougherty L, Tocco P, Campos H. Fasting whole blood as a biomarker of essential fatty acid intake in epidemiologic studies: comparison with adipose tissue and plasma. Am J Epidemiol. 2005 Aug 15;162(4):373-81. Epub 2005 Jul 13. PubMed PMID: 16014782.

Bird SS, Marur VR, Sniatynski MJ, Greenberg HK, Kristal BS. Lipidomics profiling by high-resolution LC-MS and high-energy collisional dissociation fragmentation: focus on

characterization of mitochondrial cardiolipins and monolysocardiolipins. Anal Chem. 2011 Feb 1;83(3):940-9. doi: 10.1021/ac102598u. Epub 2010 Dec 30. PubMed PMID: 21192696; PubMed Central PMCID: PMC3031668.

Bird SS, Stavrovskaya IG, Gathungu RM, Tousi F, Kristal BS. Qualitative characterization of the rat liver mitochondrial lipidome using all ion fragmentation on an Exactive benchtop Orbitrap MS. Methods Mol Biol. 2015;1264:441-52. doi: 10.1007/978-1-4939-2257-4_36. PubMed PMID: 25631033.

Bligh EG, Dyer WJ. A rapid method of total lipid extraction and purification. Can J Biochem Physiol. 1959 Aug;37(8):911-7. PubMed PMID: 13671378.

Browning LM, Walker CG, Mander AP, West AL, Madden J, Gambell JM, Young S, Wang L, Jebb SA, Calder PC. Incorporation of eicosapentaenoic and docosahexaenoic acids into lipid pools when given as supplements providing doses equivalent to typical intakes of oily fish. Am J Clin Nutr. 2012 Oct;96(4):748-58. Epub 2012 Aug 29. PubMed PMID: 22932281; PubMed Central PMCID: PMC3441107.

Buré C, Ayciriex S, Testet E, Schmitter JM. A single run LC-MS/MS method for phospholipidomics. Anal Bioanal Chem. 2013 Jan;405(1):203-13. doi: 10.1007/s00216-012-6466-9. Epub 2012 Oct 13. PubMed PMID: 23064709.

Byrdwell WC. The Updated Bottom Up Solution applied to mass spectrometry of soybean oil in a dietary supplement gelcap. Anal Bioanal Chem. 2015 Jul;407(17):5143-60. doi: 10.1007/s00216-015-8590-9. Epub 2015 Apr 9. PubMed PMID: 25855147.

Byrdwell WC. The Updated Bottom-Up Solution: Using Critical Ratios for Triacylglycerol Structural Analysis by Mass Spectrometry. The 106th Annual American Oil Chemists' Society Meeting. Rosen Shingle Creek, Orlando, FL, May 3 – 6, 2015.

Byrdwell WC. "Dilute-and-shoot" triple parallel mass spectrometry method for analysis of vitamin D and triacylglycerols in dietary supplements. Anal Bioanal Chem. 2011 Dec;401(10):3317-34. doi: 10.1007/s00216-011-5406-4. Epub 2011 Oct 2. PubMed PMID: 21964772.

Careri M. Advances in analytical mass spectrometry. Anal Bioanal Chem. 2011 Mar;399(8):2583-4. doi: 10.1007/s00216-010-4630-7. PubMed PMID: 21221539.

Cassiday L. Lipidomics comes of age. AOCS Inform Magazine. February 2014. 113-119.

Chowdhury R, Warnakula S, Kunutsor S, Crowe F, Ward HA, Johnson L, Franco OH, Butterworth AS, Forouhi NG, Thompson SG, Khaw KT, Mozaffarian D, Danesh J, Di Angelantonio E. Association of dietary, circulating, and supplement fatty acids with coronary risk: a systematic review and meta-analysis. Ann Intern Med. 2014 Mar 18;160(6):398-406. doi: 10.7326/M13-1788. Review. Erratum in: Ann Intern Med. 2014 May 6;160(9):658. PubMed PMID: 24723079.

de Oliveira Otto MC, Wu JH, Baylin A, Vaidya D, Rich SS, Tsai MY, Jacobs DR Jr, Mozaffarian D. Circulating and dietary omega-3 and omega-6 polyunsaturated fatty acids and incidence of CVD in the Multi-Ethnic Study of Atherosclerosis. J Am Heart Assoc. 2013 Dec 18;2(6):e000506. doi: 10.1161/JAHA.113.000506. PubMed PMID: 24351702; PubMed Central PMCID: PMC3886748.

Dagan S, Amirav A. Electron impact mass spectrometry of alkanes in supersonic molecular beams. J Am Soc Mass Spectrom. 1995 Feb;6(2):120-31. doi: 10.1016/S1044-0305(94)00095-H. PubMed PMID: 24222074.

De Vriese SR, Dhont M, Christophe AB. FA composition of cholesteryl esters and phospholipids in maternal plasma during pregnancy and at delivery and in cord plasma at birth. Lipids. 2003 Jan;38(1):1-7. PubMed PMID: 12669812.

Di Girolamo F, Lante I, Muraca M, Putignani L. The Role of Mass Spectrometry in the "Omics" Era. Curr Org Chem. 2013 Dec;17(23):2891-2905. PubMed PMID: 24376367; PubMed Central PMCID: PMC3873040.

Doull IJ, Ryley HC, Weller P, Goodchild MC. Cystic fibrosis-related deaths in infancy and the effect of newborn screening. Pediatr Pulmonol. 2001 May;31(5):363-6. PubMed PMID: 11340682.

Dyerberg J, Bang HO. Lipid metabolism, atherogenesis, and haemostasis in Eskimos: the role of the prostaglandin-3 family. Haemostasis. 1979;8(3-5):227-33. PubMed PMID: 511010.

Eliuk S, Makarov A. Evolution of Orbitrap Mass Spectrometry Instrumentation. Annu Rev Anal Chem (Palo Alto Calif). 2015 Jul 22;8(1):61-80. doi: 10.1146/annurev-anchem-071114-040325. PubMed PMID: 26161972.

Ellis DI, Dunn WB, Griffin JL, Allwood JW, Goodacre R. Metabolic fingerprinting as a diagnostic tool. Pharmacogenomics. 2007 Sep;8(9):1243-66. Review. PubMed PMID: 17924839.

Enriquez-Algeciras M, Bhattacharya SK. Lipidomic mass spectrometry and its application in neuroscience. World J Biol Chem. 2013 Nov 26;4(4):102-110. Review. PubMed PMID: 24340133; PubMed Central PMCID: PMC3856305.

Fahy E, Subramaniam S, Brown HA, Glass CK, Merrill AH Jr, Murphy RC, Raetz CR, Russell DW, Seyama Y, Shaw W, Shimizu T, Spener F, van Meer G, VanNieuwenhze MS, White SH, Witztum JL, Dennis EA. A comprehensive classification system for lipids. J Lipid Res.

2005 May;46(5):839-61. Epub 2005 Feb 16. Review. Erratum in: J Lipid Res. 2010 Jun;51(6):1618. PubMed PMID: 15722563.

Fahy E, Subramaniam S, Murphy RC, Nishijima M, Raetz CR, Shimizu T, Spener F, van Meer G, Wakelam MJ, Dennis EA. Update of the LIPID MAPS comprehensive classification system for lipids. J Lipid Res. 2009 Apr;50 Suppl:S9-14. doi: 10.1194/jlr.R800095-JLR200. Epub 2008 Dec 19. Review. PubMed PMID: 19098281; PubMed Central PMCID: PMC2674711.

Ferreri C, Chatgilialoglu C. Role of fatty acid-based functional lipidomics in the development of molecular diagnostic tools. Expert Rev Mol Diagn. 2012 Sep;12(7):767-80. doi: 10.1586/erm.12.73. Review. PubMed PMID: 23153242.

Firl N, Kienberger H, Hauser T, Rychlik M. Determination of the fatty acid profile of neutral lipids, free fatty acids and phospholipids in human plasma. Clin Chem Lab Med. 2013 Apr;51(4):799-810. PubMed PMID: 23006900.

Folch J. The chemical structure of phospatidyl serine. J Biol Chem. 1948 Jun;174(2):439-50. PubMed PMID: 18865612.

Folch J, Lees M, Sloane Stanley GH. A simple method for the isolation and purification of total lipides from animal tissues. J Biol Chem. 1957 May;226(1):497-509. PubMed PMID: 13428781.

Forcisi S, Moritz F, Kanawati B, Tziotis D, Lehmann R, Schmitt-Kopplin P. Liquid chromatography-mass spectrometry in metabolomics research: mass analyzers in ultra high pressure liquid chromatography coupling. J Chromatogr A. 2013 May 31;1292:51-65. doi: 10.1016/j.chroma.2013.04.017. Epub 2013 Apr 11. Review. PubMed PMID: 23631876.

Gama MR, Collins CH, Bottoli CB. Nano-liquid chromatography in pharmaceutical and biomedical research. J Chromatogr Sci. 2013 Aug;51(7):694-703. doi: 10.1093/chromsci/bmt023. Epub 2013 Apr 12. Review. PubMed PMID: 23585638.

Green A. Neonatal screening: current trends and quality control in the United Kingdom. Rinsho Byori. 1998 Mar;46(3):211-6. Review. PubMed PMID: 9564759.

Godzien J, Ciborowski M, Martínez-Alcázar MP, Samczuk P, Kretowski A, Barbas C. Rapid and Reliable Identification of Phospholipids for Untargeted Metabolomics with LC-ESI-QTOF-MS/MS. J Proteome Res. 2015 Jun 29. [Epub ahead of print] PubMed PMID: 26080858.

Goto-Inoue N, Hayasaka T, Zaima N, Setou M. Imaging mass spectrometry for lipidomics. Biochim Biophys Acta. 2011 Nov;1811(11):961-9. doi: 10.1016/j.bbalip.2011.03.004. Epub 2011 Mar 29. Review. PubMed PMID: 21440085.

Gohlke RS, McLafferty FW. Early gas chromatography/mass spectrometry. J Am Soc Mass Spectrom. 1993 May;4(5):367-71. doi: 10.1016/1044-0305(93)85001-E. PubMed PMID: 24234933.

Háková E, Vrkoslav V, Míková R, Schwarzová-Pecková K, Bosáková Z, Cvačka J. Localization of double bonds in triacylglycerols using high-performance liquid chromatography /atmospheric pressure chemical ionization ion-trap mass spectrometry. Anal Bioanal Chem. 2015 Jul;407(17):5175-88. doi: 10.1007/s00216-015-8537-1. Epub 2015 Feb 21. PubMed PMID: 25701424.

Han X. Neurolipidomics: challenges and developments. Front Biosci. 2007 Jan 1;12:2601-15. Review. PubMed PMID: 17127266; PubMed Central PMCID: PMC2141543.

Han X, Gross RW. Global analyses of cellular lipidomes directly from crude extracts of biological samples by ESI mass spectrometry: a bridge to lipidomics. J Lipid Res. 2003 Jun;44(6):1071-9. Epub 2003 Apr 1. Review. PubMed PMID: 12671038.

Hao Z, Zhang Y, Eliuk S, Blethrow J, Horn D, Zabrouskov V, Kellmann M, Huhmer A. A quadrupole-orbitrap hybrid mass spectrometer offers highest benchtop performance for in-depth analysis of complex proteomes. Thermo Scientific. Application Note 552. 2012.

Harris WS, Von Schacky C. The Omega-3 Index: a new risk factor for death from coronary heart disease? Prev Med. 2004 Jul;39(1):212-20. PubMed PMID: 15208005.

Harris WS, Dayspring TD, Moran TJ. Omega-3 fatty acids and cardiovascular disease: new developments and applications. Postgrad Med. 2013 Nov;125(6):100-13. doi: 10.3810/pgm.2013.11.2717. Review. PubMed PMID: 24200766.

Health Quality Ontario. Neonatal screening of inborn errors of metabolism using tandem mass spectrometry: an evidence-based analysis. Ont Health Technol Assess Ser. 2003;3(3):1-36. Epub 2003 May 1. PubMed PMID: 23074443; PubMed Central PMCID: PMC3387775.

Hermansson M, Uphoff A, Käkelä R, Somerharju P. Automated quantitative analysis of complex lipidomes by liquid chromatography/mass spectrometry. Anal Chem. 2005 Apr 1;77(7):2166-75. PubMed PMID: 15801751.

Ho CS, Lam CW, Chan MH, Cheung RC, Law LK, Lit LC, Ng KF, Suen MW, Tai HL. Electrospray ionisation mass spectrometry: principles and clinical applications. Clin Biochem Rev. 2003;24(1):3-12. PubMed PMID: 18568044; PubMed Central PMCID: PMC1853331.

Holub BJ, Swidinsky P, Park E. Oral docosapentaenoic acid (22:5n-3) is differentially incorporated into phospholipid pools and differentially metabolized to eicosapentaenoic acid

in tissues from young rats. Lipids. 2011 May;46(5):399-407. doi: 10.1007/s11745-011-3535-3. Epub 2011 Mar 6. PubMed PMID: 21380793.

Hong SH, Belayev L, Khoutorova L, Obenaus A, Bazan NG. Docosahexaenoic acid confers enduring neuroprotection in experimental stroke. J Neurol Sci. 2013 Dec 31. doi:pii: S0022-510X(13)03104-3. 10.1016/j.jns.2013.12.033. [Epub ahead of print] PubMed PMID: 24433927.

Honeyman TW, Strohsnitter W, Scheid CR, Schimmel RJ. Phosphatidic acid and phosphatidylinositol labelling in adipose tissue. Relationship to the metabolic effects of insulin and insulin-like agents. Biochem J. 1983 May 15;212(2):489-98. PubMed PMID: 6411068; PubMed Central PMCID: PMC1152072.

Hu C, van Dommelen J, van der Heijden R, Spijksma G, Reijmers TH, Wang M, Slee E, Lu X, Xu G, van der Greef J, Hankemeier T. RPLC-ion-trap-FTMS method for lipid profiling of plasma: method validation and application to p53 mutant mouse model. J Proteome Res. 2008 Nov;7(11):4982-91. doi: 10.1021/pr800373m. Epub 2008 Oct 8. PubMed PMID: 18841877.

Hu Q, Noll RJ, Li H, Makarov A, Hardman M, Graham Cooks R. The Orbitrap: a new mass spectrometer. J Mass Spectrom. 2005 Apr;40(4):430-43. PubMed PMID: 15838939.

Isaac G, Jeannotte R, Esch SW, Welti R. New mass-spectrometry-based strategies for lipids. Genet Eng (N Y). 2007;28:129-57. Review. PubMed PMID: 17153937.

Isobe Y, Arita M. Identification of novel omega-3 fatty acid-derived bioactive metabolites based on a targeted lipidomics approach. J Clin Biochem Nutr. 2014 Sep;55(2):79-84. doi: 10.3164/jcbn.14-18. Epub 2014 Aug 22. Review. PubMed PMID: 25320453; PubMed Central PMCID: PMC4186379.

Ji RR, Xu ZZ, Strichartz G, Serhan CN. Emerging roles of resolvins in the resolution of inflammation and pain. Trends Neurosci. 2011 Nov;34(11):599-609. doi: 10.1016/j.tins.2011.08.005. Epub 2011 Sep 30. Review. PubMed PMID: 21963090; PubMed Central PMCID: PMC3200462.

Kim H, Ahn E, Moon MH. Profiling of human urinary phospholipids by nanoflow liquid chromatography/tandem mass spectrometry. Analyst. 2008 Dec;133(12):1656-63. doi: 10.1039/b804715d. Epub 2008 Sep 3. PubMed PMID: 19082067.

Kind T, Liu KH, Lee do Y, DeFelice B, Meissen JK, Fiehn O. LipidBlast in silico tandem mass spectrometry database for lipid identification. Nat Methods. 2013 Aug;10(8):755-8. doi: 10.1038/nmeth.2551. Epub 2013 Jun 30. PubMed PMID: 23817071; PubMed Central PMCID: PMC3731409.

Kirsch S, Zarei M, Cindrić M, Müthing J, Bindila L, Peter-Katalinić J. On-line nano-HPLC/ESI QTOF MS and tandem MS for separation, detection, and structural elucidation of human erythrocytes neutral glycosphingolipid mixture. Anal Chem. 2008 Jun 15;80(12):4711-22. doi: 10.1021/ac702175f. Epub 2008 May 21. PubMed PMID: 18491926.

Klingler M, Demmelmair H, Koletzko B, Glaser C. Fatty acid status determination by cheek cell sampling combined with methanol-based ultrasound extraction of glycerophospholipids. Lipids. 2011 Oct;46(10):981-90. doi: 10.1007/s11745-011-3576-7. Epub 2011 Jun 17. PubMed PMID: 21681560.

Koivusalo M, Haimi P, Heikinheimo L, Kostiainen R, Somerharju P. Quantitative determination of phospholipid compositions by ESI-MS: effects of acyl chain length, unsaturation, and lipid concentration on instrument response. J Lipid Res. 2001 Apr;42(4):663-72. PubMed PMID: excelexcel10.1017/S0007114512001481. Review. PubMed PMID: 22591905.

Koulman A, Prentice P, Wong MC, Matthews L, Bond NJ, Eiden M, Griffin JL, Dunger DB. The development and validation of a fast and robust dried blood spot based lipid profiling method to study infant metabolism. Metabolomics. 2014;10(5):1018-1025. Epub 2014 Feb 11. PubMed PMID: 25177234; PubMed Central PMCID: PMC4145199.

Lamaziere A, Richard D, Barbe U, Kefi K, Bausero P, Wolf C, Visioli F. Differential distribution of DHA-phospholipids in rat brain after feeding: A lipidomic approach. Prostaglandins Leukot Essent Fatty Acids. 2011 Jan-Feb;84(1-2):7-11. doi: 10.1016/j.plefa.2010.11.001. Epub 2010 Nov 24. PubMed PMID: 21109411.

Lands WE. Metabolism of glycerolipides; a comparison of lecithin and triglyceride synthesis. J Biol Chem. 1958 Apr;231(2):883-8. PubMed PMID: 13539023.

Lao RC, Oja H, Thomas RS, Monkman JL. Assessment of environmental problems using the combination of gas chromatography and quadrupole mass spectrometry. Sci Total Environ. 1973 Dec;2(3):223-33. PubMed PMID: 4804496.

Lazaro MJ, Herod AA, Domin M, Zhuo Y, Islas CA, Kandiyoti R. Determining a 'safe' high-mass limit in matrix-assisted laser desorption/ionisation time-of-flight mass spectra of coal derived materials with reference to instrument noise. Rapid Commun Mass Spectrom. 1999;13(14):1401-12. PubMed PMID: 10407331.

Lee JY, Min HK, Moon MH. Simultaneous profiling of lysophospholipids and phospholipids from human plasma by nanoflow liquid chromatography-tandem mass spectrometry. Anal Bioanal Chem. 2011 Jul;400(9):2953-61. doi: 10.1007/s00216-011-4958-7. Epub 2011 Apr 18. PubMed PMID: 21499968.

Leidl K, Liebisch G, Richter D, Schmitz G. Mass spectrometric analysis of lipid species of human circulating blood cells. Biochim Biophys Acta. 2008 Oct;1781(10):655-64. doi: 10.1016/j.bbalip.2008.07.008. Epub 2008 Aug 6. PubMed PMID: 18723117.

Lowenthal MS, Andriamaharavo NR, Stein SE, Phinney KW. Characterizing Vaccinium berry Standard Reference Materials by GC-MS using NIST spectral libraries. Anal Bioanal Chem. 2013 May;405(13):4467-76. doi: 10.1007/s00216-012-6610-6. Epub 2013 Jan 6. PubMed PMID: 23291961.

Makarov A. Electrostatic axially harmonic orbital trapping: a high-performance technique of mass analysis. Anal Chem. 2000 Mar 15;72(6):1156-62. PubMed PMID: 10740853.

Matsuo T, Seyama Y. Introduction to modern biological mass spectrometry. J Mass Spectrom. 2000 Feb;35(2):114-30. Review. PubMed PMID: 10679971.

Merrill AH Jr, Stokes TH, Momin A, Park H, Portz BJ, Kelly S, Wang E, Sullards MC, Wang MD. Sphingolipidomics: a valuable tool for understanding the roles of sphingolipids in biology and disease. J Lipid Res. 2009 Apr;50 Suppl:S97-102. doi: 10.1194/jlr.R800073-JLR200. Epub 2008 Nov 21. PubMed PMID: 19029065; PubMed Central PMCID: PMC2674747.

Metherel AH, Aristizabal Henao JJ, Stark KD. EPA and DHA levels in whole blood decrease more rapidly when stored at -20 °C as compared with room temperature, 4 and -75 °C. Lipids. 2013 Nov;48(11):1079-91. doi: 10.1007/s11745-013-3827-x. Epub 2013 Aug 15. PubMed PMID: 23949919.

Metherel AH, Armstrong JM, Patterson AC, Stark KD. Assessment of blood measures of n-3 polyunsaturated fatty acids with acute fish oil supplementation and washout in men and

women. Prostaglandins Leukot Essent Fatty Acids. 2009 Jul;81(1):23-9. doi: 10.1016/j.plefa.2009.05.018. Epub 2009 Jun 9. PubMed PMID: 19515545.

Metherel AH, Buzikievich LM, Charkhzarin P, Patterson AC, Peel AC, Howorth AM, Kishi DM, Stark KD. Omega-3 polyunsaturated fatty acid profiling using fingertip-prick whole blood does not require overnight fasting before blood collection. Nutr Res. 2012 Aug;32(8):547-56. doi: 10.1016/j.nutres.2012.06.016. Epub 2012 Aug 2. PubMed PMID: 22935337.

Metherel AH, Taha AY, Izadi H, Stark KD. The application of ultrasound energy to increase lipid extraction throughput of solid matrix samples (flaxseed). Prostaglandins Leukot Essent Fatty Acids. 2009 Nov-Dec;81(5-6):417-23. doi: 10.1016/j.plefa.2009.07.003. Epub 2009 Sep 9. PubMed PMID: 19744844.

Michalski A, Damoc E, Hauschild JP, Lange O, Wieghaus A, Makarov A, Nagaraj N, Cox J, Mann M, Horning S. Mass spectrometry-based proteomics using Q Exactive, a high-performance benchtop quadrupole Orbitrap mass spectrometer. Mol Cell Proteomics. 2011 Sep;10(9):M111.011015. doi: 10.1074/mcp.M111.011015. Epub 2011 Jun 3. PubMed PMID: 21642640; PubMed Central PMCID: PMC3284220.

Moreau RA. An overview of modern mass spectrometry methods in the toolbox of lipid chemists and biochemists. *Lipid Analysis and Lipidomics – New Techniques and Applications*. AOCS Press. 2006. 29-49.

Mozaffarian D, Lemaitre RN, King IB, Song X, Huang H, Sacks FM, Rimm EB, Wang M, Siscovick DS. Plasma phospholipid long-chain ω-3 fatty acids and total and cause-specific mortality in older adults: a cohort study. Ann Intern Med. 2013 Apr 2;158(7):515-25. doi:

10.7326/0003-4819-158-7-201304020-00003. PubMed PMID: 23546563; PubMed Central PMCID: PMC3698844.

Murphy RC, Leiker TJ, Barkley RM. Glycerolipid and cholesterol ester analyses in biological samples by mass spectrometry. Biochim Biophys Acta. 2011 Nov;1811(11):776-83. doi: 10.1016/j.bbalip.2011.06.019. Epub 2011 Jun 26. Review. PubMed PMID: 21757029; PubMed Central PMCID: PMC3205286.

Murthy M, Hamilton J, Greiner RS, Moriguchi T, Salem N Jr, Kim HY. Differential effects of n-3 fatty acid deficiency on phospholipid molecular species composition in the rat hippocampus. J Lipid Res. 2002 Apr;43(4):611-7. PubMed PMID: 11907144.

Nagan N, Zoeller RA. Plasmalogens: biosynthesis and functions. Prog Lipid Res. 2001 May;40(3):199-229. Review. PubMed PMID: 11275267.

Nurhasan M, Roos N, Aristizabal Henao JJ, Chamnan C, Stark KD, Lauritzen L. Effect of storage temperature in a Cambodian field setting on the fatty acid composition in whole blood. Prostaglandins Leukot Essent Fatty Acids. 2015 May;96:57-61. doi: 10.1016/j.plefa.2015.02.001. Epub 2015 Feb 14. PubMed PMID: 25753812.

Oliver SG, Winson MK, Kell DB, Baganz F. Systematic functional analysis of the yeast genome. Trends Biotechnol. 1998 Sep;16(9):373-8. Review. Erratum in: Trends Biotechnol 1998 Oct;16(10):447. PubMed PMID: 9744112.

Olsen JV, Macek B, Lange O, Makarov A, Horning S, Mann M. Higher-energy C-trap dissociation for peptide modification analysis. Nat Methods. 2007 Sep;4(9):709-12. Epub 2007 Aug 26. PubMed PMID: 17721543.

Ottestad I, Hassani S, Borge GI, Kohler A, Vogt G, Hyötyläinen T, Orešič M, Brønner KW, Holven KB, Ulven SM, Myhrstad MC. Fish oil supplementation alters the plasma lipidomic

profile and increases long-chain PUFAs of phospholipids and triglycerides in healthy subjects. PLoS One. 2012;7(8):e42550. doi: 10.1371/journal.pone.0042550. Epub 2012 Aug 28. PubMed PMID: 22952598; PubMed Central PMCID: PMC3429454.

Pacetti D, Malavolta M, Bocci F, Boselli E, Frega NG. High-performance liquid chromatography/electrospray ionization ion-trap tandem mass spectrometric analysis and quantification of phosphatidylcholine molecular species in the serum of cystic fibrosis subjects supplemented with docosahexaenoic acid. Rapid Commun Mass Spectrom. 2004;18(20):2395-400. PubMed PMID: 15386630.

Pais P, Moyano E, Puignou L, Galceran MT. Liquid chromatography-electrospray mass spectrometry with in-source fragmentation for the identification and quantification of fourteen mutagenic amines in beef extracts. J Chromatogr A. 1997 Jul 18;775(1-2):125-36. PubMed PMID: 9253196.

Palmquist DL, Jenkins TC. Challenges with fats and fatty acid methods. J Anim Sci. 2003 Dec;81(12):3250-4. Review. PubMed PMID: 14677882.

Paul W, Reinhard HP, con Zahn U. Das elektrische Massenfilter als Massenspektrometer und Isotopentrenner. Z. Phys. 1958 (152)143. doi: 10.1007/BF01327353

Patterson AC. Evaluation of Conventional and Novel Dietary Strategies to Promote Intake of Omega-3 Highly Unsaturated Fatty Acids. Doctoral Thesis. University of Waterloo, September 27, 2012.

Patterson AC, Chalil A, Charkhzarin P, Aristizabal Henao JJ, Streit I, Ciobanu F, Stark KD. Do intakes of 250-500mg/d of EPA and DHA increase blood biomarkers? The FASEB Journal. 2012;26:646.24.

Patterson AC, Hogg RC, Kishi DM, Stark KD. Biomarker and dietary validation of a Canadian food frequency questionnaire to measure eicosapentaenoic and docosahexaenoic acid intakes from whole food, functional food, and nutraceutical sources. J Acad Nutr Diet. 2012 Jul;112(7):1005-14. doi: 10.1016/j.jand.2012.03.030. Epub 2012 May 12. PubMed PMID: 22583924.

Patterson AC, Metherel AH, Hanning RM, Stark KD. The percentage of DHA in erythrocytes can detect non-adherence to advice to increase EPA and DHA intakes. Br J Nutr. 2013 Aug 6:1-9. [Epub ahead of print] PubMed PMID: 23920312.

Peake AD, Kiyonami R, Yokoi Y, Fukamachi Y, Huang Y. Processing of a Complex Lipid Dataset for the NIST Inter-Laboratory Comparison Exercise for Lipidomics Measurements in Human Serum and Plasma

Peake DA, Yokoi Y, Wank J, Huang Y. A new lipid software workflow for processing Orbitrap-based global lipidomics data in translational and systems biology research. ASMS. 2013. ASMS13_Th591_DPeake_E 06/13S.

Pitt JJ. Principles and applications of liquid chromatography-mass spectrometry in clinical biochemistry. Clin Biochem Rev. 2009 Feb;30(1):19-34. PubMed PMID: 19224008; PubMed Central PMCID: PMC2643089.

Plumb RS, Granger JH, Stumpf CL, Johnson KA, Smith BW, Gaulitz S, Wilson ID, Castro-Perez J. A rapid screening approach to metabonomics using UPLC and oa-TOF mass spectrometry: application to age, gender and diurnal variation in normal/Zucker obese rats and black, white and nude mice. Analyst. 2005 Jun;130(6):844-9. Epub 2005 Apr 27. PubMed PMID: 15912231.

Precup-Blaga FS, Garcia-Martinez JC, Schenning AP, Meijer EW. Highly emissive

supramolecular oligo(p-phenylene vinylene) dendrimers. J Am Chem Soc. 2003 Oct 22;125(42):12953-60. PubMed PMID: 14558844.

Prentice P, Koulman A, Matthews L, Acerini CL, Ong KK, Dunger DB. Lipidomic analyses, breast- and formula-feeding, and growth in infants. J Pediatr. 2015 Feb;166(2):276-81.e6. doi: 10.1016/j.jpeds.2014.10.021. Epub 2014 Nov 18. PubMed PMID: 25454937; PubMed Central PMCID: PMC4302220.

Ramanadham S, Hsu F, Zhang S, Bohrer A, Ma Z, Turk J. Electrospray ionization mass spectrometric analyses of phospholipids from INS-1 insulinoma cells: comparison to pancreatic islets and effects of fatty acid supplementation on phospholipid composition and insulin secretion. Biochim Biophys Acta. 2000 Apr 12;1484(2-3):251-66. PubMed PMID: 10760474.

Reed CF, Swisher SN, Marinetti GV, Enen EG. Studies of the lipids of the erythrocyte. I. Quantitative analysis of the lipids of normal human red blood cells. J Lab Clin Med. 1960 Aug;56:281-9. PubMed PMID: 14436859.

Rees MK, Young M. Studies on the isolation and molecular properties of homogeneous globular actin. Evidence for a single polypeptide chain structure. J Biol Chem. 1967 Oct 10;242(19):4449-58. PubMed PMID: 6065088.

Risé P, Eligini S, Ghezzi S, Colli S, Galli C. Fatty acid composition of plasma, blood cells and whole blood: relevance for the assessment of the fatty acid status in humans. Prostaglandins Leukot Essent Fatty Acids. 2007 Jun;76(6):363-9. Epub 2007 Jun 25. PubMed PMID: 17588731.

Rocklin RE, Thistle L, Gallant L, Manku MS, Horrobin D. Altered arachidonic acid content in polymorphonuclear and mononuclear cells from patients with allergic rhinitis and/or asthma.

Lipids. 1986 Jan;21(1):17-20. Erratum in: Lipids 1990 Feb;25(2):124. PubMed PMID: 3083171.

Rouser G, Fkeischer S, Yamamoto A. Two dimensional then layer chromatographic separation of polar lipids and determination of phospholipids by phosphorus analysis of spots. Lipids. 1970 May;5(5):494-6. PubMed PMID: 5483450.

Rucker J, Paul J, Pfeifer BA, Lee K. Engineering E. coli for triglyceride accumulation through native and heterologous metabolic reactions. Appl Microbiol Biotechnol. 2013 Mar;97(6):2753-9. doi: 10.1007/s00253-013-4714-3. Epub 2013 Feb 13. PubMed PMID: 23404315.

Sahin HT, Arslan MB. A study on physical and chemical properties of cellulose paper immersed in various solvent mixtures. Int J Mol Sci. 2008 Jan;9(1):78-88. Epub 2008 Jan 25. PubMed PMID: 19325721; PubMed Central PMCID: PMC2635603.

Sandra K, Pereira Ados S, Vanhoenacker G, David F, Sandra P. Comprehensive blood plasma lipidomics by liquid chromatography/quadrupole time-of-flight mass spectrometry. J Chromatogr A. 2010 Jun 18;1217(25):4087-99. doi: 10.1016/j.chroma.2010.02.039. Epub 2010 Feb 24. PubMed PMID: 20307888.

Schmelzer K, Fahy E, Subramaniam S, Dennis EA. The lipid maps initiative in lipidomics. Methods Enzymol. 2007;432:171-83. PubMed PMID: 17954217.

Schuhmann K, Almeida R, Baumert M, Herzog R, Bornstein SR, Shevchenko A. Shotgun lipidomics on a LTQ Orbitrap mass spectrometer by successive switching between acquisition polarity modes. J Mass Spectrom. 2012 Jan;47(1):96-104. doi: 10.1002/jms.2031. PubMed PMID: 22282095.

Serna J, García-Seisdedos D, Alcázar A, Lasunción MÁ, Busto R, Pastor Ó. Quantitative

lipidomic analysis of plasma and plasma lipoproteins using MALDI-TOF mass spectrometry. Chem Phys Lipids. 2015 Jul;189:7-18. doi: 10.1016/j.chemphyslip.2015.05.005. Epub 2015 May 21. PubMed PMID: 26004846.

Shindou H, Hishikawa D, Harayama T, Eto M, Shimizu T. Generation of membrane diversity by lysophospholipid acyltransferases. J Biochem. 2013 Jul;154(1):21-8. doi: 10.1093/jb/mvt048. Epub 2013 May 21. Review. PubMed PMID: 23698096.

Simons B, Arendt B. Comprehensive lipid profiling of human liver tissue extracts if non-alcoholic fatty liver disease. AB Sciex Canada.

Sjövall P, Rossmeisl M, Hanrieder J, Kuda O, Kopecky J, Bryhn M. Dietary uptake of omega-3 fatty acids in mouse tissue studied by time-of-flight secondary ion mass spectrometry (TOF-SIMS). Anal Bioanal Chem. 2015 Jul;407(17):5101-11. doi: 10.1007/s00216-015-8515-7. Epub 2015 Feb 19. PubMed PMID: 25694146.

Snyder NW, Tombline G, Worth AJ, Parry RC, Silvers JA, Gillespie KP, Basu SS, Millen J, Goldfarb DS, Blair IA. Production of stable isotope-labeled acyl-coenzyme A thioesters by yeast stable isotope labeling by essential nutrients in cell culture. Anal Biochem. 2015 Apr 1;474:59-65. doi: 10.1016/j.ab.2014.12.014. Epub 2015 Jan 6. PubMed PMID: 25572876; PubMed Central PMCID: PMC4413507.

Ståhlman M, Ejsing CS, Tarasov K, Perman J, Borén J, Ekroos K. High-throughput shotgun lipidomics by quadrupole time-of-flight mass spectrometry. J Chromatogr B Analyt Technol Biomed Life Sci. 2009 Sep 15;877(26):2664-72. doi: 10.1016/j.jchromb.2009.02.037. Epub 2009 Feb 24. Review. PubMed PMID: 19286428.

Stanke-Labesque F, Molière P, Bessard J, Laville M, Véricel E, Lagarde M. Effect of dietary supplementation with increasing doses of docosahexaenoic acid on neutrophil lipid

composition and leukotriene production in human healthy volunteers. Br J Nutr. 2008 Oct;100(4):829-33. doi: 10.1017/S0007114508923692. Epub 2008 Feb 28. PubMed PMID: 18304388.

Stark KD. The percentage of n-3 highly unsaturated fatty acids in total HUFA as a biomarker for omega-3 fatty acid status in tissues. Lipids. 2008 Jan;43(1):45-53. Epub 2007 Nov 6. PubMed PMID: 17985169.

Stark KD, Aristizabal Henao JJ, Metherel AH, Pilot L. Development of predictive equations for omega-3 poly-unsaturated fatty acids across whole blood, erythrocytes, and plasma lipid fractions. 2015.

Stoll DR, Li X, Wang X, Carr PW, Porter SE, Rutan SC. Fast, comprehensive two-dimensional liquid chromatography. J Chromatogr A. 2007 Oct 19;1168(1-2):3-43; discussion 2. Epub 2007 Aug 30. Review. PubMed PMID: 17888443; PubMed Central PMCID: PMC3205947.

Studier MH, Hayatsu R, Fuse K. Analyses of pyrimidine and purine bases by a combination of paper chromatography and time-of-flight mass spectrometry. Anal Biochem. 1968 Nov;26(2):320-4. PubMed PMID: 5758046.

Tanaka T, Isezaki T, Nakano H, Iwasaki Y. Synthesis of phospholipids containing polyunsaturated fatty acids by phospholipase A(2)-mediated esterification with food-compatible reagents. J Oleo Sci. 2010;59(7):375-80. PubMed PMID: 20513971.

Uhl O, Demmelmair H, Klingler M, Koletzko B. Changes of molecular glycerophospholipid species in plasma and red blood cells during docosahexaenoic acid supplementation. Lipids. 2013 Nov;48(11):1103-13. doi: 10.1007/s11745-013-3837-8. Epub 2013 Sep 17. PubMed PMID: 24043586.

Varma D, Ganti S, Gilles T, Diaz M, Thompson T, Stull J, Jansen SA. Comparison of UHPLC

and HPLC methods for the assay of prostanoids: "are the methods equivalent in terms of accuracy and precision?". Bioanalysis. 2011 Apr;3(8):853-62. doi: 10.4155/bio.11.58. PubMed PMID: 21510759.

von Schacky C, Harris WS. Cardiovascular risk and the omega-3 index. J Cardiovasc Med (Hagerstown). 2007 Sep;8 Suppl 1:S46-9. Review. PubMed PMID: 17876200.

Wang C, Yang J, Gao P, Lu X, Xu G. Identification of phospholipid structures in human blood by direct-injection quadrupole-linear ion-trap mass spectrometry. Rapid Commun Mass Spectrom. 2005;19(17):2443-53. PubMed PMID: 16059884.

Wang WQ, Gustafson A. One-dimensional thin-layer chromatographic separation of phospholipids and lysophospholipids from tissue lipid extracts. J Chromatogr. 1992 Oct 2;581(1):139-42. PubMed PMID: 1429997.

Wang M, Hayakawa J, Yang K, Han X. Characterization and Quantification of Diacylglycerol Species in Biological Extracts after One-Step Derivatization: A Shotgun Lipidomics Approach. Anal Chem. 2014 Jan 28. [Epub ahead of print] PubMed PMID: 24432906.

Waters – The Science of What's Possible. HPLC – High Performance Liquid Chromatography. Primers. 2014.

Weir JM, Wong G, Barlow CK, Greeve MA, Kowalczyk A, Almasy L, Comuzzie AG, Mahaney MC, Jowett JB, Shaw J, Curran JE, Blangero J, Meikle PJ. Plasma lipid profiling in a large population-based cohort. J Lipid Res. 2013 Oct;54(10):2898-908. doi: 10.1194/jlr.P035808. Epub 2013 Jul 18. PubMed PMID: 23868910; PubMed Central PMCID: PMC3770102.

West AA, Yan J, Jiang X, Perry CA, Innis SM, Caudill MA. Choline intake influences phosphatidylcholine DHA enrichment in nonpregnant women but not in pregnant women in

the third trimester. Am J Clin Nutr. 2013 Apr;97(4):718-27. doi: 10.3945/ajcn.112.050211. Epub 2013 Feb 27. PubMed PMID: 23446897.

Wiley WC, McLaren IH. Time-of-Flight Mass Spectrometer with Improved Resolution. Rev.Sci.Instrum. 1955 (26) 1150. Doi: 10.1002/(SICI)1096-9888(199701)32:1<1::AID-JMS467>3.0.CO;2-6

Williams ER, Furlong JJ, McLafferty FW. Efficiency of collisionally-activated dissociation and 193-nm photodissociation of peptide ions in fourier transform mass spectrometry. J Am Soc Mass Spectrom. 1990 Jul;1(4):288-94. doi: 10.1016/1044-0305(90)85003-5. PubMed PMID: 24248821.

Xu Z, Riediger N, Innis S, Moghadasian MH. Fish oil significantly alters fatty acid profiles in various lipid fractions but not atherogenesis in apo E-KO mice. Eur J Nutr. 2007 Mar;46(2):103-10. PubMed PMID: 17225919.

Yost RA, Boyd RK. Tandem mass spectrometry: quadrupole and hybrid instruments. Methods Enzymol. 1990;193:154-200. Review. PubMed PMID: 2074819.

Yuan M, Breitkopf SB, Yang X, Asara JM. A positive/negative ion-switching, targeted mass spectrometry-based metabolomics platform for bodily fluids, cells, and fresh and fixed tissue. Nat Protoc. 2012 Apr 12;7(5):872-81. doi: 10.1038/nprot.2012.024. PubMed PMID: 22498707; PubMed Central PMCID: PMC3685491.

Zhang J, Wang C, Gao Y, Li L, Man Q, Song P, Meng L, Du ZY, Miles EA, Lie Ø, Calder PC, Frøyland L. Different intakes of n-3 fatty acids among pregnant women in 3 regions of China with contrasting dietary patterns are reflected in maternal but not in umbilical erythrocyte phosphatidylcholine fatty acid composition. Nutr Res. 2013 Aug;33(8):613-21. doi: 10.1016/j.nutres.2013.05.009. Epub 2013 Jun 27. PubMed PMID: 23890350.

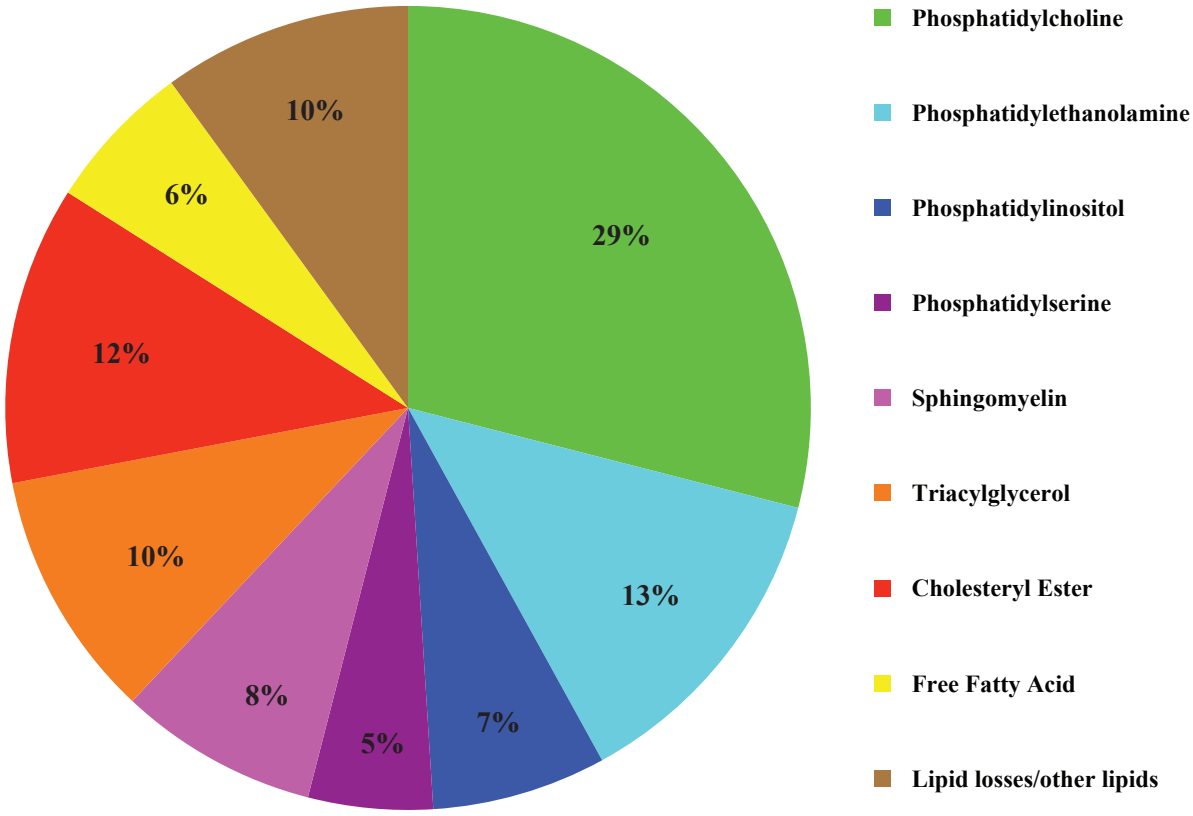

Figure A.1. Lipid Pool Composition of Human Whole Blood after Folch Lipid Extraction. Distribution of total fatty acids in whole blood across the predominant lipid pools. Data represents the percent weight of total fatty acids in each pool divided by the total fatty acid concentration of whole blood. Lipids were extracted using 2:1 chloroform:methanol as described previously (Folch et al., 1957). Lipid classes from lipid extracts (n = 12) were separated with thin layer chromatography, lipids were extracted, derivatized to fatty acid methyl esters with 14% BF_3 in methanol, and analyzed using gas chromatography-flame ionization detection. C22:3n-3 methyl ester was used for quantitation.

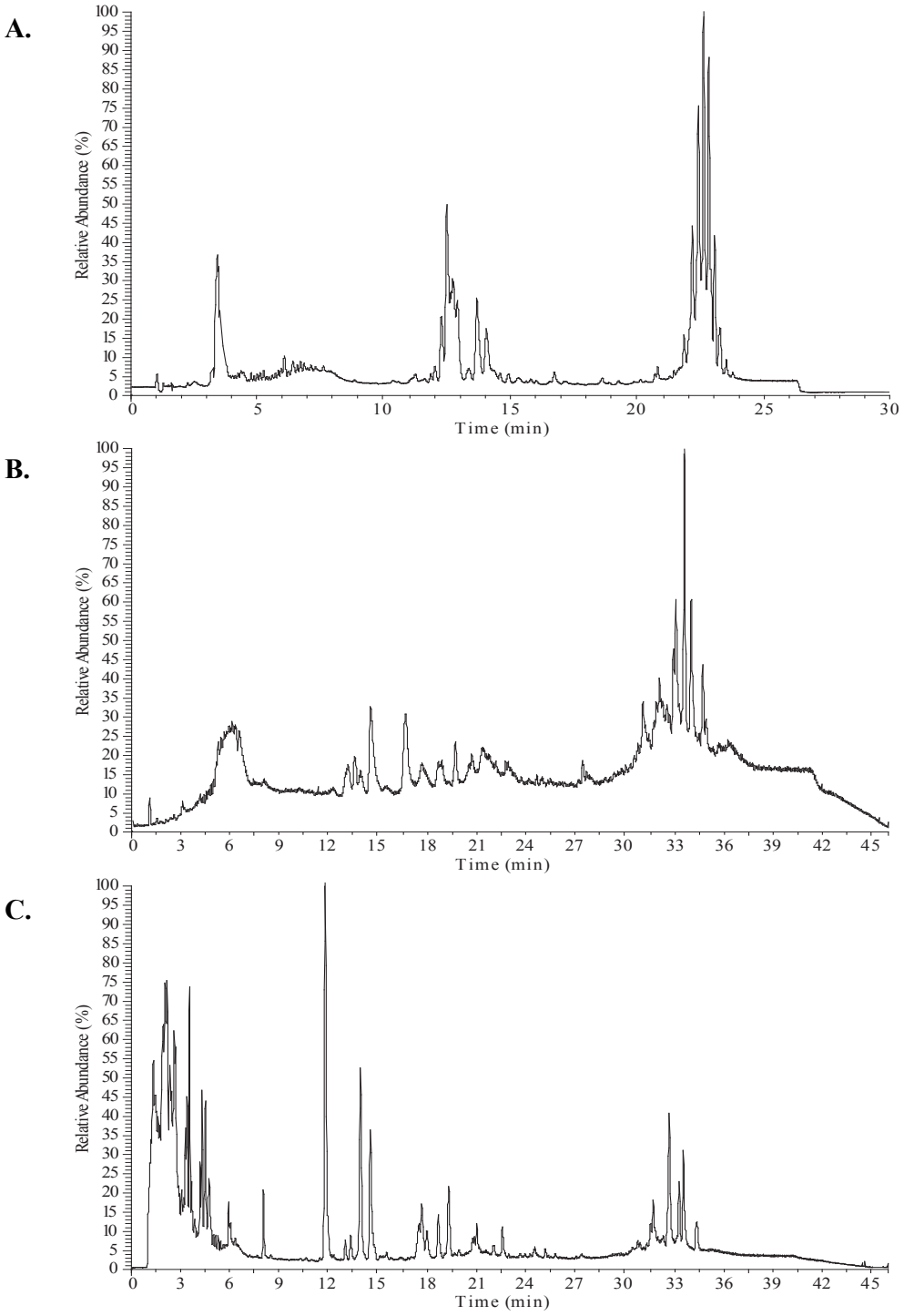

Figure A.2. **A.**10 µL blood lipid extract run with Bird et al., 2011 chromatographic protocol. **B.**10 µL blood lipid extract run with optimized chromatographic protocol. **C.** 10 µL blood lipid extract run with optimized chromatographic protocol and 2.0 µm C18 column.

Appendix A. Method Development (Chapter 5)

Table A.1. *Matrix for the Determination of Acyl-Specific Phosphatidylcholine m/z ratios*[ϟ]

Acyl Chains	C12:0	C14:0	C16:0	C16:1	C18:0	C18:1	C18:2	C18:3	C20:0	C20:1	C20:2
C12:0	622.4442	650.4755	678.5068	676.4912	706.5381	704.5225	702.5068	700.4912	734.5694	732.5538	730.5381
C14:0	650.4755	678.5068	706.5381	704.5225	734.5694	732.5538	730.5381	728.5225	762.6007	760.5851	758.5694
C16:0	678.5068	706.5381	734.5694	732.5538	762.6007	760.5851	758.5694	756.5538	790.6320	788.6164	786.6007
C16:1	676.4912	704.5225	732.5538	730.5381	760.5851	758.5694	756.5538	754.5381	788.6164	786.6007	784.5851
C18:0	706.5381	734.5694	762.6007	760.5851	790.6320	788.6164	786.6007	784.5851	818.6633	816.6477	814.6320
C18:1	704.5225	732.5538	760.5851	758.5694	788.6164	786.6007	784.5851	782.5694	816.6477	814.6320	812.6164
C18:2	702.5068	730.5381	758.5694	756.5538	786.6007	784.5851	782.5694	780.5538	814.6320	812.6164	810.6007
C18:3	700.4912	728.5225	756.5538	754.5381	784.5851	782.5694	780.5538	778.5381	812.6164	810.6007	808.5851
C20:0	734.5694	762.6007	790.6320	788.6164	818.6633	816.6477	814.6320	812.6164	846.6946	844.6790	842.6633
C20:1	732.5538	760.5851	788.6164	786.6007	816.6477	814.6320	812.6164	810.6007	844.6790	842.6633	840.6477
C20:2	730.5381	758.5694	786.6007	784.5851	814.6320	812.6164	810.6007	808.5851	842.6633	840.6477	838.6320
C20:3	728.5225	756.5538	784.5851	782.5694	812.6164	810.6007	808.5851	806.5694	840.6477	838.6320	836.6164
C20:4	726.5069	754.5381	782.5694	780.5538	810.6007	808.5851	806.5694	804.5538	838.6320	836.6164	834.6007
C20:5	724.4912	752.5225	780.5538	778.5381	808.5851	806.5694	804.5538	802.5381	836.6164	834.6007	832.5851
C22:0	762.6007	790.6320	818.6633	816.6477	846.6946	844.6790	842.6633	840.6477	874.7259	872.7103	870.6946
C22:1	760.5851	788.6164	816.6477	814.6320	844.6790	842.6633	840.6477	838.6320	872.7103	870.6946	868.6790
C22:2	758.5694	786.6007	814.6320	812.6164	842.6633	840.6477	838.6320	836.6164	870.6946	868.6790	866.6633
C22:4	754.5381	782.5694	810.6007	808.5851	838.6320	836.6164	834.6007	832.5851	866.6633	864.6477	862.6320
C22:5	752.5225	780.5538	808.5851	806.5694	836.6164	834.6007	832.5851	830.5694	864.6477	862.6320	860.6164
C22:6	750.5068	778.5381	806.5694	804.5538	834.6007	832.5851	830.5694	828.5538	862.6320	860.6164	858.6007
C24:0	790.6320	818.6633	846.6946	844.6790	874.7259	872.7103	870.6946	868.6790	902.7572	900.7416	898.7259
C24:1	788.6164	816.6477	844.6790	842.6633	872.7103	870.6946	868.6790	866.6633	900.7416	898.7259	896.7103

Acyl Chains	C20:3	C20:4	C20:5	C22:0	C22:1	C22:2	C22:4	C22:5	C22:6	C24:0	C24:1
C12:0	728.5225	726.5069	724.4912	762.6007	760.5851	758.5694	754.5381	752.5225	750.5068	790.6320	788.6164
C14:0	756.5538	754.5381	752.5225	790.6320	788.6164	786.6007	782.5694	780.5538	778.5381	818.6633	816.6477
C16:0	784.5851	782.5694	780.5538	818.6633	816.6477	814.6320	810.6007	808.5851	806.5694	846.6946	844.6790
C16:1	782.5694	780.5538	778.5381	816.6477	814.6320	812.6164	808.5851	806.5694	804.5538	844.6790	842.6633
C18:0	812.6164	810.6007	808.5851	846.6946	844.6790	842.6633	838.6320	836.6164	834.6007	874.7259	872.7103
C18:1	810.6007	808.5851	806.5694	844.6790	842.6633	840.6477	836.6164	834.6007	832.5851	872.7103	870.6946
C18:2	808.5851	806.5694	804.5538	842.6633	840.6477	838.6320	834.6007	832.5851	830.5694	870.6946	868.6790
C18:3	806.5694	804.5538	802.5381	840.6477	838.6320	836.6164	832.5851	830.5694	828.5538	868.6790	866.6633
C20:0	840.6477	838.6320	836.6164	874.7259	872.7103	870.6946	866.6633	864.6477	862.6320	902.7572	900.7416
C20:1	838.6320	836.6164	834.6007	872.7103	870.6946	868.6790	864.6477	862.6320	860.6164	900.7416	898.7259
C20:2	836.6164	834.6007	832.5851	870.6946	868.6790	866.6633	862.6320	860.6164	858.6007	898.7259	896.7103
C20:3	834.6007	832.5851	830.5694	868.6790	866.6633	864.6477	860.6164	858.6007	856.5851	896.7103	894.6946
C20:4	832.5851	830.5694	828.5538	866.6633	864.6477	862.6320	858.6007	856.5851	854.5694	894.6946	892.6790
C20:5	830.5694	828.5538	826.5381	864.6477	862.6320	860.6164	856.5851	854.5694	852.5538	892.6790	890.6633
C22:0	868.6790	866.6633	864.6477	902.7572	900.7416	898.7259	894.6946	892.6790	890.6633	930.7885	928.7729
C22:1	866.6633	864.6477	862.6320	900.7416	898.7259	896.7103	892.6790	890.6633	888.6477	928.7729	926.7572
C22:2	864.6477	862.6320	860.6164	898.7259	896.7103	894.6946	890.6633	888.6477	886.6320	926.7572	924.7416
C22:4	860.6164	858.6007	856.5851	894.6946	892.6790	890.6633	886.6320	884.6164	882.6007	922.7259	920.7103
C22:5	858.6007	856.5851	854.5694	892.6790	890.6633	888.6477	884.6164	882.6007	880.5851	920.7103	918.6946
C22:6	856.5851	854.5694	852.5538	890.6633	888.6477	886.6320	882.6007	880.5851	878.5694	918.6946	916.6790
C24:0	896.7103	894.6946	892.6790	930.7885	928.7729	926.7572	922.7259	920.7103	918.6946	958.8198	956.8042
C24:1	894.6946	892.6790	890.6633	928.7729	926.7572	924.7416	920.7103	918.6946	916.6790	956.8042	954.7885

[ϟ]Matrix used for the identification of precursor $[M+H]^+$ *m/z* ratios for phosphatidylcholines with specific fatty acyl chains. The intersection between a fatty acid across the top row and down the first column would reveal its *m/z* ratio.

Table A.2. ***Matrix for the Determination of Acyl-Specific Phosphatidylethanolamine m/z ratios***[ϟ]

Acyl Chains	C12:0	C14:0	C16:0	C16:1	C18:0	C18:1	C18:2	C18:3	C20:0	C20:1	C20:2
C12:0	580.3973	608.4286	636.4599	634.4442	664.4912	662.4755	660.4599	658.4442	692.5225	690.5068	688.4912
C14:0	608.4286	636.4599	664.4912	662.4755	692.5225	690.5068	688.4912	686.4755	720.5538	718.5381	716.5225
C16:0	636.4599	664.4912	692.5225	690.5068	720.5538	718.5381	716.5225	714.5068	748.5851	746.5694	744.5538
C16:1	634.4442	662.4755	690.5068	688.4912	718.5381	716.5225	714.5068	712.4912	746.5694	744.5538	742.5381
C18:0	664.4912	692.5225	720.5538	718.5381	748.5851	746.5694	744.5538	742.5381	776.6164	774.6007	772.5851
C18:1	662.4755	690.5068	718.5381	716.5225	746.5694	744.5538	742.5381	740.5225	774.6007	772.5851	770.5694
C18:2	660.4599	688.4912	716.5225	714.5068	744.5538	742.5381	740.5225	738.5068	772.5851	770.5694	768.5538
C18:3	658.4442	686.4755	714.5068	712.4912	742.5381	740.5225	738.5068	736.4912	770.5694	768.5538	766.5381
C20:0	692.5225	720.5538	748.5851	746.5694	776.6164	774.6007	772.5851	770.5694	804.6477	802.6320	800.6164
C20:1	690.5068	718.5381	746.5694	744.5538	774.6007	772.5851	770.5694	768.5538	802.6320	800.6164	798.6007
C20:2	688.4912	716.5225	744.5538	742.5381	772.5851	770.5694	768.5538	766.5381	800.6164	798.6007	796.5851
C20:3	686.4755	714.5068	742.5381	740.5225	770.5694	768.5538	766.5381	764.5225	798.6007	796.5851	794.5694
C20:4	684.4599	712.4912	740.5225	738.5068	768.5538	766.5381	764.5225	762.5068	796.5851	794.5694	792.5538
C20:5	682.4442	710.4755	738.5068	736.4912	766.5381	764.5225	762.5068	760.4912	794.5694	792.5538	790.5381
C22:0	720.5538	748.5851	776.6164	774.6007	804.6477	802.6320	800.6164	798.6007	832.6790	830.6633	828.6477
C22:1	718.5381	746.5694	774.6007	772.5851	802.6320	800.6164	798.6007	796.5851	830.6633	828.6477	826.6320
C22:2	716.5225	744.5538	772.5851	770.5694	800.6164	798.6007	796.5851	794.5694	828.6477	826.6320	824.6164
C22:4	712.4912	740.5225	768.5538	766.5381	796.5851	794.5694	792.5538	790.5381	824.6164	822.6007	820.5851
C22:5	710.4755	738.5068	766.5381	764.5225	794.5694	792.5538	790.5381	788.5225	822.6007	820.5851	818.5694
C22:6	708.4599	736.4912	764.5225	762.5068	792.5538	790.5381	788.5225	786.5068	820.5851	818.5694	816.5538
C24:0	748.5851	776.6164	804.6477	802.6320	832.6790	830.6633	828.6477	826.6320	860.7103	858.6946	856.6790
C24:1	746.5694	774.6007	802.6320	800.6164	830.6633	828.6477	826.6320	824.6164	858.6946	856.6790	854.6633

Acyl Chains	C20:3	C20:4	C20:5	C22:0	C22:1	C22:2	C22:4	C22:5	C22:6	C24:0	C24:1
C12:0	686.4755	684.4599	682.4442	720.5538	718.5381	716.5225	712.4912	710.4755	708.4599	748.5851	746.5694
C14:0	714.5068	712.4912	710.4755	748.5851	746.5694	744.5538	740.5225	738.5068	736.4912	776.6164	774.6007
C16:0	742.5381	740.5225	738.5068	776.6164	774.6007	772.5851	768.5538	766.5381	764.5225	804.6477	802.6320
C16:1	740.5225	738.5068	736.4912	774.6007	772.5851	770.5694	766.5381	764.5225	762.5068	802.6320	800.6164
C18:0	770.5694	768.5538	766.5381	804.6477	802.6320	800.6164	796.5851	794.5694	792.5538	832.6790	830.6633
C18:1	768.5538	766.5381	764.5225	802.6320	800.6164	798.6007	794.5694	792.5538	790.5381	830.6633	828.6477
C18:2	766.5381	764.5225	762.5068	800.6164	798.6007	796.5851	792.5538	790.5381	788.5225	828.6477	826.6320
C18:3	764.5225	762.5068	760.4912	798.6007	796.5851	794.5694	790.5381	788.5225	786.5068	826.6320	824.6164
C20:0	798.6007	796.5851	794.5694	832.6790	830.6633	828.6477	824.6164	822.6007	820.5851	860.7103	858.6946
C20:1	796.5851	794.5694	792.5538	830.6633	828.6477	826.6320	822.6007	820.5851	818.5694	858.6946	856.6790
C20:2	794.5694	792.5538	790.5381	828.6477	826.6320	824.6164	820.5851	818.5694	816.5538	856.6790	854.6633
C20:3	792.5538	790.5381	788.5225	826.6320	824.6164	822.6007	818.5694	816.5538	814.5381	854.6633	852.6477
C20:4	790.5381	788.5225	786.5068	824.6164	822.6007	820.5851	816.5538	814.5381	812.5225	852.6477	850.6320
C20:5	788.5225	786.5068	784.4912	822.6007	820.5851	818.5694	814.5381	812.5225	810.5068	850.6320	848.6164
C22:0	826.6320	824.6164	822.6007	860.7103	858.6946	856.6790	852.6477	850.6320	848.6164	888.7416	886.7259
C22:1	824.6164	822.6007	820.5851	858.6946	856.6790	854.6633	850.6320	848.6164	846.6007	886.7259	884.7103
C22:2	822.6007	820.5851	818.5694	856.6790	854.6633	852.6477	848.6164	846.6007	844.5851	884.7103	882.6946
C22:4	818.5694	816.5538	814.5381	852.6477	850.6320	848.6164	844.5851	842.5694	840.5538	880.6790	878.6633
C22:5	816.5538	814.5381	812.5225	850.6320	848.6164	846.6007	842.5694	840.5538	838.5381	878.6633	876.6477
C22:6	814.5381	812.5225	810.5068	848.6164	846.6007	844.5851	840.5538	838.5381	836.5225	876.6477	874.6320
C24:0	854.6633	852.6477	850.6320	888.7416	886.7259	884.7103	880.6790	878.6633	876.6477	916.7729	914.7572
C24:1	852.6477	850.6320	848.6164	886.7259	884.7103	882.6946	878.6633	876.6477	874.6320	914.7572	912.7416

[ϟ]Matrix used for the identification of precursor $[M+H]^+$ *m/z* ratios for phosphatidylethanolamines with specific fatty acyl chains. The intersection between a fatty acid across the top row and down the first column would reveal its *m/z* ratio.

Table A.3. *Matrix for the Determination of Acyl-Specific Phosphatidylserine m/z ratios*[ϟ]

Acyl Chains	C12:0	C14:0	C16:0	C16:1	C18:0	C18:1	C18:2	C18:3	C20:0	C20:1	C20:2
C12:0	624.3871	652.4184	680.4497	678.4341	708.4810	706.4654	704.4497	702.4341	736.5123	734.4967	732.4810
C14:0	652.4184	680.4497	708.4810	706.4654	736.5123	734.4967	732.4810	730.4654	764.5436	762.5280	760.5123
C16:0	680.4497	708.4810	736.5123	734.4967	764.5436	762.5280	760.5123	758.4967	792.5749	790.5593	788.5436
C16:1	678.4341	706.4654	734.4967	732.4810	762.5280	760.5123	758.4967	756.4810	790.5593	788.5436	786.5280
C18:0	708.4810	736.5123	764.5436	762.5280	792.5749	790.5593	788.5436	786.5280	820.6062	818.5906	816.5749
C18:1	706.4654	734.4967	762.5280	760.5123	790.5593	788.5436	786.5280	784.5123	818.5906	816.5749	814.5593
C18:2	704.4497	732.4810	760.5123	758.4967	788.5436	786.5280	784.5123	782.4967	816.5749	814.5593	812.5436
C18:3	702.4341	730.4654	758.4967	756.4810	786.5280	784.5123	782.4967	780.4810	814.5593	812.5436	810.5280
C20:0	736.5123	764.5436	792.5749	790.5593	820.6062	818.5906	816.5749	814.5593	848.6375	846.6219	844.6062
C20:1	734.4967	762.5280	790.5593	788.5436	818.5906	816.5749	814.5593	812.5436	846.6219	844.6062	842.5906
C20:2	732.4810	760.5123	788.5436	786.5280	816.5749	814.5593	812.5436	810.5280	844.6062	842.5906	840.5749
C20:3	730.4654	758.4967	786.5280	784.5123	814.5593	812.5436	810.5280	808.5123	842.5906	840.5749	838.5593
C20:4	728.4498	756.4810	784.5123	782.4967	812.5436	810.5280	808.5123	806.4967	840.5749	838.5593	836.5436
C20:5	726.4341	754.4654	782.4967	780.4810	810.5280	808.5123	806.4967	804.4810	838.5593	836.5436	834.5280
C22:0	764.5436	792.5749	820.6062	818.5906	848.6375	846.6219	844.6062	842.5906	876.6688	874.6532	872.6375
C22:1	762.5280	790.5593	818.5906	816.5749	846.6219	844.6062	842.5906	840.5749	874.6532	872.6375	870.6219
C22:2	760.5123	788.5436	816.5749	814.5593	844.6062	842.5906	840.5749	838.5593	872.6375	870.6219	868.6062
C22:4	756.4810	784.5123	812.5436	810.5280	840.5749	838.5593	836.5436	834.5280	868.6062	866.5906	864.5749
C22:5	754.4654	782.4967	810.5280	808.5123	838.5593	836.5436	834.5280	832.5123	866.5906	864.5749	862.5593
C22:6	752.4497	780.4810	808.5123	806.4967	836.5436	834.5280	832.5123	830.4967	864.5749	862.5593	860.5436
C24:0	792.5749	820.6062	848.6375	846.6219	876.6688	874.6532	872.6375	870.6219	904.7001	902.6845	900.6688
C24:1	790.5593	818.5906	846.6219	844.6062	874.6532	872.6375	870.6219	868.6062	902.6845	900.6688	898.6532

Acyl Chains	C20:3	C20:4	C20:5	C22:0	C22:1	C22:2	C22:4	C22:5	C22:6	C24:0	C24:1
C12:0	730.4654	728.4498	726.4341	764.5436	762.5280	760.5123	756.4810	754.4654	752.4497	792.5749	790.5593
C14:0	758.4967	756.4810	754.4654	792.5749	790.5593	788.5436	784.5123	782.4967	780.4810	820.6062	818.5906
C16:0	786.5280	784.5123	782.4967	820.6062	818.5906	816.5749	812.5436	810.5280	808.5123	848.6375	846.6219
C16:1	784.5123	782.4967	780.4810	818.5906	816.5749	814.5593	810.5280	808.5123	806.4967	846.6219	844.6062
C18:0	814.5593	812.5436	810.5280	848.6375	846.6219	844.6062	840.5749	838.5593	836.5436	876.6688	874.6532
C18:1	812.5436	810.5280	808.5123	846.6219	844.6062	842.5906	838.5593	836.5436	834.5280	874.6532	872.6375
C18:2	810.5280	808.5123	806.4967	844.6062	842.5906	840.5749	836.5436	834.5280	832.5123	872.6375	870.6219
C18:3	808.5123	806.4967	804.4810	842.5906	840.5749	838.5593	834.5280	832.5123	830.4967	870.6219	868.6062
C20:0	842.5906	840.5749	838.5593	876.6688	874.6532	872.6375	868.6062	866.5906	864.5749	904.7001	902.6845
C20:1	840.5749	838.5593	836.5436	874.6532	872.6375	870.6219	866.5906	864.5749	862.5593	902.6845	900.6688
C20:2	838.5593	836.5436	834.5280	872.6375	870.6219	868.6062	864.5749	862.5593	860.5436	900.6688	898.6532
C20:3	836.5436	834.5280	832.5123	870.6219	868.6062	866.5906	862.5593	860.5436	858.5280	898.6532	896.6375
C20:4	834.5280	832.5123	830.4967	868.6062	866.5906	864.5749	860.5436	858.5280	856.5123	896.6375	894.6219
C20:5	832.5123	830.4967	828.4810	866.5906	864.5749	862.5593	858.5280	856.5123	854.4967	894.6219	892.6062
C22:0	870.6219	868.6062	866.5906	904.7001	902.6845	900.6688	896.6375	894.6219	892.6062	932.7314	930.7158
C22:1	868.6062	866.5906	864.5749	902.6845	900.6688	898.6532	894.6219	892.6062	890.5906	930.7158	928.7001
C22:2	866.5906	864.5749	862.5593	900.6688	898.6532	896.6375	892.6062	890.5906	888.5749	928.7001	926.6845
C22:4	862.5593	860.5436	858.5280	896.6375	894.6219	892.6062	888.5749	886.5593	884.5436	924.6688	922.6532
C22:5	860.5436	858.5280	856.5123	894.6219	892.6062	890.5906	886.5593	884.5436	882.5280	922.6532	920.6375
C22:6	858.5280	856.5123	854.4967	892.6062	890.5906	888.5749	884.5436	882.5280	880.5123	920.6375	918.6219
C24:0	898.6532	896.6375	894.6219	932.7314	930.7158	928.7001	924.6688	922.6532	920.6375	960.7627	958.7471
C24:1	896.6375	894.6219	892.6062	930.7158	928.7001	926.6845	922.6532	920.6375	918.6219	958.7471	956.7314

[ϟ]Matrix used for the identification of precursor $[M+H]^+$ *m/z* ratios for phosphatidylserines with specific fatty acyl chains. The intersection between a fatty acid across the top row and down the first column would reveal its *m/z* ratio.

Table A.4. *Matrix for the Determination of Acyl-Specific Phosphatidylinositol m/z ratios*[ϟ]

Acyl Chains	C12:0	C14:0	C16:0	C16:1	C18:0	C18:1	C18:2	C18:3	C20:0	C20:1	C20:2
C12:0	699.4079	727.4392	755.4705	753.4549	783.5018	781.4862	779.4705	777.4549	811.5331	809.5175	807.5018
C14:0	727.4392	755.4705	783.5018	781.4862	811.5331	809.5175	807.5018	805.4862	839.5644	837.5488	835.5331
C16:0	755.4705	783.5018	811.5331	809.5175	839.5644	837.5488	835.5331	833.5175	867.5957	865.5801	863.5644
C16:1	753.4549	781.4862	809.5175	807.5018	837.5488	835.5331	833.5175	831.5018	865.5801	863.5644	861.5488
C18:0	783.5018	811.5331	839.5644	837.5488	867.5957	865.5801	863.5644	861.5488	895.6270	893.6114	891.5957
C18:1	781.4862	809.5175	837.5488	835.5331	865.5801	863.5644	861.5488	859.5331	893.6114	891.5957	889.5801
C18:2	779.4705	807.5018	835.5331	833.5175	863.5644	861.5488	859.5331	857.5175	891.5957	889.5801	887.5644
C18:3	777.4549	805.4862	833.5175	831.5018	861.5488	859.5331	857.5175	855.5018	889.5801	887.5644	885.5488
C20:0	811.5331	839.5644	867.5957	865.5801	895.6270	893.6114	891.5957	889.5801	923.6583	921.6427	919.6270
C20:1	809.5175	837.5488	865.5801	863.5644	893.6114	891.5957	889.5801	887.5644	921.6427	919.6270	917.6114
C20:2	807.5018	835.5331	863.5644	861.5488	891.5957	889.5801	887.5644	885.5488	919.6270	917.6114	915.5957
C20:3	805.4862	833.5175	861.5488	859.5331	889.5801	887.5644	885.5488	883.5331	917.6114	915.5957	913.5801
C20:4	803.4706	831.5018	859.5331	857.5175	887.5644	885.5488	883.5331	881.5175	915.5957	913.5801	911.5644
C20:5	801.4549	829.4862	857.5175	855.5018	885.5488	883.5331	881.5175	879.5018	913.5801	911.5644	909.5488
C22:0	839.5644	867.5957	895.6270	893.6114	923.6583	921.6427	919.6270	917.6114	951.6896	949.6740	947.6583
C22:1	837.5488	865.5801	893.6114	891.5957	921.6427	919.6270	917.6114	915.5957	949.6740	947.6583	945.6427
C22:2	835.5331	863.5644	891.5957	889.5801	919.6270	917.6114	915.5957	913.5801	947.6583	945.6427	943.6270
C22:4	831.5018	859.5331	887.5644	885.5488	915.5957	913.5801	911.5644	909.5488	943.6270	941.6114	939.5957
C22:5	829.4862	857.5175	885.5488	883.5331	913.5801	911.5644	909.5488	907.5331	941.6114	939.5957	937.5801
C22:6	827.4705	855.5018	883.5331	881.5175	911.5644	909.5488	907.5331	905.5175	939.5957	937.5801	935.5644
C24:0	867.5957	895.6270	923.6583	921.6427	951.6896	949.6740	947.6583	945.6427	979.7209	977.7053	975.6896
C24:1	865.5801	893.6114	921.6427	919.6270	949.6740	947.6583	945.6427	943.6270	977.7053	975.6896	973.6740

Acyl Chains	C20:3	C20:4	C20:5	C22:0	C22:1	C22:2	C22:4	C22:5	C22:6	C24:0	C24:1
C12:0	805.4862	803.4706	801.4549	839.5644	837.5488	835.5331	831.5018	829.4862	827.4705	867.5957	865.5801
C14:0	833.5175	831.5018	829.4862	867.5957	865.5801	863.5644	859.5331	857.5175	855.5018	895.6270	893.6114
C16:0	861.5488	859.5331	857.5175	895.6270	893.6114	891.5957	887.5644	885.5488	883.5331	923.6583	921.6427
C16:1	859.5331	857.5175	855.5018	893.6114	891.5957	889.5801	885.5488	883.5331	881.5175	921.6427	919.6270
C18:0	889.5801	887.5644	885.5488	923.6583	921.6427	919.6270	915.5957	913.5801	911.5644	951.6896	949.6740
C18:1	887.5644	885.5488	883.5331	921.6427	919.6270	917.6114	913.5801	911.5644	909.5488	949.6740	947.6583
C18:2	885.5488	883.5331	881.5175	919.6270	917.6114	915.5957	911.5644	909.5488	907.5331	947.6583	945.6427
C18:3	883.5331	881.5175	879.5018	917.6114	915.5957	913.5801	909.5488	907.5331	905.5175	945.6427	943.6270
C20:0	917.6114	915.5957	913.5801	951.6896	949.6740	947.6583	943.6270	941.6114	939.5957	979.7209	977.7053
C20:1	915.5957	913.5801	911.5644	949.6740	947.6583	945.6427	941.6114	939.5957	937.5801	977.7053	975.6896
C20:2	913.5801	911.5644	909.5488	947.6583	945.6427	943.6270	939.5957	937.5801	935.5644	975.6896	973.6740
C20:3	911.5644	909.5488	907.5331	945.6427	943.6270	941.6114	937.5801	935.5644	933.5488	973.6740	971.6583
C20:4	909.5488	907.5331	905.5175	943.6270	941.6114	939.5957	935.5644	933.5488	931.5331	971.6583	969.6427
C20:5	907.5331	905.5175	903.5018	941.6114	939.5957	937.5801	933.5488	931.5331	929.5175	969.6427	967.6270
C22:0	945.6427	943.6270	941.6114	979.7209	977.7053	975.6896	971.6583	969.6427	967.6270	1007.7522	1005.7366
C22:1	943.6270	941.6114	939.5957	977.7053	975.6896	973.6740	969.6427	967.6270	965.6114	1005.7366	1003.7209
C22:2	941.6114	939.5957	937.5801	975.6896	973.6740	971.6583	967.6270	965.6114	963.5957	1003.7209	1001.7053
C22:4	937.5801	935.5644	933.5488	971.6583	969.6427	967.6270	963.5957	961.5801	959.5644	999.6896	997.6740
C22:5	935.5644	933.5488	931.5331	969.6427	967.6270	965.6114	961.5801	959.5644	957.5488	997.6740	995.6583
C22:6	933.5488	931.5331	929.5175	967.6270	965.6114	963.5957	959.5644	957.5488	955.5331	995.6583	993.6427
C24:0	973.6740	971.6583	969.6427	1007.7522	1005.7366	1003.7209	999.6896	997.6740	995.6583	1035.7835	1033.7679
C24:1	971.6583	969.6427	967.6270	1005.7366	1003.7209	1001.7053	997.6740	995.6583	993.6427	1033.7679	1031.7522

[ϟ]Matrix used for the identification of precursor $[M+H]^+$ *m/z* ratios for phosphatidylinositols with specific fatty acyl chains. The intersection between a fatty acid across the top row and down the first column would reveal its *m/z* ratio.

Table A.5. *Matrix for the Determination of Acyl-Specific Phosphatidylglycerol m/z ratios*[ϟ]

Acyl Chains	C12:0	C14:0	C16:0	C16:1	C18:0	C18:1	C18:2	C18:3	C20:0	C20:1	C20:2
C12:0	611.3919	639.4232	667.4545	665.4388	695.4858	693.4701	691.4545	689.4388	723.5171	721.5014	719.4858
C14:0	639.4232	667.4545	695.4858	693.4701	723.5171	721.5014	719.4858	717.4701	751.5484	749.5327	747.5171
C16:0	667.4545	695.4858	723.5171	721.5014	751.5484	749.5327	747.5171	745.5014	779.5797	777.5640	775.5484
C16:1	665.4388	693.4701	721.5014	719.4858	749.5327	747.5171	745.5014	743.4858	777.5640	775.5484	773.5327
C18:0	695.4858	723.5171	751.5484	749.5327	779.5797	777.5640	775.5484	773.5327	807.6110	805.5953	803.5797
C18:1	693.4701	721.5014	749.5327	747.5171	777.5640	775.5484	773.5327	771.5171	805.5953	803.5797	801.5640
C18:2	691.4545	719.4858	747.5171	745.5014	775.5484	773.5327	771.5171	769.5014	803.5797	801.5640	799.5484
C18:3	689.4388	717.4701	745.5014	743.4858	773.5327	771.5171	769.5014	767.4858	801.5640	799.5484	797.5327
C20:0	723.5171	751.5484	779.5797	777.5640	807.6110	805.5953	803.5797	801.5640	835.6423	833.6266	831.6110
C20:1	721.5014	749.5327	777.5640	775.5484	805.5953	803.5797	801.5640	799.5484	833.6266	831.6110	829.5953
C20:2	719.4858	747.5171	775.5484	773.5327	803.5797	801.5640	799.5484	797.5327	831.6110	829.5953	827.5797
C20:3	717.4701	745.5014	773.5327	771.5171	801.5640	799.5484	797.5327	795.5171	829.5953	827.5797	825.5640
C20:4	715.4545	743.4858	771.5171	769.5014	799.5484	797.5327	795.5171	793.5014	827.5797	825.5640	823.5484
C20:5	713.4388	741.4701	769.5014	767.4858	797.5327	795.5171	793.5014	791.4858	825.5640	823.5484	821.5327
C22:0	751.5484	779.5797	807.6110	805.5953	835.6423	833.6266	831.6110	829.5953	863.6736	861.6579	859.6423
C22:1	749.5327	777.5640	805.5953	803.5797	833.6266	831.6110	829.5953	827.5797	861.6579	859.6423	857.6266
C22:2	747.5171	775.5484	803.5797	801.5640	831.6110	829.5953	827.5797	825.5640	859.6423	857.6266	855.6110
C22:4	743.4858	771.5171	799.5484	797.5327	827.5797	825.5640	823.5484	821.5327	855.6110	853.5953	851.5797
C22:5	741.4701	769.5014	797.5327	795.5171	825.5640	823.5484	821.5327	819.5171	853.5953	851.5797	849.5640
C22:6	739.4545	767.4858	795.5171	793.5014	823.5484	821.5327	819.5171	817.5014	851.5797	849.5640	847.5484
C24:0	779.5797	807.6110	835.6423	833.6266	863.6736	861.6579	859.6423	857.6266	891.7049	889.6892	887.6736
C24:1	777.5640	805.5953	833.6266	831.6110	861.6579	859.6423	857.6266	855.6110	889.6892	887.6736	885.6579

Acyl Chains	C20:3	C20:4	C20:5	C22:0	C22:1	C22:2	C22:4	C22:5	C22:6	C24:0	C24:1
C12:0	717.4701	715.4545	713.4388	751.5484	749.5327	747.5171	743.4858	741.4701	739.4545	779.5797	777.5640
C14:0	745.5014	743.4858	741.4701	779.5797	777.5640	775.5484	771.5171	769.5014	767.4858	807.6110	805.5953
C16:0	773.5327	771.5171	769.5014	807.6110	805.5953	803.5797	799.5484	797.5327	795.5171	835.6423	833.6266
C16:1	771.5171	769.5014	767.4858	805.5953	803.5797	801.5640	797.5327	795.5171	793.5014	833.6266	831.6110
C18:0	801.5640	799.5484	797.5327	835.6423	833.6266	831.6110	827.5797	825.5640	823.5484	863.6736	861.6579
C18:1	799.5484	797.5327	795.5171	833.6266	831.6110	829.5953	825.5640	823.5484	821.5327	861.6579	859.6423
C18:2	797.5327	795.5171	793.5014	831.6110	829.5953	827.5797	823.5484	821.5327	819.5171	859.6423	857.6266
C18:3	795.5171	793.5014	791.4858	829.5953	827.5797	825.5640	821.5327	819.5171	817.5014	857.6266	855.6110
C20:0	829.5953	827.5797	825.5640	863.6736	861.6579	859.6423	855.6110	853.5953	851.5797	891.7049	889.6892
C20:1	827.5797	825.5640	823.5484	861.6579	859.6423	857.6266	853.5953	851.5797	849.5640	889.6892	887.6736
C20:2	825.5640	823.5484	821.5327	859.6423	857.6266	855.6110	851.5797	849.5640	847.5484	887.6736	885.6579
C20:3	823.5484	821.5327	819.5171	857.6266	855.6110	853.5953	849.5640	847.5484	845.5327	885.6579	883.6423
C20:4	821.5327	819.5171	817.5014	855.6110	853.5953	851.5797	847.5484	845.5327	843.5171	883.6423	881.6266
C20:5	819.5171	817.5014	815.4858	853.5953	851.5797	849.5640	845.5327	843.5171	841.5014	881.6266	879.6110
C22:0	857.6266	855.6110	853.5953	891.7049	889.6892	887.6736	883.6423	881.6266	879.6110	919.7362	917.7205
C22:1	855.6110	853.5953	851.5797	889.6892	887.6736	885.6579	881.6266	879.6110	877.5953	917.7205	915.7049
C22:2	853.5953	851.5797	849.5640	887.6736	885.6579	883.6423	879.6110	877.5953	875.5797	915.7049	913.6892
C22:4	849.5640	847.5484	845.5327	883.6423	881.6266	879.6110	875.5797	873.5640	871.5484	911.6736	909.6579
C22:5	847.5484	845.5327	843.5171	881.6266	879.6110	877.5953	873.5640	871.5484	869.5327	909.6579	907.6423
C22:6	845.5327	843.5171	841.5014	879.6110	877.5953	875.5797	871.5484	869.5327	867.5171	907.6423	905.6266
C24:0	885.6579	883.6423	881.6266	919.7362	917.7205	915.7049	911.6736	909.6579	907.6423	947.7675	945.7518
C24:1	883.6423	881.6266	879.6110	917.7205	915.7049	913.6892	909.6579	907.6423	905.6266	945.7518	943.7362

[ϟ]Matrix used for the identification of precursor $[M+H]^+$ *m/z* ratios for phosphatidylglycerols with specific fatty acyl chains. The intersection between a fatty acid across the top row and down the first column would reveal its *m/z* ratio.

Table A.6 ***Predicted Glycerophospholipid Precursor Accurate Masses***[#]

	Accurate Mass, *m/z* $[M+H]^+$		
Lipid Group	**Phosphatidylcholines**	**Phosphatidylethanolamines**	**Phosphatidylserines**
24:0	622.4442	580.3973	624.3871
24:1	620.4286	578.3817	622.3715
24:2	618.4130	576.3661	620.3559
26:0	650.4755	608.4286	652.4184
26:1	648.4599	606.4130	650.4028
26:2	646.4443	604.3974	648.3872
28:0	678.5068	636.4599	680.4497
28:1	676.4912	634.4443	678.4341
28:2	674.4756	632.4287	676.4185
30:0	706.5381	664.4912	708.4810
30:1	704.5225	662.4756	706.4654
30:2	702.5069	660.4600	704.4498
30:3	700.4913	658.4444	702.4342
30:4	698.4757	656.4288	700.4186
32:0	734.5694	692.5225	736.5123
32:1	732.5538	690.5069	734.4967
32:2	730.5382	688.4913	732.4811
32:3	728.5226	686.4757	730.4655
32:4	726.5070	684.4601	728.4499
32:5	724.4914	682.4445	726.4343
32:6	722.4758	680.4289	724.4187
34:0	762.6007	720.5538	764.5436
34:1	760.5851	718.5382	762.5280
34:2	758.5695	716.5226	760.5124
34:3	756.5539	714.5070	758.4968
34:4	754.5383	712.4914	756.4812
34:5	752.5227	710.4758	754.4656
34:6	750.5071	708.4602	752.4500
34:7	748.4915	706.4446	750.4344
36:0	790.6320	748.5851	792.5749
36:1	788.6164	746.5695	790.5593
36:2	786.6008	744.5539	788.5437
36:3	784.5852	742.5383	786.5281
36:4	782.5696	740.5227	784.5125
36:5	780.5540	738.5071	782.4969
36:6	778.5384	736.4915	780.4813
36:7	776.5228	734.4759	778.4657
38:0	818.6633	776.6164	820.6062
30:1	816.6477	774.6008	818.5906
38:2	814.6321	772.5852	816.5750

38:3	812.6165	770.5696	814.5594
38:4	810.6009	768.5540	812.5438
38:5	808.5853	766.5384	810.5282
38:6	806.5697	764.5228	808.5126
38:7	804.5541	762.5072	806.4970
40:0	846.6946	804.6477	848.6375
40:1	844.6790	802.6321	846.6219
40:2	842.6634	800.6165	844.6063
40:3	840.6478	798.6009	842.5907
40:4	838.6322	796.5853	840.5751
40:5	836.6166	794.5697	838.5595
40:6	834.6010	792.5541	836.5439
40:7	832.5854	790.5385	834.5283
40:8	830.5698	788.5229	832.5127
40:9	828.5542	786.5073	830.4971
42:0	874.7259	832.6790	876.6688
42:1	872.7103	830.6634	874.6532
42:2	870.6947	828.6478	872.6376
42:3	868.6791	826.6322	870.6220
42:4	866.6635	824.6166	868.6064
42:5	864.6479	822.6010	866.5908
42:6	862.6323	820.5854	864.5752
42:7	860.6167	818.5698	862.5596
42:8	858.6011	816.5542	860.5440
42:9	856.5855	814.5386	858.5284
42:10	854.5699	812.5230	856.5128
42:11	852.5543	810.5074	854.4972
44:0	902.7572	860.7103	904.7001
44:1	900.7416	858.6947	902.6845
44:2	898.7260	856.6791	900.6689
44:3	896.7104	854.6635	898.6533
44:4	894.6948	852.6479	896.6377
44:5	892.6792	850.6323	894.6221
44:6	890.6636	848.6167	892.6065
44:7	888.6480	846.6011	890.5909
44:8	886.6324	844.5855	888.5753
44:9	884.6168	842.5699	886.5597
44:10	882.6012	840.5543	884.5441
44:11	880.5856	838.5387	882.5285
44:12	878.5700	836.5231	880.5129
46:0	930.7885	888.7416	932.7314
46:1	928.7729	886.7260	930.7158
46:2	926.7573	884.7104	928.7002

46:3	924.7417	882.6948	926.6846
46:4	922.7261	880.6792	924.6690
46:5	920.7105	878.6636	922.6534
46:6	918.6949	876.6480	920.6378
46:7	916.6793	874.6324	918.6222
48:0	958.8198	916.7729	960.7627
48:1	956.8042	914.7573	958.7471
48:2	954.7886	912.7417	956.7315

[#]Matrix for the identification of precursor *m/z* ratios for phosphatidylcholine, phosphatidylethanolamine and phosphatidylserine lipid groups (non-acyl specific).

Table A.7 ***Predicted Triacylglycerol Precursor Accurate Masses***[#]

Lipid Group	Accurate Mass, *m/z* $[M+NH_4]^+$
42:0	740.6763
42:1	738.6606
42:2	736.6450
44:0	768.7076
44:1	766.6919
44:2	764.6763
44:3	762.6606
46:0	796.7467
46:1	794.7232
46:2	792.7076
46:3	790.6919
46:4	788.6763
48:0	824.7720
48:1	822.2553
48:2	820.7436
50:0	852.8020
50:1	850.7812
50:2	848.7726
52:0	880.8328
52:1	878.8175
52:2	876.7986
52:3	874.7862
52:4	872.7674
52:5	870.7514
54:0	908.8641
54:1	906.8534
54:2	904.8312
54:3	902.8143
54:4	900.7988
54:5	898.7857
54:6	896.7463
54:7	894.7069
56:0	936.8954
56:1	934.8797
56:2	932.8641
56:3	930.8484
56:4	928.8328
56:5	926.7880
56:6	924.8015
56:7	922.7840
56:8	920.7164

58:0	964.9267
58:1	962.9110
58:10	944.7702
58:11	942.7545
58:12	940.7389
58:2	960.8954
58:3	958.8797
58:4	956.8641
58:5	954.8484
58:6	952.8328
58:7	950.8171
58:8	948.8015
58:9	946.7858
60:0	992.9580
60:1	990.9423
60:10	972.8015
60:11	970.7858
60:12	968.7702
60:13	966.7545
60:2	988.9267
60:3	986.9110
60:4	984.8954
60:5	982.8797
60:6	980.8641
60:7	978.8484
60:8	976.8328
60:9	974.8171
62:0	1020.9893
62:1	1018.9737
62:10	1000.8333
62:11	998.8177
62:12	996.8021
62:2	1016.9581
62:3	1014.9425
62:4	1012.9269
62:5	1010.9113
62:6	1008.8957
62:7	1006.8801
62:8	1004.8645
62:9	1002.8489
64:0	1049.0206
64:1	1047.0050
64:10	1028.8646

64:11	1026.8490
64:12	1024.8334
64:2	1044.9894
64:3	1042.9738
64:4	1040.9582
64:5	1038.9426
64:6	1036.9270
64:7	1034.9114
64:8	1032.8958
64:9	1030.8802
66:0	1077.0519
66:1	1075.0363
66:10	1056.8959
66:11	1054.8803
66:2	1073.0207
66:3	1071.0051
66:4	1068.9895
66:6	1064.9583
66:7	1062.9427
66:8	1060.9271
66:9	1058.9115

[#]Matrix for the identification of precursor *m/z* ratios for triacylglycerol lipid groups (non-acyl specific).

Appendix B. Method Validation (Chapter 6)

Table B.1 ***Comprehensive Lipidomics of Cholesterol and Cholesteryl Ester Species in Whole Blood***

m/z Ratio	Molecular Adduct	Lipid	Area Under the Curve
369.3516	$[M+H-H_2O]^+$	Free Cholesterol	44074511
640.6027	$[M+NH_4]^+$	CE 16:1	1941979
642.6183	$[M+NH_4]^+$	CE 16:0	17929076
664.6027	$[M+NH_4]^+$	CE 18:3	18726347
666.6183	$[M+NH_4]^+$	CE 18:2	1471637361
668.6340	$[M+NH_4]^+$	CE 18:1	146302004
670.6496	$[M+NH_4]^+$	CE 18:0	21039879
688.6027	$[M+NH_4]^+$	CE 20:5	34869072
690.6183	$[M+NH_4]^+$	CE 20:4	330830276
692.6340	$[M+NH_4]^+$	CE 20:3	17734717
694.6496	$[M+NH_4]^+$	CE 20:2	54850605
696.6653	$[M+NH_4]^+$	CE 20:1	14691256
698.6809	$[M+NH_4]^+$	CE 20:0	3560071
714.6183	$[M+NH_4]^+$	CE 22:6	55135656
716.6340	$[M+NH_4]^+$	CE 22:5	4879891
718.6496	$[M+NH_4]^+$	CE 22:4	20319563
724.6966	$[M+NH_4]^+$	CE 22:1	5505764
726.7122	$[M+NH_4]^+$	CE 22:0	1903873
752.7279	$[M+NH_4]^+$	CE 24:1	3760657
754.7435	$[M+NH_4]^+$	CE 24:0	514724

Mass-to-charge ratio (*m/z*); Cholesteryl ester (CE).

Appendix B. Method Validation (Chapter 6)

Table B.2 ***Comprehensive Lipidomics of Phosphatidylcholine Species in Whole Blood***

m/z Ratio	Molecular Adduct	Lipid	Lipid Group	Area under the Curve
496.3399	$[M+H]^+$	lyso-16:0 PC		1054184678
522.3556	$[M+H]^+$	lyso-18:1 PC		246445199
524.3710	$[M+H]^+$	lyso-18:0 PC		381953150
618.4130	$[M+H]^+$		PC 24:2	5293777
620.4286	$[M+H]^+$		PC 24:1	8683479
622.4442	$[M+H]^+$		PC 24:0	283579
646.4443	$[M+H]^+$		PC 26:2	<LOD
648.4599	$[M+H]^+$		PC 26:1	13869347
650.4755	$[M+H]^+$		PC 26:0	<LOD
674.4756	$[M+H]^+$		PC 28:2	<LOD
676.4912	$[M+H]^+$		PC 28:1	<LOD
678.5068	$[M+H]^+$		PC 28:0	1032753
698.4757	$[M+H]^+$		PC 30:4	<LOD
700.4913	$[M+H]^+$		PC 30:3	356366
702.5069	$[M+H]^+$		PC 30:2	2850946
704.5225	$[M+H]^+$		PC 30:1	11496406
706.5381	$[M+H]^+$		PC 30:0	130414318
722.4758	$[M+H]^+$		PC 32:6	2216626
724.4914	$[M+H]^+$		PC 32:5	4335569
726.5070	$[M+H]^+$		PC 32:4	1801215
728.5226	$[M+H]^+$		PC 32:3	5977234
730.5378	$[M+H]^+$	PC 14:0/18:2	PC 32:2	43413080
730.5378	$[M+H]^+$			18711386
732.5538	$[M+H]^+$		PC 32:1	456884323
732.5538	$[M+H]^+$	PC 16:0/16:1		401103023
734.5694	$[M+H]^+$		PC 32:0	736489764
734.5694	$[M+H]^+$	PC 16:0/16:0		673269675
748.4915	$[M+H]^+$		PC 34:7	<LOD
750.5071	$[M+H]^+$		PC 34:6	4904911
752.5227	$[M+H]^+$		PC 34:5	13563503
754.5383	$[M+H]^+$		PC 34:4	50472182
756.5539	$[M+H]^+$		PC 34:3	300224436
758.5695	$[M+H]^+$		PC 34:2	13540304839
758.5695	$[M+H]^+$	PC 16:0/18:2		13085851102
760.5843	$[M+H]^+$	PC 16:0/18:1	PC 34:1	6792037828
760.5843	$[M+H]^+$			8603126442
762.6007	$[M+H]^+$		PC 34:0	2272134454
776.5228	$[M+H]^+$		PC 36:7	<LOD
778.5384	$[M+H]^+$		PC 36:6	<LOD
780.5537	$[M+H]^+$	PC 16:0/20:5	PC 36:5	566524647
780.5537	$[M+H]^+$			798112731

782.5693	$[M+H]^+$	PC 18:2/18:2		234439064
782.5696	$[M+H]^+$		PC 36:4	12013187125
782.5699	$[M+H]^+$	PC 16:0/20:4		11232517157
784.5255	$[M+H]^+$	PC 18:1/18:2		1384783855
784.5852	$[M+H]^+$		PC 36:3	4276038119
784.5858	$[M+H]^+$	PC 16:0/20:3		783986453
786.6008	$[M+H]^+$			5684295432
786.6021	$[M+H]^+$	PC 18:1/18:1	PC 36:2	735455506
786.6022	$[M+H]^+$	PC 18:0/18:2		4381677582
788.6164	$[M+H]^+$		PC 36:1	2408553034
788.6178	$[M+H]^+$	PC 18:0/18:1		1656390362
790.6320	$[M+H]^+$		PC 36:0	246908217
804.5541	$[M+H]^+$		PC 38:7	584316889
806.5697	$[M+H]^+$		PC 38:6	1225689021
806.5701	$[M+H]^+$	PC 16:0/22:6		849451102
808.5853	$[M+H]^+$			1681214263
808.5862	$[M+H]^+$	PC 18:0/20:5	PC 38:5	200965596
808.5872	$[M+H]^+$	PC 18:1/20:4		828143821
810.6008	$[M+H]^+$	PC 18:0/20:4		1866759061
810.6009	$[M+H]^+$		PC 38:4	2476911499
810.6028	$[M+H]^+$	PC 18:1/20:3		62773961
812.6165	$[M+H]^+$		PC 38:3	474034308
812.6178	$[M+H]^+$	PC 18:0/20:3		341037865
814.6321	$[M+H]^+$		PC 38:2	157403704
816.6477	$[M+H]^+$		PC 38:1	25828217
818.6633	$[M+H]^+$		PC 38:0	3604768
828.5542	$[M+H]^+$		PC 40:9	71745446
830.5698	$[M+H]^+$		PC 40:8	77675246
832.5848	$[M+H]^+$	PC 18:1/22:6	PC 40:7	43263364
832.5854	$[M+H]^+$			266831772
834.6010	$[M+H]^+$		PC 40:6	325786223
834.6014	$[M+H]^+$	PC 18:0/22:6		247551540
836.6166	$[M+H]^+$		PC 40:5	111124185
838.6322	$[M+H]^+$		PC 40:4	73202889
838.6367	$[M+H]^+$	PC 18:0/22:4		24522523
840.6478	$[M+H]^+$		PC 40:3	2306992
842.6634	$[M+H]^+$		PC 40:2	<LOD
844.6790	$[M+H]^+$		PC 40:1	<LOD
846.6946	$[M+H]^+$		PC 40:0	<LOD
852.5543	$[M+H]^+$		PC 42:11	<LOD
854.5699	$[M+H]^+$		PC 42:10	<LOD
856.5855	$[M+H]^+$		PC 42:9	19768308
858.6011	$[M+H]^+$		PC 42:8	8440167

860.6167	$[M+H]^+$	PC 42:7	3124636
862.6323	$[M+H]^+$	PC 42:6	24941042
864.6479	$[M+H]^+$	PC 42:5	<LOD
866.6635	$[M+H]^+$	PC 42:4	<LOD
868.6791	$[M+H]^+$	PC 42:3	<LOD
870.6947	$[M+H]^+$	PC 42:2	<LOD
872.7103	$[M+H]^+$	PC 42:1	<LOD
874.7259	$[M+H]^+$	PC 42:0	<LOD
878.5700	$[M+H]^+$	PC 44:12	<LOD
880.5856	$[M+H]^+$	PC 44:11	8639161
882.6012	$[M+H]^+$	PC 44:10	<LOD
884.6168	$[M+H]^+$	PC 44:9	<LOD
886.6324	$[M+H]^+$	PC 44:8	<LOD
888.6480	$[M+H]^+$	PC 44:7	<LOD
890.6636	$[M+H]^+$	PC 44:6	<LOD
892.6792	$[M+H]^+$	PC 44:5	<LOD
894.6948	$[M+H]^+$	PC 44:4	<LOD
896.7104	$[M+H]^+$	PC 44:3	<LOD
898.7260	$[M+H]^+$	PC 44:2	<LOD
900.7416	$[M+H]^+$	PC 44:1	<LOD
902.7572	$[M+H]^+$	PC 44:0	<LOD
916.6793	$[M+H]^+$	PC 46:7	<LOD
918.6949	$[M+H]^+$	PC 46:6	<LOD
920.7105	$[M+H]^+$	PC 46:5	<LOD
922.7261	$[M+H]^+$	PC 46:4	<LOD
924.7417	$[M+H]^+$	PC 46:3	<LOD
926.7573	$[M+H]^+$	PC 46:2	<LOD
928.7729	$[M+H]^+$	PC 46:1	<LOD
930.7885	$[M+H]^+$	PC 46:0	<LOD
954.7886	$[M+H]^+$	PC 48:2	<LOD
956.8042	$[M+H]^+$	PC 48:1	<LOD
958.8198	$[M+H]^+$	PC 48:0	<LOD

Mass-to-charge ratio (*m/z*); Phosphatidylcholine (PC); Limit of detection (LOD).

Appendix B. Method Validation (Chapter 6)

Table B.3. ***Comprehensive Lipidomics of Phosphatidylethanolamine and Plasmenyl-Phosphatidylethanolamine Species in Whole Blood***

m/z Ratio	Molecular Adduct	Lipid	Lipid Group	Area Under the Curve
576.3661	$[M+H]^+$		PE 24:2	<LOD
578.3817	$[M+H]^+$		PE 24:1	<LOD
580.3973	$[M+H]^+$		PE 24:0	1866840
604.3974	$[M+H]^+$		PE 26:2	<LOD
606.4130	$[M+H]^+$		PE 26:1	<LOD
608.4286	$[M+H]^+$		PE 26:0	3519976
632.4287	$[M+H]^+$		PE 28:2	<LOD
634.4443	$[M+H]^+$		PE 28:1	7990002
636.4599	$[M+H]^+$		PE 28:0	<LOD
656.4288	$[M+H]^+$		PE 30:4	<LOD
658.4444	$[M+H]^+$		PE 30:3	<LOD
660.4600	$[M+H]^+$		PE 30:2	<LOD
662.4756	$[M+H]^+$		PE 30:1	<LOD
664.4912	$[M+H]^+$		PE 30:0	<LOD
680.4289	$[M+H]^+$		PE 32:6	<LOD
682.4445	$[M+H]^+$		PE 32:5	<LOD
684.4601	$[M+H]^+$		PE 32:4	<LOD
686.4757	$[M+H]^+$		PE 32:3	<LOD
688.4913	$[M+H]^+$		PE 32:2	<LOD
690.5069	$[M+H]^+$		PE 32:1	63548261
692.5225	$[M+H]^+$		PE 32:0	11690609
706.4446	$[M+H]^+$		PE 34:7	<LOD
708.4602	$[M+H]^+$		PE 34:6	<LOD
710.4758	$[M+H]^+$		PE 34:5	<LOD
712.4914	$[M+H]^+$		PE 34:4	<LOD
714.5070	$[M+H]^+$		PE 34:3	1027096
716.5226	$[M+H]^+$		PE 34:2	140866889
716.5322	$[M+H]^+$	PE 16:0/18:2		115800324
718.5380	$[M+H]^+$	PE 16:0/18:1	PE 34:1	316732311
718.5382	$[M+H]^+$			352269192
720.5538	$[M+H]^+$		PE 34:0	62109295
722.5094	$[M+H]^+$	Plasmenyl-PE P-16:0/20:5		28813754
724.5284	$[M+H]^+$	Plasmenyl-PE P-16:0/20:4		235265833
730.5733	$[M+H]^+$	Plasmenyl-PE P-18:0/18:1	54946073	
734.4759	$[M+H]^+$		PE 36:7	<LOD
736.4915	$[M+H]^+$		PE 36:6	<LOD
738.5069	$[M+H]^+$	PE 16:0/20:5	PE 36:5	17290571
738.5071	$[M+H]^+$			19289309

740.5227	$[M+H]^+$		PE 36:4	332524679
740.5247	$[M+H]^+$	PE 16:0/20:4		267961188
742.5381	$[M+H]^+$	PE 18:1/18:2	PE 36:3	138352337
742.5383	$[M+H]^+$			269068248
744.5539	$[M+H]^+$		PE 36:2	218373496
744.5897	$[M+H]^+$	PE 18:1/18:1		86650818
746.5690	$[M+H]^+$	PE 18:0/18:1	PE 36:1	111455765
746.5695	$[M+H]^+$			220162562
748.5298	$[M+H]^+$	Plasmenyl-PE P-16:0/22:6		75173546
748.5851	$[M+H]^+$		PE 36:0	5036671
750.5428	$[M+H]^+$	Plasmenyl-PE P-16:0/22:5		142621474
752.5598	$[M+H]^+$	Plasmenyl-PE P-18:0/20:4		445638736
762.5072	$[M+H]^+$		PE 38:7	39960549
764.5228	$[M+H]^+$		PE 38:6	296147456
764.5229	$[M+H]^+$	PE 16:0/22:6		259526686
766.5370	$[M+H]^+$	PE 18:1/20:4	PE 38:5	213226059
766.5384	$[M+H]^+$			300220305
768.5512	$[M+H]^+$	PE 18:0/20:4	PE 38:4	291632129
768.5540	$[M+H]^+$			397548274
770.5696	$[M+H]^+$		PE 38:3	57089712
772.5852	$[M+H]^+$		PE 38:2	147731642
774.6008	$[M+H]^+$		PE 38:1	113010509
776.6164	$[M+H]^+$		PE 38:0	10404390
780.5911	$[M+H]^+$	Plasmenyl-PE P-18:0/22:4	106184046	
786.5073	$[M+H]^+$		PE 40:9	<LOD
788.5229	$[M+H]^+$		PE 40:8	44500366
790.5385	$[M+H]^+$		PE 40:7	131989503
792.5541	$[M+H]^+$		PE 40:6	56883074
794.5697	$[M+H]^+$		PE 40:5	59570445
796.5853	$[M+H]^+$		PE 40:4	89050243
798.6009	$[M+H]^+$		PE 40:3	35482485
800.6165	$[M+H]^+$		PE 40:2	<LOD
802.6321	$[M+H]^+$		PE 40:1	<LOD
804.6477	$[M+H]^+$		PE 40:0	27820806
810.5074	$[M+H]^+$		PE 42:11	<LOD
812.5230	$[M+H]^+$		PE 42:10	<LOD
814.5386	$[M+H]^+$		PE 42:9	<LOD
816.5542	$[M+H]^+$		PE 42:8	<LOD
818.5698	$[M+H]^+$		PE 42:7	<LOD
820.5854	$[M+H]^+$		PE 42:6	26330221
822.6010	$[M+H]^+$		PE 42:5	<LOD

824.6166	$[M+H]^+$	PE 42:4	16589395
826.6322	$[M+H]^+$	PE 42:3	9659705
828.6478	$[M+H]^+$	PE 42:2	<LOD
830.6634	$[M+H]^+$	PE 42:1	<LOD
832.6790	$[M+H]^+$	PE 42:0	<LOD
836.5231	$[M+H]^+$	PE 44:12	<LOD
838.5387	$[M+H]^+$	PE 44:11	<LOD
840.5543	$[M+H]^+$	PE 44:10	<LOD
842.5699	$[M+H]^+$	PE 44:9	<LOD
844.5855	$[M+H]^+$	PE 44:8	<LOD
846.6011	$[M+H]^+$	PE 44:7	<LOD
848.6167	$[M+H]^+$	PE 44:6	<LOD
850.6323	$[M+H]^+$	PE 44:5	<LOD
852.6479	$[M+H]^+$	PE 44:4	<LOD
854.6635	$[M+H]^+$	PE 44:3	<LOD
856.6791	$[M+H]^+$	PE 44:2	<LOD
858.6947	$[M+H]^+$	PE 44:1	<LOD
860.7103	$[M+H]^+$	PE 44:0	<LOD
874.6324	$[M+H]^+$	PE 46:7	<LOD
876.6480	$[M+H]^+$	PE 46:6	<LOD
878.6636	$[M+H]^+$	PE 46:5	<LOD
880.6792	$[M+H]^+$	PE 46:4	<LOD
882.6948	$[M+H]^+$	PE 46:3	<LOD
884.7104	$[M+H]^+$	PE 46:2	<LOD
886.7260	$[M+H]^+$	PE 46:1	<LOD
888.7416	$[M+H]^+$	PE 46:0	<LOD
912.7417	$[M+H]^+$	PE 48:2	<LOD
914.7573	$[M+H]^+$	PE 48:1	<LOD
916.7729	$[M+H]^+$	PE 48:0	<LOD

Mass-to-charge ratio (*m/z*); Phosphatidylethanolamine (PE); Limit of detection (LOD).

Appendix B. Method Validation (Chapter 6)

Table B.4 ***Comprehensive Lipidomics of Phosphatidylserine Species in Whole Blood***

m/z Ratio	Molecular Adduct	Lipid	Lipid Group	Area Under the Curve
620.3559	$[M+H]^+$		PS 24:2	<LOD
622.3715	$[M+H]^+$		PS 24:1	<LOD
624.3871	$[M+H]^+$		PS 24:0	<LOD
648.3872	$[M+H]^+$		PS 26:2	<LOD
650.4028	$[M+H]^+$		PS 26:1	<LOD
652.4184	$[M+H]^+$		PS 26:0	650991
676.4185	$[M+H]^+$		PS 28:2	<LOD
678.4341	$[M+H]^+$		PS 28:1	<LOD
680.4497	$[M+H]^+$		PS 28:0	420877
700.4186	$[M+H]^+$		PS 30:4	<LOD
702.4342	$[M+H]^+$		PS 30:3	<LOD
704.4498	$[M+H]^+$		PS 30:2	<LOD
706.4654	$[M+H]^+$		PS 30:1	<LOD
708.4810	$[M+H]^+$		PS 30:0	661455
724.4187	$[M+H]^+$		PS 32:6	<LOD
726.4343	$[M+H]^+$		PS 32:5	<LOD
728.4499	$[M+H]^+$		PS 32:4	<LOD
730.4655	$[M+H]^+$		PS 32:3	<LOD
732.4811	$[M+H]^+$		PS 32:2	<LOD
734.4967	$[M+H]^+$		PS 32:1	<LOD
736.5123	$[M+H]^+$		PS 32:0	822370
750.4344	$[M+H]^+$		PS 34:7	<LOD
752.4500	$[M+H]^+$		PS 34:6	<LOD
754.4656	$[M+H]^+$		PS 34:5	<LOD
756.4812	$[M+H]^+$		PS 34:4	<LOD
758.4968	$[M+H]^+$		PS 34:3	1357458
760.5124	$[M+H]^+$		PS 34:2	<LOD
762.5280	$[M+H]^+$		PS 34:1	5189348
764.5436	$[M+H]^+$		PS 34:0	14408944
778.4657	$[M+H]^+$		PS 36:7	16740318
780.4813	$[M+H]^+$		PS 36:6	<LOD
782.4969	$[M+H]^+$		PS 36:5	<LOD
784.5125	$[M+H]^+$		PS 36:4	<LOD
786.5281	$[M+H]^+$		PS 36:3	<LOD
788.5437	$[M+H]^+$		PS 36:2	30759943
790.5593	$[M+H]^+$		PS 36:1	77869885
790.5593	$[M+H]^+$	PS 18:0/18:1		65018065
792.5749	$[M+H]^+$		PS 36:0	<LOD
806.4970	$[M+H]^+$		PS 38:7	<LOD
808.5126	$[M+H]^+$		PS 38:6	<LOD
810.5282	$[M+H]^+$		PS 38:5	67450286

812.5438	$[M+H]^+$		PS 38:4	788138088
812.5553	$[M+H]^+$	PS 18:0/20:4		738414886
814.5512	$[M+H]^+$	PS 18:0/20:3	PS 38:3	28998762
814.5594	$[M+H]^+$			133024430
816.5750	$[M+H]^+$		PS 38:2	8024747
818.5906	$[M+H]^+$		PS 38:1	<LOD
820.6062	$[M+H]^+$		PS 38:0	<LOD
830.4971	$[M+H]^+$		PS 40:9	<LOD
832.5127	$[M+H]^+$		PS 40:8	<LOD
834.5283	$[M+H]^+$		PS 40:7	<LOD
836.5407	$[M+H]^+$	PS 18:0/22:6	PS 40:6	543442262
836.5439	$[M+H]^+$			564797028
838.5588	$[M+H]^+$	PS 18:0/22:5	PS 40:5	2344653
838.5595	$[M+H]^+$			148621873
840.5751	$[M+H]^+$		PS 40:4	67518015
842.5907	$[M+H]^+$		PS 40:3	<LOD
844.6063	$[M+H]^+$		PS 40:2	<LOD
846.6219	$[M+H]^+$		PS 40:1	<LOD
848.6375	$[M+H]^+$		PS 40:0	<LOD
854.4972	$[M+H]^+$		PS 42:11	<LOD
856.5128	$[M+H]^+$		PS 42:10	<LOD
858.5284	$[M+H]^+$		PS 42:9	<LOD
860.5440	$[M+H]^+$		PS 42:8	<LOD
862.5596	$[M+H]^+$		PS 42:7	11896503
864.5752	$[M+H]^+$		PS 42:6	<LOD
866.5908	$[M+H]^+$		PS 42:5	<LOD
868.6064	$[M+H]^+$		PS 42:4	<LOD
870.6220	$[M+H]^+$		PS 42:3	<LOD
872.6376	$[M+H]^+$		PS 42:2	<LOD
874.6532	$[M+H]^+$		PS 42:1	<LOD
876.6688	$[M+H]^+$		PS 42:0	<LOD
880.5129	$[M+H]^+$		PS 44:12	<LOD
882.5285	$[M+H]^+$		PS 44:11	<LOD
884.5441	$[M+H]^+$		PS 44:10	<LOD
886.5597	$[M+H]^+$		PS 44:9	<LOD
888.5753	$[M+H]^+$		PS 44:8	<LOD
890.5909	$[M+H]^+$		PS 44:7	<LOD
892.6065	$[M+H]^+$		PS 44:6	<LOD
894.6221	$[M+H]^+$		PS 44:5	<LOD
896.6377	$[M+H]^+$		PS 44:4	<LOD
898.6533	$[M+H]^+$		PS 44:3	<LOD
900.6689	$[M+H]^+$		PS 44:2	<LOD
902.6845	$[M+H]^+$		PS 44:1	<LOD

904.7001	$[M+H]^+$	PS 44:0	<LOD
918.6222	$[M+H]^+$	PS 46:7	<LOD
920.6378	$[M+H]^+$	PS 46:6	16454351
922.6534	$[M+H]^+$	PS 46:5	6851312
924.6690	$[M+H]^+$	PS 46:4	<LOD
926.6846	$[M+H]^+$	PS 46:3	<LOD
928.7002	$[M+H]^+$	PS 46:2	<LOD
930.7158	$[M+H]^+$	PS 46:1	<LOD
932.7314	$[M+H]^+$	PS 46:0	<LOD
956.7315	$[M+H]^+$	PS 48:2	<LOD
958.7471	$[M+H]^+$	PS 48:1	<LOD
960.7627	$[M+H]^+$	PS 48:0	<LOD

Mass-to-charge ratio (*m/z*); Phosphatidylserine (PS); Limit of detection (LOD).

Appendix B. Method Validation (Chapter 6)

Table B.5 ***Comprehensive Lipidomics of Sphingomyelin Species in Whole Blood***

m/z Ratio	Molecular Adduct	Lipid	Lipid Group	Area Under the Curve
703.5755	$[M+H]^+$		SM 34:1	2373406140
725.5565	$[M+Na]^+$		SM 34:1	376987084
701.5595	$[M+H]^+$		SM 34:2	194385143
731.6069	$[M+H]^+$		SM 36:1	247459601
729.5918	$[M+H]^+$		SM 36:2	717627881

Mass-to-charge ratio (*m/z*); Sphingomyelin (SM).

Appendix B. Method Validation (Chapter 6)

Table B.6 ***Comprehensive Lipidomics of Triacylglycerol Species in Whole Blood***

m/z Ratio	Molecular Adduct	Lipid	Lipid Group	Area Under the Curve
736.6450	$[M+NH_4]^+$		TAG 42:2	4186014
738.6606	$[M+NH_4]^+$		TAG 42:1	17664651
740.6763	$[M+NH_4]^+$		TAG 42:0	46929040
762.6606	$[M+NH_4]^+$		TAG 44:3	3430004
764.6763	$[M+NH_4]^+$		TAG 44:2	31060791
766.6919	$[M+NH_4]^+$	TAG 12:0/14:1/18:0		
766.6919	$[M+NH_4]^+$	TAG 14:0/14:0/16:1	TAG 44:1	
766.6919	$[M+NH_4]^+$	TAG 14:0/14:1/16:0		
766.6919	$[M+NH_4]^+$			92627876
768.7076	$[M+NH_4]^+$	TAG 12:0/14:0/18:0		
768.7076	$[M+NH_4]^+$	TAG 14:0/14:0/16:0	TAG 44:0	
768.7076	$[M+NH_4]^+$			146311692
788.6763	$[M+NH_4]^+$		TAG 46:4	17338363
790.6919	$[M+NH_4]^+$		TAG 46:3	23758702
792.7076	$[M+NH_4]^+$	TAG 12:0/14:1/18:2		
792.7076	$[M+NH_4]^+$	TAG 12:0/16:1/18:1		
792.7076	$[M+NH_4]^+$	TAG 14:0/16:1/16:1	TAG 46:2	
792.7076	$[M+NH_4]^+$	TAG 14:1/16:0/16:1		
792.7076	$[M+NH_4]^+$			132990657
794.7232	$[M+NH_4]^+$	TAG 12:0/16:1/18:0		
794.7232	$[M+NH_4]^+$	TAG 14:0/16:0/16:1	TAG 46:1	115479784
794.7232	$[M+NH_4]^+$			275697544
796.7467	$[M+NH_4]^+$	TAG 12:0/16:0/18:0		
796.7467	$[M+NH_4]^+$	TAG 14:0/16:0/16:0	TAG 46:0	
796.7467	$[M+NH_4]^+$			349068286
820.7436	$[M+NH_4]^+$	TAG 12:0/18:1/18:1		
820.7436	$[M+NH_4]^+$	TAG 14:0/14:0/20:2		
820.7436	$[M+NH_4]^+$	TAG 14:0/16:0/18:2		
820.7436	$[M+NH_4]^+$	TAG 14:0/16:1/18:1	TAG 48:2	78240364
820.7436	$[M+NH_4]^+$	TAG 14:1/16:0/18:1		
820.7436	$[M+NH_4]^+$	TAG 16:0/16:1/16:1		
820.7436	$[M+NH_4]^+$			363551003
822.2553	$[M+NH_4]^+$	TAG 14:0/16:0/18:1		236386132
822.2553	$[M+NH_4]^+$	TAG 16:0/16:0/16:1	TAG 48:1	127001336
822.2553	$[M+NH_4]^+$			515410069
824.7720	$[M+NH_4]^+$	TAG 12:0/16:0/20:0		
824.7720	$[M+NH_4]^+$	TAG 12:0/18:0/18:0		
824.7720	$[M+NH_4]^+$	TAG 14:0/14:0/20:0	TAG 48:0	
824.7720	$[M+NH_4]^+$	TAG 14:0/16:0/18:0		
824.7720	$[M+NH_4]^+$	TAG 16:0/16:0/16:0		137360765
824.7720	$[M+NH_4]^+$			413048012

848.7726	$[M+NH_4]^+$	TAG 14:0/18:1/18:1		
848.7726	$[M+NH_4]^+$	TAG 16:0/16:0/18:2		
848.7726	$[M+NH_4]^+$	TAG 16:0/16:1/18:1	TAG 50:2	
848.7726	$[M+NH_4]^+$	TAG 16:1/16:0/18:0		
848.7726	$[M+NH_4]^+$	TAG 16:1/16:1/18:0		
848.7726	$[M+NH_4]^+$			1065347409
850.7812	$[M+NH_4]^+$	TAG 14:0/16:0/20:1		
850.7812	$[M+NH_4]^+$	TAG 16:0/16:0/18:1	TAG 50:1	398027936
850.7812	$[M+NH_4]^+$			479183927
852.8020	$[M+NH_4]^+$	TAG 14:0/18:0/20:0		
852.8020	$[M+NH_4]^+$	TAG 16:0/16:0/18:0	TAG 50:0	503657742
852.8020	$[M+NH_4]^+$			95674075
870.7514	$[M+NH_4]^+$	TAG 16:0/18:2/18:3		
870.7514	$[M+NH_4]^+$	TAG 16:1/18:1/18:3	TAG 52:5	
870.7514	$[M+NH_4]^+$	TAG 16:1/18:2/18:2		31525771
870.7514	$[M+NH_4]^+$			302425017
872.7674	$[M+NH_4]^+$	TAG 16:0/18:1/18:3		302184166
872.7674	$[M+NH_4]^+$	TAG 16:0/18:2/18:2	TAG 52:4	600636961
872.7674	$[M+NH_4]^+$	TAG 16:1/18:1/18:2		219315443
872.7674	$[M+NH_4]^+$			1152786133
874.7862	$[M+NH_4]^+$	TAG 16:0/18:1/18:2		2695509654
874.7862	$[M+NH_4]^+$	TAG 16:1/18:1/18:1	TAG 52:3	272298752
874.7862	$[M+NH_4]^+$			3093089589
876.7986	$[M+NH_4]^+$	TAG 14:0/18:1/20:1		81396930
876.7986	$[M+NH_4]^+$	TAG 16:0/18:1/18:1	TAG 52:2	2870568710
876.7986	$[M+NH_4]^+$			2917011757
878.8175	$[M+NH_4]^+$	TAG 14:0/18:1/20:0		15355180
878.8175	$[M+NH_4]^+$	TAG 16:0/18:0/18:1	TAG 52:1	155316559
878.8175	$[M+NH_4]^+$			192326441
880.8328	$[M+NH_4]^+$	TAG 12:0/16:0/22:0		
880.8328	$[M+NH_4]^+$	TAG 14:0/16:0/18:0	TAG 52:0	
880.8328	$[M+NH_4]^+$	TAG 16:0/18:0/18:0		
880.8328	$[M+NH_4]^+$			65781339
894.7069	$[M+NH_4]^+$	TAG 14:0/18:2/22:5		
894.7069	$[M+NH_4]^+$	TAG 16:0/18:2/20:5		
894.7069	$[M+NH_4]^+$	TAG 18:1/18:3/18:3	TAG 54:7	17147086
894.7069	$[M+NH_4]^+$	TAG 18:2/18:2/18:3		24418374
894.7069	$[M+NH_4]^+$			147616344
896.7463	$[M+NH_4]^+$	TAG 14:0/18:1/22:5		
896.7463	$[M+NH_4]^+$	TAG 16:0/18:1/20:5		67166181
896.7463	$[M+NH_4]^+$	TAG 16:0/18:2/20:4	TAG 54:6	
896.7463	$[M+NH_4]^+$	TAG 18:1/18:2/18:3		156879087
896.7463	$[M+NH_4]^+$	TAG 18:2/18:2/18:2		40560451

896.7463	$[M+NH_4]^+$			484025594
898.7857	$[M+NH_4]^+$	TAG 16:0/16:0/22:5		
898.7857	$[M+NH_4]^+$	TAG 16:0/18:1/20:4		134277520
898.7857	$[M+NH_4]^+$	TAG 16:0/18:2/20:3	TAG 54:5	
898.7857	$[M+NH_4]^+$	TAG 18:1/18:1/18:3		205752055
898.7857	$[M+NH_4]^+$	TAG 18:1/18:2/18:2		426220158
898.7857	$[M+NH_4]^+$			909030524
900.7988	$[M+NH_4]^+$	TAG 16:0/18:1/20:3		172551468
900.7988	$[M+NH_4]^+$	TAG 18:1/18:1/18:2	TAG 54:4	1563813145
900.7988	$[M+NH_4]^+$			2203244769
902.8143	$[M+NH_4]^+$	TAG 16:0/18:1/20:2		
902.8143	$[M+NH_4]^+$	TAG 18:0/18:1/18:2	TAG 54:3	258388211
902.8143	$[M+NH_4]^+$	TAG 18:1/18:1/18:1		1338600628
902.8143	$[M+NH_4]^+$			2265063290
904.8312	$[M+NH_4]^+$	TAG 16:0/18:0/20:2		
904.8312	$[M+NH_4]^+$	TAG 16:0/18:1/20:1	TAG 54:2	
904.8312	$[M+NH_4]^+$	TAG 18:0/18:1/18:1		
904.8312	$[M+NH_4]^+$			1225901399
906.8534	$[M+NH_4]^+$	TAG 16:0/16:1/22:0		
906.8534	$[M+NH_4]^+$	TAG 16:0/18:0/20:1		
906.8534	$[M+NH_4]^+$	TAG 16:0/18:1/20:0	TAG 54:1	
906.8534	$[M+NH_4]^+$	TAG 16:1/18:0/20:0		
906.8534	$[M+NH_4]^+$	TAG 18:0/18:0/18:1		
906.8534	$[M+NH_4]^+$			344023487
908.8641	$[M+NH_4]^+$		TAG 54:0	140684022
920.7164	$[M+NH_4]^+$	TAG 16:0/18:2/22:6		
920.7164	$[M+NH_4]^+$	TAG 16:0/18:3/22:5		
920.7164	$[M+NH_4]^+$	TAG 16:0/20:4/20:4		
920.7164	$[M+NH_4]^+$	TAG 18:1/18:2/20:5	TAG 56:8	
920.7164	$[M+NH_4]^+$	TAG 18:1/18:3/20:4		
920.7164	$[M+NH_4]^+$	TAG 18:2/18:2/20:4		
920.7164	$[M+NH_4]^+$			164657162
922.7840	$[M+NH_4]^+$	TAG 16:0/18:1/22:6		133460906
922.7840	$[M+NH_4]^+$	TAG 16:0/18:2/22:5		
922.7840	$[M+NH_4]^+$	TAG 16:0/20:3/20:4	TAG 56:7	
922.7840	$[M+NH_4]^+$	TAG 18:1/18:1/20:5		
922.7840	$[M+NH_4]^+$			343796330
924.8015	$[M+NH_4]^+$	TAG 16:0/18:1/22:5		
924.8015	$[M+NH_4]^+$	TAG 16:0/20:2/20:4	TAG 56:6	
924.8015	$[M+NH_4]^+$			511904034
926.7880	$[M+NH_4]^+$	TAG 16:0/18:0/22:5		
926.7880	$[M+NH_4]^+$	TAG 18:0/18:1/20:4	TAG 56:5	97606884
926.7880	$[M+NH_4]^+$	TAG 18:1/18:1/20:3		

926.7880	$[M+NH_4]^+$			523769967
928.8328	$[M+NH_4]^+$		TAG 56:4	532758186
930.8484	$[M+NH_4]^+$	TAG 18:0/18:1/20:2		
930.8484	$[M+NH_4]^+$	TAG 18:0/18:2/20:1		
930.8484	$[M+NH_4]^+$	TAG 18:1/18:1/20:1	TAG 56:3	
930.8484	$[M+NH_4]^+$	TAG 18:1/18:2/20:0		
930.8484	$[M+NH_4]^+$			701215457
932.8641	$[M+NH_4]^+$		TAG 56:2	566747136
934.8797	$[M+NH_4]^+$		TAG 56:1	210937697
936.8954	$[M+NH_4]^+$		TAG 56:0	67035881
940.7389	$[M+NH_4]^+$		TAG 58:12	2375764
942.7545	$[M+NH_4]^+$		TAG 58:11	11774262
944.7702	$[M+NH_4]^+$		TAG 58:10	39590063
946.7858	$[M+NH_4]^+$		TAG 58:9	11508803
948.8015	$[M+NH_4]^+$		TAG 58:8	179183287
950.8171	$[M+NH_4]^+$		TAG 58:7	199447504
952.8328	$[M+NH_4]^+$		TAG 58:6	190990099
954.8484	$[M+NH_4]^+$		TAG 58:5	199355344
956.8641	$[M+NH_4]^+$		TAG 58:4	325814221
958.8797	$[M+NH_4]^+$		TAG 58:3	495400242
960.8954	$[M+NH_4]^+$		TAG 58:2	371319258
962.9110	$[M+NH_4]^+$		TAG 58:1	121311166
964.9267	$[M+NH_4]^+$		TAG 58:0	25088472
966.7545	$[M+NH_4]^+$		TAG 60:13	1165179
968.7702	$[M+NH_4]^+$		TAG 60:12	7540026
970.7858	$[M+NH_4]^+$		TAG 60:11	15166455
972.8015	$[M+NH_4]^+$		TAG 60:10	22921778
974.8171	$[M+NH_4]^+$		TAG 60:9	33170155
976.8328	$[M+NH_4]^+$		TAG 60:8	55402051
978.8484	$[M+NH_4]^+$		TAG 60:7	78243871
980.8641	$[M+NH_4]^+$		TAG 60:6	96924672
982.8797	$[M+NH_4]^+$		TAG 60:5	143914935
984.8954	$[M+NH_4]^+$		TAG 60:4	178872795
986.9110	$[M+NH_4]^+$		TAG 60:3	2252155662
988.9267	$[M+NH_4]^+$		TAG 60:2	52650137
990.9423	$[M+NH_4]^+$		TAG 60:1	27269602
992.9580	$[M+NH_4]^+$		TAG 60:0	12942781
996.8021	$[M+NH_4]^+$		TAG 62:12	2594211
998.8177	$[M+NH_4]^+$		TAG 62:11	2171482
1000.8333	$[M+NH_4]^+$		TAG 62:10	4770559
1002.8489	$[M+NH_4]^+$		TAG 62:9	10449710
1004.8645	$[M+NH_4]^+$		TAG 62:8	29642858
1006.8801	$[M+NH_4]^+$		TAG 62:7	46555212

1008.8957	$[M+NH_4]^+$	TAG 62:6	45556733
1010.9113	$[M+NH_4]^+$	TAG 62:5	9159493
1012.9269	$[M+NH_4]^+$	TAG 62:4	12950277
1014.9425	$[M+NH_4]^+$	TAG 62:3	6561222
1016.9581	$[M+NH_4]^+$	TAG 62:2	7670887
1018.9737	$[M+NH_4]^+$	TAG 62:1	7194299
1020.9893	$[M+NH_4]^+$	TAG 62:0	5586068
1024.8334	$[M+NH_4]^+$	TAG 64:12	<LOD
1026.8490	$[M+NH_4]^+$	TAG 64:11	<LOD
1028.8646	$[M+NH_4]^+$	TAG 64:10	2365080
1030.8802	$[M+NH_4]^+$	TAG 64:9	6043299
1032.8958	$[M+NH_4]^+$	TAG 64:8	11664077
1034.9114	$[M+NH_4]^+$	TAG 64:7	7898949
1036.9270	$[M+NH_4]^+$	TAG 64:6	2302619
1038.9426	$[M+NH_4]^+$	TAG 64:5	<LOD
1040.9582	$[M+NH_4]^+$	TAG 64:4	<LOD
1042.9738	$[M+NH_4]^+$	TAG 64:3	1410872
1044.9894	$[M+NH_4]^+$	TAG 64:2	3068418
1047.0050	$[M+NH_4]^+$	TAG 64:1	1759337
1049.0206	$[M+NH_4]^+$	TAG 64:0	857072
1054.8803	$[M+NH_4]^+$	TAG 66:11	1321467
1056.8959	$[M+NH_4]^+$	TAG 66:10	10553978
1058.9115	$[M+NH_4]^+$	TAG 66:9	3662434
1060.9271	$[M+NH_4]^+$	TAG 66:8	<LOD
1062.9427	$[M+NH_4]^+$	TAG 66:7	<LOD
1064.9583	$[M+NH_4]^+$	TAG 66:6	<LOD
1068.9895	$[M+NH_4]^+$	TAG 66:4	<LOD
1071.0051	$[M+NH_4]^+$	TAG 66:3	<LOD
1073.0207	$[M+NH_4]^+$	TAG 66:2	<LOD
1075.0363	$[M+NH_4]^+$	TAG 66:1	<LOD
1077.0519	$[M+NH_4]^+$	TAG 66:0	<LOD

Mass-to-charge ratio (*m/z*); Triacylglycerol (TAG); Limit of detection (LOD).

Appendix C. Lipidomic Validation of Dried Blood Spots (Chapter 7)

Table C.1. ***Fatty Acid Composition of Whole Blood – Relative Percent***

Whole Blood Total Lipids
(% weight fatty acid in total fatty acids)

Name	P1	P2	P3	Average	SD
C 12:0	0.07	0.05	0.04	0.05	0.01
C 14:0	0.68	0.83	0.68	0.73	0.09
C 16:0	20.75	20.15	21.12	20.67	0.49
C 17:0	0.31	0.29	0.28	0.29	0.02
C 18:0	11.52	12.42	12.90	12.28	0.70
C 20:0	0.30	0.36	0.36	0.34	0.04
C 22:0	0.70	0.84	0.83	0.79	0.08
C 23:0	0.18	0.20	0.18	0.19	0.01
C 24:0	1.19	1.63	1.58	1.47	0.24
SFAs	**35.68**	**36.78**	**37.97**	**36.81**	**1.15**
C 12:1	0.01	0.01	0.01	0.01	<0.01
C 14:1	0.03	0.03	0.01	0.02	0.01
C 16:1	0.77	0.78	0.65	0.73	0.07
C 18:1n-7	1.54	1.52	1.80	1.62	0.16
C 18:1n-9	15.02	16.11	15.89	15.68	0.58
C 20:1n-9	0.22	0.26	0.25	0.24	0.02
C 22:1n-9	0.04	0.07	0.08	0.06	0.02
C 24:1n-9	1.67	1.92	1.73	1.77	0.13
MUFAs	**19.29**	**20.71**	**20.42**	**20.14**	**0.75**
C 18:2n-6	24.24	18.44	19.83	20.83	3.03
C 18:3n-6	0.06	0.32	0.11	0.16	0.14
C 20:2n-6	0.25	0.20	0.22	0.22	0.02
C 20:3n-6	0.98	1.22	1.12	1.10	0.12
C 20:4n-6	7.77	10.11	10.13	9.33	1.35
C 22:2n-6	0.08	0.09	0.09	0.09	0.01
C 22:4n-6	0.66	1.00	1.46	1.04	0.40
C 22:5n-6	0.24	0.35	0.43	0.34	0.10
N-6	**34.26**	**31.72**	**33.40**	**33.13**	**1.30**
C 18:3n-3	0.70	0.47	0.38	0.52	0.16
C 20:3n-3	0.05	0.04	0.04	0.04	0.01
C 20:5n-3	0.96	0.84	0.25	0.68	0.38
C 22:5n-3	1.00	1.23	1.12	1.12	0.11
C 22:6n-3	2.98	2.69	1.63	2.43	0.71
N-3	**5.69**	**5.27**	**3.42**	**4.79**	**1.21**
C 20:3n-9	**0.07**	**0.12**	**0.08**	0.09	0.03
PUFAs	**40.02**	**37.11**	**36.90**	**38.01**	**1.75**
HUFAs	**14.70**	**17.60**	**16.25**	**16.18**	**1.45**
EPA+DHA	**3.94**	**3.53**	**1.88**	**3.12**	**1.09**
Total	**94.99**	**94.59**	**95.29**	**94.96**	**0.35**

Saturated fatty acids (SFAs); Mono-unsaturated fatty acids (MUFAs); Omega-6 fatty acids (N-6); Omega-3 fatty acids (N-3); Polyunsaturated fatty acids (PUFAs); Highly unsaturated fatty acids (HUFAs); Eicosapentaenoic acid (EPA); Docosahexaenoic acid (DHA).

Appendix D. Fish Oil Supplementation-Fatty Acid Composition of Lipid Pools (Chapter 8)

Table D.1. ***Fatty Acid Composition of Blood Cholesteryl Esters (n = 3)***

Concentration (*µg fatty acid/100 µL whole blood*)				
Fatty Acid	**Baseline**	**Week 4**	**Week 8**	**Week 12**
C 14:0	0.21 ± 0.13	0.21 ± 0.08	0.29 ± 0.08	0.51 ± 0.21
C 16:0	3.91 ± 0.73	4.65 ± 1.53	4.33 ± 0.96	5.70 ± 2.18
C 18:0	2.73 ± 0.56	4.02 ± 1.81	2.81 ± 0.49	4.37 ± 2.01
C 20:0	0.07 ± 0.01	0.13 ± 0.08	0.06 ± 0.01	0.25 ± 0.26
C 22:0	0.03 ± <0.01[a]	0.04 ± 0.01[ab]	0.05 ± <0.01[ab]	0.07 ± 0.02[b]
C 24:0	0.03 ± 0.01[a]	0.03 ± 0.01[a]	0.03 ± 0.01[a]	0.06 ± <0.01[b]
SFAs	**7.11 ± 1.02**	**9.25 ± 3.37**	**7.77 ± 1.38**	**11.29 ± 4.78**
C 12:1	<0.01 ± <0.01	0.01 ± <0.01	0.07 ± 0.07	0.08 ± 0.01
C 14:1	0.01 ± 0.01	0.01 ± 0.01	0.02 ± 0.01	0.02 ± 0.01
C 16:1	0.60 ± 0.58	0.38 ± 0.30	0.53 ± 0.41	0.43 ± 0.19
C 18:1n-7	0.24 ± 0.07	0.24 ± 0.04	0.27 ± 0.07	0.33 ± 0.08
C 18:1n-9	4.89 ± 3.17	4.45 ± 0.45	5.32 ± 2.99	6.80 ± 2.63
C 20:1n-9	0.03 ± 0.01[a]	0.05 ± 0.03[ab]	0.04 ± 0.02[a]	0.13 ± 0.05[b]
C 22:1n-9	0.28 ± 0.02	0.25 ± 0.03	0.25 ± 0.05	0.23 ± 0.03
C 24:1n-9	<0.01 ± <0.01[a]	0.01 ± 0.01[a]	0.01 ± <0.01[a]	0.03 ± 0.01[b]
MUFAs	**6.06 ± 3.87**	**5.41 ± 0.48**	**6.51 ± 3.45**	**8.05 ± 2.89**
C 18:2n-6	7.36 ± 1.80	7.39 ± 2.40	8.86 ± 3.52	9.96 ± 2.64
C 18:3n-6	0.15 ± 0.15	0.18 ± 0.08	0.23 ± 0.11	0.20 ± 0.10
C 20:2n-6	<0.01 ± <0.01	<0.01 ± <0.01	<0.01 ± <0.01	0.01 ± 0.01
C 20:3n-6	0.14 ± 0.04	0.13 ± 0.06	0.15 ± 0.04	0.15 ± 0.04
C 20:4n-6	1.06 ± 0.34	0.94 ± 0.46	1.12 ± 0.34	1.20 ± 0.32
C 22:2n-6	0.02 ± <0.01[a]	0.03 ± 0.01[ab]	0.02 ± 0.01[a]	0.05 ± 0.02[b]
C 22:4n-6	0.01 ± 0.01	<0.01 ± <0.01	<0.01 ± <0.01	0.01 ± 0.01
C 22:5n-6	0.01 ± <0.01	0.01 ± 0.01	0.01 ± <0.01	0.01 ± <0.01
N-6	**8.75 ± 2.19**	**8.69 ± 3.00**	**10.40 ± 3.99**	**11.59 ± 3.07**
C 18:3n-3	0.08 ± 0.03	0.09 ± 0.03	0.11 ± 0.04	0.12 ± 0.02
C 20:3n-3	<0.01 ± <0.01	<0.01 ± <0.01	0.01 ± 0.01	0.01 ± <0.01
C 20:5n-3	0.08 ± 0.06[a]	0.14 ± 0.11[a]	0.29 ± 0.15[ab]	0.50 ± 0.14[b]
C 22:5n-3	0.03 ± 0.03[a]	0.04 ± 0.04[ab]	0.05 ± 0.03[ab]	0.26 ± 0.16[b]
C 22:6n-3	0.05 ± 0.01[a]	0.06 ± 0.04[ab]	0.09 ± 0.03[ab]	0.14 ± 0.03[b]
N-3	**0.24 ± 0.12[a]**	**0.33 ± 0.19[a]**	**0.55 ± 0.24[a]**	**1.03 ± 0.12[b]**
C 20:3n-9	0.01 ± <0.01	<0.01 ± <0.01	<0.01 ± <0.01	0.01 ± <0.01
PUFAs	**8.99 ± 2.27**	**9.02 ± 3.19**	**10.95 ± 4.23**	**12.62 ± 3.14**
HUFAs	**1.39 ± 0.43**	**1.34 ± 0.68**	**1.74 ± 0.58**	**2.28 ± 0.40**
EPA+DHA	**0.13 ± 0.07[a]**	**0.21 ± 0.14[a]**	**0.38 ± 0.18[ab]**	**0.64 ± 0.17[b]**
N6/N3	**39.63 ± 11.16[a]**	**31.16 ± 13.64[ab]**	**19.33 ± 1.25[ab]**	**11.20 ± 2.58[b]**
%n-3 HUFA in total HUFA	**11.69 ± 4.64[a]**	**16.98 ± 4.99[ab]**	**24.59 ± 3.59[b]**	**40.30 ± 5.76[c]**
Total	**22.17 ± 6.13**	**23.69 ± 4.95**	**25.23 ± 7.99**	**31.97 ± 10.70**

Saturated fatty acids (SFAs); Mono-unsaturated fatty acids (MUFAs); Omega-6 fatty acids (N-6); Omega-3 fatty acids (N-3); Polyunsaturated fatty acids (PUFAs); Highly unsaturated fatty acids (HUFAs); Eicosapentaenoic acid (EPA); Docosahexaenoic acid (DHA). Omega-6:Omega-3 ratio (N-6/N-3). Superscript differences represent significantly different values after one-way ANOVA + Tukey HSD ($p < 0.05$).

Appendix D. Fish Oil Supplementation-Fatty Acid Composition of Lipid Pools (Chapter 8)

Table D.2. ***Fatty Acid Composition of Blood Free Fatty Acids (n = 3)***

Concentration (*µg fatty acid/100 µL whole blood*)				
Fatty Acid	**Baseline**	**Week 4**	**Week 8**	**Week 12**
C 14:0	0.69 ± 0.32	0.49 ± 0.30	0.30 ± 0.02	0.29 ± 0.14
C 16:0	3.93 ± 0.68	4.48 ± 0.76	4.03 ± 0.36	3.93 ± 0.94
C 18:0	3.67 ± 0.46	4.06 ± 0.36	3.89 ± 0.49	3.45 ± 0.45
C 20:0	0.12 ± 0.03	0.14 ± 0.04	0.14 ± 0.05	0.10 ± 0.01
C 22:0	0.03 ± 0.01	0.03 ± 0.02	0.03 ± 0.01	0.01 ± 0.01
C 24:0	0.03 ± 0.02	0.03 ± 0.02	0.03 ± 0.01	0.01 ± 0.01
SFAs	**9.28 ± 1.84**	**9.56 ± 1.55**	**8.72 ± 0.84**	**8.00 ± 1.57**
C 12:1	<0.01 ± <0.01	0.01 ± 0.01	<0.01 ± <0.01	<0.01 ± <0.01
C 14:1	0.01 ± <0.01	0.01 ± <0.01	0.02 ± 0.01	0.02 ± 0.01
C 16:1	0.35 ± 0.43	0.17 ± 0.17	0.13 ± 0.06	0.15 ± 0.07
C 18:1n-7	0.13 ± 0.07	0.15 ± 0.04	0.11 ± 0.01	0.17 ± 0.09
C 18:1n-9	4.27 ± 2.87	3.51 ± 0.63	3.27 ± 0.28	3.22 ± 2.05
C 20:1n-9	0.03 ± 0.01	0.04 ± <0.01	0.02 ± 0.01	0.02 ± 0.01
C 22:1n-9	0.18 ± 0.03	0.19 ± 0.01	0.18 ± <0.01	0.22 ± 0.03
C 24:1n-9	0.01 ± <0.01	0.01 ± 0.01	<0.01 ± <0.01	<0.01 ± <0.01
MUFAs	**4.98 ± 3.23**	**4.09 ± 0.85**	**3.73 ± 0.30**	**3.80 ± 2.23**
C 18:2n-6	0.75 ± 0.35	0.95 ± 0.22	1.03 ± 0.01	1.10 ± 0.50
C 18:3n-6	0.16 ± 0.02	0.19 ± 0.05	0.16 ± <0.01	0.15 ± 0.01
C 20:2n-6	0.01 ± <0.01	<0.01 ± <0.01	0.01 ± <0.01	0.01 ± <0.01
C 20:3n-6	0.04 ± 0.02	0.03 ± 0.01	0.03 ± 0.02	0.02 ± 0.01
C 20:4n-6	0.02 ± 0.01	0.01 ± 0.01	0.02 ± <0.01	0.03 ± 0.01
C 22:2n-6	0.04 ± 0.01[a]	0.03 ± <0.01[ab]	0.02 ± <0.01[b]	0.02 ± <0.01[b]
C 22:4n-6	0.01 ± <0.01	0.01 ± 0.01	0.01 ± 0.01	0.01 ± 0.01
C 22:5n-6	0.01 ± <0.01	0.01 ± 0.01	0.01 ± 0.01	0.01 ± 0.01
N-6	**1.03 ± 0.35**	**1.24 ± 0.23**	**1.30 ± 0.01**	**1.35 ± 0.50**
C 18:3n-3	0.03 ± 0.01	0.05 ± 0.01	0.03 ± 0.01	0.04 ± 0.02
C 20:3n-3	0.01 ± <0.01	<0.01 ± <0.01	0.01 ± 0.01	0.01 ± <0.01
C 20:5n-3	0.02 ± <0.01[a]	0.01 ± 0.01[ab]	<0.01 ± <0.01[b]	<0.01 ± <0.01[b]
C 22:5n-3	<0.01 ± <0.01[ab]	<0.01 ± <0.01[ab]	<0.01 ± <0.01[ab]	0.01 ± <0.01[b]
C 22:6n-3	0.01 ± 0.01	0.01 ± 0.01	0.01 ± <0.01	<0.01 ± <0.01
N-3	**0.07 ± <0.01**	**0.08 ± <0.01**	**0.05 ± 0.01**	**0.06 ± 0.02**
C 20:3n-9	<0.01 ± <0.01	0.01 ± <0.01	<0.01 ± <0.01	0.01 ± 0.01
PUFAs	**1.10 ± 0.35**	**1.32 ± 0.24**	**1.35 ± 0.02**	**1.41 ± 0.50**
HUFAs	**0.12 ± 0.02**	**0.09 ± 0.03**	**0.10 ± 0.02**	**0.10 ± 0.02**
EPA+DHA	**0.03 ± 0.01[a]**	**0.02 ± 0.01[ab]**	**0.01 ± <0.01[ab]**	**0.01 ± 0.01[b]**
N6/N3	**15.51 ± 4.85**	**15.94 ± 2.59**	**27.51 ± 7.63**	**24.42 ± 11.18**
%n-3 HUFA in total HUFA	**33.47 ± 13.85**	**24.77 ± 9.93**	**17.53 ± 5.99**	**22.21 ± 4.56**
Total	**15.37 ± 5.21**	**14.97 ± 2.23**	**13.81 ± 0.95**	**13.21 ± 4.22**

Saturated fatty acids (SFAs); Mono-unsaturated fatty acids (MUFAs); Omega-6 fatty acids (N-6); Omega-3 fatty acids (N-3); Polyunsaturated fatty acids (PUFAs); Highly unsaturated fatty acids (HUFAs); Eicosapentaenoic acid (EPA); Docosahexaenoic acid (DHA). Omega-6:Omega-3 ratio (N-6/N-3). Superscript differences represent significantly different values after one-way ANOVA + Tukey HSD ($p < 0.05$).

Appendix D. Fish Oil Supplementation-Fatty Acid Composition of Lipid Pools (Chapter 8)

Table D.3. ***Fatty Acid Composition of Blood Phosphatidylcholines (n = 3)***

Concentration (*μg fatty acid/100 μL whole blood*)				
Fatty Acid	**Baseline**	**Week 4**	**Week 8**	**Week 12**
C 14:0	0.39 ± 0.12	0.17 ± 0.07	0.24 ± 0.04	0.32 ± 0.08
C 16:0	18.75 ± 6.74	16.83 ± 6.51	20.28 ± 4.84	20.59 ± 3.27
C 18:0	9.71 ± 3.35	10.16 ± 3.39	12.04 ± 4.38	11.28 ± 2.05
C 20:0	0.16 ± 0.03	0.15 ± 0.03	0.18 ± 0.09	0.15 ± 0.01
C 22:0	0.06 ± 0.02	0.05 ± 0.03	0.05 ± 0.01	0.06 ± 0.02
C 24:0	0.11 ± 0.04	0.08 ± 0.05	0.07 ± 0.02	0.10 ± 0.04
SFAs	**29.62 ± 10.27**	**27.71 ± 10.08**	**33.17 ± 9.06**	**32.84 ± 5.39**
C 12:1	<0.01 ± <0.01	<0.01 ± <0.01	<0.01 ± <0.01	<0.01 ± <0.01
C 14:1	0.01 ± <0.01	<0.01 ± <0.01	<0.01 ± <0.01	<0.01 ± <0.01
C 16:1	0.39 ± 0.28	0.22 ± 0.13	0.37 ± 0.27	0.28 ± 0.07
C 18:1n-7	1.01 ± 0.48	0.96 ± 0.25	1.05 ± 0.14	1.17 ± 0.10
C 18:1n-9	9.66 ± 4.58	7.12 ± 2.94	7.73 ± 1.97	7.59 ± 1.40
C 20:1n-9	0.12 ± 0.07	0.10 ± 0.04	0.10 ± 0.01	0.11 ± 0.01
C 22:1n-9	0.27 ± 0.03	0.26 ± 0.01	0.26 ± 0.01	0.26 ± 0.01
C 24:1n-9	0.07 ± 0.03	0.06 ± 0.02	0.05 ± 0.01	0.06 ± 0.02
MUFAs	**11.53 ± 5.30**	**8.73 ± 3.36**	**9.56 ± 2.34**	**9.48 ± 1.47**
C 18:2n-6	10.85 ± 5.53	9.99 ± 5.10	11.28 ± 3.40	12.57 ± 1.89
C 18:3n-6	0.05 ± 0.03	0.04 ± 0.02	0.09 ± 0.10	0.03 ± 0.01
C 20:2n-6	0.19 ± 0.10	0.15 ± 0.07	0.17 ± 0.04	0.17 ± 0.03
C 20:3n-6	1.45 ± 0.93	1.14 ± 0.72	1.24 ± 0.56	1.10 ± 0.42
C 20:4n-6	4.54 ± 2.60	3.98 ± 2.28	4.29 ± 1.00	4.41 ± 0.73
C 22:2n-6	0.04 ± <0.01	0.03 ± 0.02	0.03 ± <0.01	0.03 ± 0.01
C 22:4n-6	0.15 ± 0.07	0.12 ± 0.06	0.11 ± 0.03	0.09 ± 0.02
C 22:5n-6	0.10 ± 0.06	0.07 ± 0.05	0.07 ± 0.03	0.06 ± 0.03
N-6	**17.38 ± 9.23**	**15.53 ± 8.29**	**17.29 ± 5.03**	**18.47 ± 3.05**
C 18:3n-3	0.13 ± 0.06	0.11 ± 0.04	0.11 ± 0.03	0.14 ± 0.04
C 20:3n-3	0.01 ± <0.01	0.01 ± <0.01	0.01 ± <0.01	0.02 ± 0.01
C 20:5n-3	0.23 ± 0.14[a]	0.39 ± 0.24[a]	0.70 ± 0.25[ab]	1.05 ± 0.20[b]
C 22:5n-3	0.27 ± 0.13	0.32 ± 0.18	0.39 ± 0.13	0.43 ± 0.08
C 22:6n-3	0.76 ± 0.45	0.97 ± 0.59	1.18 ± 0.36	1.58 ± 0.38
N-3	**1.40 ± 0.74**	**1.80 ± 1.05**	**2.39 ± 0.76**	**3.22 ± 0.65**
C 20:3n-9	0.07 ± 0.06	0.06 ± 0.05	0.07 ± 0.04	0.05 ± 0.02
PUFAs	**18.85 ± 10.01**	**17.39 ± 9.39**	**19.74 ± 5.81**	**21.74 ± 3.71**
HUFAs	**7.58 ± 4.30**	**7.06 ± 4.16**	**8.07 ± 2.33**	**8.80 ± 1.75**
EPA+DHA	**0.99 ± 0.56**	**1.36 ± 0.83**	**1.88 ± 0.60**	**2.63 ± 0.54**
N6/N3	**12.65 ± 1.61[a]**	**8.89 ± 1.02[b]**	**7.30 ± 0.45[bc]**	**5.76 ± 0.25[c]**
%n-3 HUFA in total HUFA	**16.88 ± 1.62[a]**	**23.79 ± 0.66[b]**	**28.08 ± 1.15[c]**	**35.03 ± 0.43[d]**
Total	**<0.01 ± 25.37**	**53.82 ± 22.72**	**62.48 ± 16.35**	**64.06 ± 10.17**

Saturated fatty acids (SFAs); Mono-unsaturated fatty acids (MUFAs); Omega-6 fatty acids (N-6); Omega-3 fatty acids (N-3); Polyunsaturated fatty acids (PUFAs); Highly unsaturated fatty acids (HUFAs); Eicosapentaenoic acid (EPA); Docosahexaenoic acid (DHA). Omega-6:Omega-3 ratio (N-6/N-3). Superscript differences represent significantly different values after one-way ANOVA + Tukey HSD ($p < 0.05$).

Appendix D. Fish Oil Supplementation-Fatty Acid Composition of Lipid Pools (Chapter 8)

Table D.4. ***Fatty Acid Composition of Blood Phosphatidylserines (n = 3)***

Concentration (*µg fatty acid/100 µL whole blood*)				
Fatty Acid	**Baseline**	**Week 4**	**Week 8**	**Week 12**
C 14:0	0.14 ± 0.02	0.14 ± 0.07	0.21 ± 0.12	0.05 ± 0.01
C 16:0	2.55 ± 0.61	2.33 ± 0.57	2.50 ± 0.45	1.38 ± 0.04
C 18:0	4.65 ± 0.89[a]	4.35 ± 0.59[a]	3.24 ± 0.60[ab]	2.42 ± 0.21[b]
C 20:0	0.10 ± 0.02[a]	0.09 ± 0.01[ab]	0.10 ± <0.01[ab]	0.08 ± 0.01[b]
C 22:0	0.03 ± 0.01[ab]	0.03 ± 0.01[a]	0.05 ± 0.01[b]	0.04 ± 0.01[ab]
C 24:0	0.05 ± 0.01	0.05 ± 0.02	0.05 ± <0.01	0.05 ± 0.01
SFAs	**7.64 ± 1.46[a]**	**7.07 ± 1.30[a]**	**6.29 ± 0.56[ab]**	**4.09 ± 0.21[b]**
C 12:1	0.01 ± <0.01	<0.01 ± <0.01	<0.01 ± <0.01	<0.01 ± <0.01
C 14:1	0.01 ± 0.01	0.01 ± <0.01	<0.01 ± <0.01	<0.01 ± <0.01
C 16:1	0.05 ± 0.03	0.07 ± 0.08	0.08 ± 0.08	0.01 ± 0.01
C 18:1n-7	0.11 ± 0.02	0.10 ± 0.07	0.11 ± 0.07	0.06 ± 0.05
C 18:1n-9	2.15 ± 0.75	1.38 ± 0.98	2.71 ± 1.61	0.59 ± 0.29
C 20:1n-9	0.03 ± 0.01	0.03 ± 0.03	0.03 ± 0.01	0.02 ± <0.01
C 22:1n-9	0.23 ± 0.01	0.25 ± 0.03	0.22 ± <0.01	0.24 ± 0.01
C 24:1n-9	0.03 ± 0.01	0.03 ± 0.01	0.03 ± 0.01	0.04 ± 0.01
MUFAs	**2.62 ± 0.74**	**1.88 ± 1.20**	**3.19 ± 1.72**	**0.96 ± 0.35**
C 18:2n-6	0.36 ± 0.11	0.35 ± 0.27	0.46 ± 0.35	0.12 ± 0.04
C 18:3n-6	0.01 ± <0.01	0.01 ± <0.01	0.01 ± <0.01	0.01 ± <0.01
C 20:2n-6	0.02 ± <0.01	0.02 ± 0.01	0.02 ± 0.01	0.01 ± <0.01
C 20:3n-6	0.07 ± 0.03[a]	0.07 ± 0.03[ab]	0.04 ± 0.01[ab]	0.02 ± <0.01[b]
C 20:4n-6	0.70 ± 0.10	0.79 ± 0.44	0.38 ± 0.08	0.26 ± 0.02
C 22:2n-6	0.03 ± 0.01	0.02 ± 0.01	0.02 ± <0.01	0.02 ± <0.01
C 22:4n-6	0.15 ± 0.07	0.14 ± 0.05	0.08 ± 0.01	0.05 ± 0.01
C 22:5n-6	0.04 ± 0.01	0.04 ± 0.01	0.02 ± 0.01	0.02 ± 0.01
N-6	**1.37 ± 0.20**	**1.45 ± 0.77**	**1.02 ± 0.40**	**0.50 ± 0.06**
C 18:3n-3	0.04 ± 0.02	0.04 ± 0.02	0.04 ± 0.04	0.02 ± <0.01
C 20:3n-3	0.01 ± <0.01	<0.01 ± <0.01	<0.01 ± <0.01	<0.01 ± <0.01
C 20:5n-3	0.02 ± <0.01	0.03 ± 0.02	0.02 ± <0.01	0.03 ± <0.01
C 22:5n-3	0.11 ± 0.02	0.12 ± 0.05	0.07 ± 0.01	0.06 ± 0.01
C 22:6n-3	0.13 ± 0.01	0.19 ± 0.11	0.09 ± 0.02	0.09 ± 0.02
N-3	**0.29 ± 0.03**	**0.38 ± 0.19**	**0.22 ± 0.06**	**0.20 ± 0.02**
C 20:3n-9	0.01 ± 0.01	0.01 ± <0.01	0.01 ± 0.01	<0.01 ± <0.01
PUFAs	**1.80 ± 0.20**	**1.83 ± 0.97**	**1.25 ± 0.46**	**1.08 ± 0.73**
HUFAs	**1.28 ± 0.20**	**1.39 ± 0.69**	**0.71 ± 0.12**	**0.80 ± 0.51**
EPA+DHA	**0.15 ± 0.02**	**0.21 ± 0.13**	**0.11 ± 0.02**	**0.12 ± 0.02**
N6/N3	**4.64 ± 0.64[a]**	**3.82 ± 0.11[ab]**	**4.68 ± 1.02[a]**	**2.53 ± 0.16[b]**
%n-3 HUFA in total HUFA	**20.66 ± 3.69**	**24.31 ± 0.83**	**25.69 ± 1.31**	**26.94 ± 11.24**
Total	**11.61 ± 0.43**	**10.78 ± 3.41**	**10.73 ± 2.18**	**7.54 ± 3.31**

Saturated fatty acids (SFAs); Mono-unsaturated fatty acids (MUFAs); Omega-6 fatty acids (N-6); Omega-3 fatty acids (N-3); Polyunsaturated fatty acids (PUFAs); Highly unsaturated fatty acids (HUFAs); Eicosapentaenoic acid (EPA); Docosahexaenoic acid (DHA). Omega-6:Omega-3 ratio (N-6/N-3). Superscript differences represent significantly different values after one-way ANOVA + Tukey HSD ($p < 0.05$).

Appendix D. Fish Oil Supplementation-Fatty Acid Composition of Lipid Pools (Chapter 8)

Table D.5. ***Fatty Acid Composition of Blood Phosphatidylinositols (n = 3)***

Concentration (*μg fatty acid/100 μL whole blood*)				
Fatty Acid	**Baseline**	**Week 4**	**Week 8**	**Week 12**
C 14:0	0.25 ± 0.18	0.30 ± 0.31	0.10 ± 0.03	0.20 ± 0.11
C 16:0	3.35 ± 0.56	5.65 ± 2.72	2.61 ± 0.44	3.45 ± 0.49
C 18:0	4.31 ± 1.22	7.17 ± 4.47	5.15 ± 0.35	6.36 ± 0.30
C 20:0	0.12 ± 0.03	0.18 ± 0.09	0.10 ± <0.01	0.13 ± 0.03
C 22:0	0.04 ± 0.02	0.05 ± 0.03	0.03 ± 0.01	0.05 ± 0.01
C 24:0	0.05 ± 0.02	0.05 ± 0.03	0.03 ± 0.01	0.05 ± 0.03
SFAs	**8.33 ± 1.40**	**13.68 ± 7.08**	**8.18 ± 0.78**	**10.49 ± 0.70**
C 12:1	<0.01 ± <0.01	<0.01 ± <0.01	<0.01 ± <0.01	0.01 ± <0.01
C 14:1	0.01 ± 0.02	0.02 ± 0.04	<0.01 ± <0.01	0.01 ± 0.01
C 16:1	0.13 ± 0.06	0.11 ± 0.09	0.05 ± 0.01	0.08 ± 0.02
C 18:1n-7	0.13 ± 0.02^{a}	0.23 ± 0.06^{b}	0.12 ± 0.02^{a}	0.18 ± <0.01^{ab}
C 18:1n-9	2.89 ± 1.60	4.18 ± 3.28	1.42 ± 0.33	3.08 ± 1.53
C 20:1n-9	0.03 ± 0.01	0.05 ± 0.02	0.02 ± <0.01	0.04 ± <0.01
C 22:1n-9	0.22 ± 0.01	0.24 ± 0.04	0.22 ± <0.01	0.22 ± 0.01
C 24:1n-9	0.03 ± 0.01	0.03 ± 0.02	0.04 ± 0.02	0.05 ± 0.02
MUFAs	**3.45 ± 1.66**	**4.87 ± 3.51**	**1.87 ± 0.35**	**3.67 ± 1.56**
C 18:2n-6	0.69 ± 0.14	0.95 ± 0.34	0.46 ± 0.11	0.75 ± 0.19
C 18:3n-6	0.01 ± <0.01	0.02 ± 0.02	0.01 ± <0.01	0.01 ± <0.01
C 20:2n-6	0.02 ± <0.01	0.02 ± 0.02	0.02 ± <0.01	0.03 ± 0.02
C 20:3n-6	0.10 ± 0.04	0.14 ± 0.04	0.13 ± 0.03	0.19 ± 0.07
C 20:4n-6	1.08 ± 0.55	1.90 ± 0.53	1.33 ± 0.09	2.05 ± 0.26
C 22:2n-6	0.01 ± <0.01	0.03 ± 0.01	0.02 ± <0.01	0.02 ± <0.01
C 22:4n-6	0.17 ± 0.07^{a}	0.38 ± 0.07^{b}	0.22 ± 0.07^{ab}	0.30 ± 0.08^{ab}
C 22:5n-6	0.05 ± 0.03	0.04 ± 0.01	0.05 ± 0.01	0.07 ± 0.02
N-6	**2.12 ± 0.63**	**3.47 ± 0.81**	**2.24 ± 0.10**	**3.42 ± 0.31**
C 18:3n-3	0.04 ± 0.01	0.05 ± 0.03	0.02 ± 0.01	0.04 ± 0.02
C 20:3n-3	<0.01 ± <0.01	<0.01 ± <0.01	0.01 ± 0.01	0.01 ± <0.01
C 20:5n-3	0.02 ± 0.01^{a}	0.07 ± 0.02^{bc}	0.03 ± <0.01^{ab}	0.10 ± 0.02^{c}
C 22:5n-3	0.11 ± 0.04^{a}	0.25 ± 0.03^{bc}	0.20 ± 0.05^{ab}	0.36 ± 0.08^{c}
C 22:6n-3	0.16 ± 0.08^{a}	0.31 ± 0.09^{ab}	0.26 ± 0.01^{a}	0.53 ± 0.13^{b}
N-3	**0.33 ± 0.12^{a}**	**0.69 ± 0.16^{bc}**	**0.52 ± 0.05^{ab}**	**1.04 ± 0.18^{c}**
C 20:3n-9	0.01 ± <0.01	0.01 ± 0.01	0.01 ± <0.01	0.01 ± 0.01
PUFAs	**2.47 ± 0.75**	**3.71 ± 1.76**	**2.77 ± 0.06**	**3.66 ± 1.74**
HUFAs	**1.69 ± 0.79**	**2.62 ± 1.49**	**2.24 ± 0.07**	**2.80 ± 1.66**
EPA+DHA	**0.18 ± 0.08^{a}**	**0.38 ± 0.11^{ab}**	**0.30 ± 0.02^{a}**	**0.63 ± 0.16^{b}**
N6/N3	**6.51 ± 0.54^{a}**	**5.04 ± 0.03^{b}**	**4.36 ± 0.61^{bc}**	**3.35 ± 0.48^{c}**
%n-3 HUFA in total HUFA	**17.39 ± 1.78**	**30.29 ± 16.43**	**22.20 ± 1.96**	**51.67 ± 42.97**
Total	**14.25 ± 2.79**	**22.37 ± 9.64**	**12.82 ± 1.06**	**17.01 ± 5.01**

Saturated fatty acids (SFAs); Mono-unsaturated fatty acids (MUFAs); Omega-6 fatty acids (N-6); Omega-3 fatty acids (N-3); Polyunsaturated fatty acids (PUFAs); Highly unsaturated fatty acids (HUFAs); Eicosapentaenoic acid (EPA); Docosahexaenoic acid (DHA). Omega-6:Omega-3 ratio (N-6/N-3). Superscript differences represent significantly different values after one-way ANOVA + Tukey HSD ($p < 0.05$).

Appendix D. Fish Oil Supplementation-Fatty Acid Composition of Lipid Pools (Chapter 8)

Table D.6. ***Fatty Acid Composition of Blood Sphingomyelins (n = 3)***

Concentration (*μg fatty acid/100 μL whole blood*)				
Fatty Acid	**Baseline**	**Week 4**	**Week 8**	**Week 12**
C 14:0	0.51 ± 0.40	0.50 ± 0.57	0.12 ± 0.01	0.14 ± 0.08
C 16:0	6.34 ± 2.37	5.73 ± 1.04	5.09 ± 1.07	5.23 ± 0.70
C 18:0	5.05 ± 0.33	4.51 ± 0.87	3.52 ± 0.68	4.06 ± 1.50
C 20:0	0.32 ± 0.10	0.32 ± 0.03	0.34 ± 0.15	0.31 ± 0.02
C 22:0	0.74 ± 0.29	0.69 ± 0.18	0.98 ± 0.32	0.84 ± 0.12
C 24:0	1.14 ± 0.58	1.06 ± 0.38	1.31 ± 0.13	1.26 ± 0.26
SFAs	**14.56 ± 4.29**	**13.18 ± 1.46**	**11.67 ± 2.03**	**12.13 ± 1.76**
C 12:1	<0.01 ± <0.01	<0.01 ± <0.01	<0.01 ± <0.01	<0.01 ± <0.01
C 14:1	0.02 ± 0.02	0.02 ± 0.02	<0.01 ± <0.01	0.01 ± <0.01
C 16:1	0.07 ± 0.02	0.09 ± 0.10	0.04 ± 0.01	0.05 ± 0.03
C 18:1n-7	0.11 ± 0.03	0.15 ± 0.03	0.07 ± 0.01	0.14 ± 0.09
C 18:1n-9	3.33 ± 2.11	5.20 ± 5.58	1.24 ± 0.50	1.78 ± 0.96
C 20:1n-9	0.02 ± 0.01	0.04 ± 0.02	0.03 ± 0.01	0.03 ± 0.01
C 22:1n-9	0.27 ± 0.02	0.29 ± 0.02	0.26 ± 0.02	0.26 ± <0.01
C 24:1n-9	1.33 ± 0.45	1.26 ± 0.19	1.58 ± 0.13	1.63 ± 0.32
MUFAs	**5.15 ± 2.51**	**7.05 ± 5.71**	**3.22 ± 0.42**	**3.90 ± 1.04**
C 18:2n-6	0.46 ± 0.20	0.63 ± 0.38	0.40 ± 0.11	0.49 ± 0.14
C 18:3n-6	<0.01 ± <0.01	0.01 ± <0.01	<0.01 ± <0.01	<0.01 ± <0.01
C 20:2n-6	0.02 ± <0.01	0.02 ± 0.01	0.02 ± <0.01	0.02 ± 0.01
C 20:3n-6	0.02 ± 0.01	0.02 ± 0.01	0.02 ± 0.01	0.02 ± 0.01
C 20:4n-6	0.09 ± 0.05	0.10 ± 0.05	0.12 ± 0.02	0.12 ± <0.01
C 22:2n-6	0.02 ± 0.01	0.03 ± 0.01	0.03 ± 0.01	0.02 ± 0.01
C 22:4n-6	0.01 ± <0.01	0.01 ± <0.01	0.01 ± <0.01	0.01 ± <0.01
C 22:5n-6	0.01 ± <0.01	0.02 ± 0.02	0.01 ± <0.01	0.01 ± <0.01
N-6	**0.64 ± 0.28**	**0.83 ± 0.42**	**0.60 ± 0.12**	**0.70 ± 0.15**
C 18:3n-3	0.03 ± 0.02	0.03 ± 0.01	0.02 ± 0.01	0.02 ± <0.01
C 20:3n-3	<0.01 ± <0.01	<0.01 ± <0.01	0.01 ± <0.01	<0.01 ± <0.01
C 20:5n-3	0.01 ± <0.01[a]	0.02 ± <0.01[b]	0.02 ± <0.01[b]	0.03 ± <0.01[c]
C 22:5n-3	0.01 ± <0.01	0.01 ± <0.01	0.01 ± <0.01	0.01 ± <0.01
C 22:6n-3	0.02 ± 0.01	0.04 ± 0.02	0.04 ± <0.01	0.04 ± 0.01
N-3	**0.07 ± 0.03**	**0.10 ± 0.03**	**0.10 ± 0.01**	**0.11 ± 0.01**
C 20:3n-9	0.01 ± <0.01	0.01 ± <0.01	<0.01 ± <0.01	0.01 ± 0.01
PUFAs	**0.71 ± 0.28**	**0.93 ± 0.45**	**0.70 ± 0.12**	**0.82 ± 0.15**
HUFAs	**0.18 ± 0.08**	**0.22 ± 0.07**	**0.23 ± 0.04**	**0.26 ± 0.01**
EPA+DHA	**0.03 ± 0.02[a]**	**0.06 ± 0.02[ab]**	**0.06 ± <0.01[ab]**	**0.07 ± 0.01[b]**
N6/N3	**10.03 ± 4.98**	**7.76 ± 1.94**	**6.07 ± 1.51**	**6.70 ± 1.81**
%n-3 HUFA in total HUFA	**24.89 ± 6.22**	**34.04 ± 7.11**	**34.42 ± 6.48**	**34.12 ± 2.39**
Total	**20.43 ± 7.06**	**21.16 ± 7.57**	**15.59 ± 2.00**	**16.84 ± 1.31**

Saturated fatty acids (SFAs); Mono-unsaturated fatty acids (MUFAs); Omega-6 fatty acids (N-6); Omega-3 fatty acids (N-3); Polyunsaturated fatty acids (PUFAs); Highly unsaturated fatty acids (HUFAs); Eicosapentaenoic acid (EPA); Docosahexaenoic acid (DHA). Omega-6:Omega-3 ratio (N-6/N-3). Superscript differences represent significantly different values after one-way ANOVA + Tukey HSD ($p < 0.05$).

Appendix D. Fish Oil Supplementation-Fatty Acid Composition of Lipid Pools (Chapter 8)

Table D.7. ***Fatty Acid Composition of Blood Triacylglycerols (n = 3)***

Concentration (*μg fatty acid/100 μL whole blood*)				
Fatty Acid	**Baseline**	**Week 4**	**Week 8**	**Week 12**
C 14:0	0.47 ± 0.47	0.29 ± 0.10	0.36 ± 0.06	0.29 ± 0.03
C 16:0	5.50 ± 2.64	4.58 ± 1.72	5.73 ± 1.56	4.23 ± 0.84
C 18:0	3.14 ± 1.25	2.98 ± 1.01	3.37 ± 0.40	2.76 ± 0.44
C 20:0	0.07 ± 0.03	0.07 ± 0.01	0.07 ± 0.01	0.06 ± 0.02
C 22:0	0.03 ± 0.01	0.03 ± 0.02	0.03 ± 0.01	0.03 ± <0.01
C 24:0	0.02 ± <0.01	0.03 ± 0.01	0.03 ± <0.01	0.02 ± 0.01
SFAs	**9.39 ± 2.78**	**8.18 ± 2.85**	**9.83 ± 1.53**	**7.53 ± 1.32**
C 12:1	<0.01 ± <0.01	<0.01 ± <0.01	0.01 ± <0.01	0.01 ± <0.01
C 14:1	0.03 ± 0.02	0.03 ± 0.02	0.03 ± 0.02	0.02 ± <0.01
C 16:1	0.64 ± 0.72	0.39 ± 0.28	0.50 ± 0.37	0.35 ± 0.15
C 18:1n-7	0.36 ± 0.31	0.30 ± 0.08	0.37 ± 0.15	0.28 ± 0.04
C 18:1n-9	5.00 ± 2.81	7.46 ± 4.24	6.41 ± 1.51	4.69 ± 1.94
C 20:1n-9	0.06 ± 0.02	0.07 ± 0.04	0.08 ± 0.01	0.05 ± 0.02
C 22:1n-9	0.27 ± 0.02[a]	0.23 ± 0.01[ab]	0.24 ± <0.01[ab]	0.22 ± 0.02[b]
C 24:1n-9	0.01 ± 0.01	0.01 ± 0.01	0.01 ± 0.01	0.01 ± 0.01
MUFAs	**6.37 ± 3.87**	**8.50 ± 4.19**	**7.64 ± 1.95**	**5.63 ± 1.99**
C 18:2n-6	1.37 ± 0.46	1.88 ± 0.68	2.17 ± 0.58	1.81 ± 0.57
C 18:3n-6	0.07 ± 0.02	0.05 ± 0.03	0.09 ± 0.03	0.07 ± 0.02
C 20:2n-6	0.01 ± 0.01	0.02 ± 0.01	0.02 ± 0.01	0.01 ± <0.01
C 20:3n-6	0.07 ± 0.02	0.05 ± 0.01	0.08 ± 0.02	0.06 ± 0.01
C 20:4n-6	0.10 ± 0.05	0.10 ± 0.02	0.14 ± 0.02	0.10 ± 0.02
C 22:2n-6	0.02 ± <0.01	0.03 ± 0.02	0.03 ± 0.01	0.02 ± 0.01
C 22:4n-6	0.02 ± 0.01	0.02 ± <0.01	0.02 ± 0.01	0.01 ± <0.01
C 22:5n-6	0.02 ± 0.01	0.02 ± 0.01	0.02 ± 0.02	0.01 ± <0.01
N-6	**1.68 ± 0.59**	**2.17 ± 0.68**	**2.57 ± 0.62**	**2.09 ± 0.63**
C 18:3n-3	0.10 ± 0.05	0.11 ± 0.04	0.13 ± 0.02	0.14 ± 0.03
C 20:3n-3	0.01 ± <0.01	0.01 ± 0.01	0.01 ± <0.01	0.01 ± <0.01
C 20:5n-3	0.02 ± 0.01[a]	0.06 ± 0.01[ab]	0.10 ± 0.02[b]	0.07 ± 0.02[b]
C 22:5n-3	0.03 ± 0.02	0.13 ± 0.17	0.14 ± 0.07	0.10 ± 0.08
C 22:6n-3	0.03 ± 0.02[a]	0.04 ± 0.01[ab]	0.07 ± 0.02[ab]	0.08 ± 0.02[b]
N-3	**0.18 ± 0.10**	**0.34 ± 0.21**	**0.46 ± 0.03**	**0.40 ± 0.10**
C 20:3n-9	0.02 ± 0.01	0.01 ± 0.01	0.01 ± 0.01	<0.01 ± <0.01
PUFAs	**1.86 ± 0.69**	**2.51 ± 0.86**	**3.03 ± 0.63**	**2.49 ± 0.73**
HUFAs	**0.30 ± 0.15[a]**	**0.43 ± 0.16[a]**	**0.60 ± 0.03[b]**	**0.45 ± 0.12[ab]**
EPA+DHA	**0.04 ± 0.04[a]**	**0.10 ± 0.02[ab]**	**0.17 ± 0.03[c]**	**0.16 ± 0.02[bc]**
N6/N3	**9.92 ± 2.50**	**7.15 ± 2.52**	**5.57 ± 1.19**	**5.19 ± 0.28**
%n-3 HUFA in total HUFA	**24.84 ± 4.57[a]**	**49.06 ± 21.60[ab]**	**54.89 ± 9.53[ab]**	**57.43 ± 5.69[b]**
Total	**17.63 ± 7.04**	**24.22 ± 13.13**	**20.50 ± 3.50**	**15.65 ± 3.68**

Saturated fatty acids (SFAs); Mono-unsaturated fatty acids (MUFAs); Omega-6 fatty acids (N-6); Omega-3 fatty acids (N-3); Polyunsaturated fatty acids (PUFAs); Highly unsaturated fatty acids (HUFAs); Eicosapentaenoic acid (EPA); Docosahexaenoic acid (DHA). Omega-6:Omega-3 ratio (N-6/N-3). Superscript differences represent significantly different values after one-way ANOVA + Tukey HSD ($p < 0.05$).

Appendix D. Fish Oil Supplementation-Fatty Acid Composition of Lipid Pools (Chapter 8)

Table D.8. ***Fatty Acid Composition of Whole Blood (n = 20)****

	Concentration (*µg fatty acid per 100 µL whole blood)*		
Fatty Acid	**Baseline**	**Week 4**	**Week 8**
C 12:0	0.14 ± 0.07[a]	0.20 ± 0.09[ab]	0.21 ± 0.08[b]
C 14:0	1.20 ± 0.50	1.65 ± 0.70	1.61 ± 0.55
C 16:0	33.02 ± 7.90[a]	43.43 ± 10.84[b]	43.60 ± 8.79[b]
C 18:0	18.61 ± 3.36[a]	23.12 ± 5.02[b]	23.72 ± 4.87[b]
C 20:0	0.44 ± 0.09[a]	0.59 ± 0.12[ab]	0.75 ± 0.48[b]
C 22:0	1.21 ± 0.29[a]	1.67 ± 0.34[b]	1.82 ± 0.22[b]
C 24:0	2.36 ± 0.56[a]	3.25 ± 0.712[b]	3.65 ± 0.53[b]
SFAs	**61.12 ± 12.53[a]**	**79.06 ± 17.23[b]**	**82.12 ± 15.31[b]**
C 12:1	<0.01 ± <0.01[a]	<0.01 ± <0.01[a]	0.01 ± <0.01[b]
C 14:1	0.05 ± 0.05	0.08 ± 0.06	0.08 ± 0.06
C 16:1	1.53 ± 0.98	2.05 ± 0.98	2.12 ± 1.03
C 18:1n-7	2.36 ± 0.56[a]	2.99 ± 0.59[b]	3.06 ± 0.48[b]
C 18:1n-9	22.68 ± 5.85[a]	31.27 ± 7.14[b]	31.31 ± 5.57[b]
C 20:1n-9	0.37 ± 0.08[a]	0.44 ± 0.09[b]	0.45 ± 0.06[b]
C 22:1n-9	0.47 ± 0.03[a]	0.32 ± 0.05[b]	0.49 ± 0.08[a]
C 24:1n-9	2.67 ± 0.61[a]	3.63 ± 0.62[b]	4.16 ± 0.46[c]
MUFAs	**30.83 ± 8.53[1]**	**41.36 ± 8.95[b]**	**42.37 ± 7.07[b]**
C 18:2n-6	28.41 ± 5.33[a]	41.22 ± 7.40[b]	40.16 ± 7.11[b]
C 18:3n-6	0.29 ± 0.14[a]	0.49 ± 0.29[b]	0.49 ± 0.23[b]
C 20:2n-6	0.40 ± 0.12[a]	0.59 ± 0.18[b]	0.59 ± 0.12[b]
C 20:3n-6	2.76 ± 1.13	3.28 ± 1.38	3.35 ± 1.02
C 20:4n-6	17.16 ± 4.14[a]	20.51 ± 4.81[b]	20.92 ± 3.09[b]
C 22:2n-6	0.09 ± 0.02	0.10 ± 0.03	0.11 ± 0.04
C 22:4n-6	2.53 ± 0.80	2.91 ± 0.84	2.86 ± 0.35
C 22:5n-6	0.58 ± 0.16	0.68 ± 0.15	0.68 ± 0.13
N-6	**52.22 ± 10.16[a]**	**69.78 ± 13.06[b]**	**69.16 ± 10.31[b]**
C 18:3n-3	0.67 ± 0.28[a]	0.94 ± 0.35[b]	0.97 ± 0.29[b]
C 20:3n-3	0.05 ± 0.02	0.07 ± 0.03	0.06 ± 0.03
C 20:5n-3	0.80 ± 0.36[a]	1.64 ± 0.43[b]	2.68 ± 0.58[c]
C 22:5n-3	2.17 ± 0.59[a]	2.82 ± 0.90[b]	3.26 ± 0.51[b]
C 22:6n-3	3.95 ± 0.75[a]	5.39 ± 1.05[b]	6.88 ± 1.26[c]
N-3	**7.65 ± 1.50[a]**	**10.85 ± 2.28[b]**	**13.85 ± 2.04[c]**
PUFAs	**59.87 ± 11.36[a]**	**80.63 ± 15.08[b]**	**83.01 ± 12.04[b]**
HUFAs	**30.02 ± 6.73[a]**	**37.28 ± 8.22[b]**	**40.70 ± 4.99[b]**
EPA+DHA	**4.76 ± 0.97[a]**	**7.03 ± 1.34[b]**	**9.57 ± 1.67[c]**
N-6/N-3	**6.89 ± 0.84[a]**	**6.51 ± 0.73[a]**	**5.01 ± 0.43[b]**
%n-3 HUFA in total HUFA	**23.48 ± 2.51[a]**	**26.73 ± 2.10[b]**	**31.65 ± 2.52[c]**
Total	**151.82 ± 31.14[a]**	**201.04 ± 39.79[b]**	**207.51 ± 31.37[b]**

Saturated fatty acids (SFAs); Mono-unsaturated fatty acids (MUFAs); Omega-6 fatty acids (N-6); Omega-3 fatty acids (N-3); Polyunsaturated fatty acids (PUFAs); Highly unsaturated fatty acids (HUFAs); Eicosapentaenoic acid (EPA); Docosahexaenoic acid (DHA). Omega-6:Omega-3 ratio (N-6/N-3). Superscript differences represent significantly different values after one-way ANOVA + Tukey HSD ($p < 0.05$).

* supporting data from Dr. Ashley Patterson's Doctoral Thesis (Reference: Patterson, 2012)

Appendix D. Fish Oil Supplementation-Fatty Acid Composition of Lipid Pools (Chapter 8)

Table D.9. ***Fatty Acid Composition of Whole Blood (n = 5)****

	Concentration (*µg fatty acid per 100 µL whole blood)*			
Fatty Acid	**Baseline**	**Week 4**	**Week 8**	**Week 12**
C 12:0	0.14 ± 0.06^{ab}	0.22 ± 0.14^{b}	0.19 ± 0.08^{ab}	0.07 ± 0.02^{a}
C 14:0	1.42 ± 0.74	1.70 ± 0.90	1.63 ± 0.54	1.11 ± 0.26
C 16:0	37.60 ± 9.34	44.77 ± 8.42	45.07 ± 14.16	41.84 ± 7.05
C 18:0	20.92 ± 4.91	24.02 ± 3.62	25.39 ± 9.20	22.97 ± 3.82
C 20:0	0.50 ± 0.13	0.58 ± 0.08	0.98 ± 0.97	0.56 ± 0.12
C 22:0	1.42 ± 0.40	1.55 ± 0.35	1.83 ± 0.28	1.60 ± 0.24
C 24:0	2.58 ± 0.45	2.90 ± 0.69	3.46 ± 0.83	2.86 ± 0.51
SFAs	**69.20 ± 14.94**	**81.53 ± 14.47**	**86.11 ± 27.06**	**76.21 ± 11.77**
C 12:1	<0.01 ± <0.01^{a}	<0.01 ± <0.01^{a}	0.01 ± <0.01^{ab}	0.01 ± <0.01^{b}
C 14:1	0.07 ± 0.09	0.10 ± 0.10	0.08 ± 0.05	0.06 ± 0.02
C 16:1	1.89 ± 1.72	2.21 ± 0.98	2.20 ± 1.63	1.89 ± 0.50
C 18:1n-7	2.74 ± 0.57	3.19 ± 0.25	2.99 ± 0.63	3.33 ± 0.26
C 18:1n-9	26.01 ± 6.68	33.62 ± 5.75	30.65 ± 8.30	34.90 ± 9.55
C 20:1n-9	0.39 ± 0.09	0.44 ± 0.07	0.40 ± 0.03	0.42 ± 0.07
C 22:1n-9	0.47 ± 0.04^{a}	0.30 ± 0.04^{b}	0.51 ± 0.05^{a}	0.53 ± 0.04^{a}
C 24:1n-9	3.11 ± 0.64^{a}	3.33 ± 0.40^{ab}	4.06 ± 0.48^{b}	3.30 ± 0.37^{ab}
MUFAs	**36.23 ± 11.46**	**43.85 ± 7.06**	**41.66 ± 10.68**	**44.81 ± 9.84**
C 18:2n-6	29.90 ± 5.38^{a}	42.38 ± 7.69^{ab}	38.94 ± 9.94^{ab}	51.42 ± 15.21^{b}
C 18:3n-6	0.37 ± 0.21	0.71 ± 0.47	0.65 ± 0.28	0.53 ± 0.18
C 20:2n-6	0.42 ± 0.12	0.46 ± 0.07	0.57 ± 0.11	0.45 ± 0.05
C 20:3n-6	2.99 ± 1.30	3.21 ± 0.93	3.20 ± 1.07	2.67 ± 0.57
C 20:4n-6	21.83 ± 3.32	23.43 ± 3.38	21.88 ± 3.90	22.76 ± 4.31
C 22:2n-6	0.08 ± 0.02	0.12 ± 0.04	0.12 ± 0.07	0.11 ± 0.02
C 22:4n-6	3.31 ± 1.03	3.46 ± 1.00	3.07 ± 0.29	2.56 ± 0.58
C 22:5n-6	0.68 ± 0.14	0.71 ± 0.09	0.68 ± 0.18	0.51 ± 0.08
N-6	**59.59 ± 10.46**	**74.47 ± 12.49**	**69.11 ± 15.07**	**81.02 ± 19.33**
C 18:3n-3	0.64 ± 0.14^{a}	0.85 ± 0.21^{ab}	0.85 ± 0.18^{ab}	1.04 ± 0.14^{b}
C 20:3n-3	0.06 ± 0.03	0.06 ± 0.01	0.04 ± 0.02	0.06 ± 0.01
C 20:5n-3	0.89 ± 0.31^{a}	1.74 ± 0.48^{ab}	2.71 ± 0.87^{bc}	4.11 ± 1.21^{c}
C 22:5n-3	2.52 ± 0.51^{a}	3.04 ± 0.44^{ab}	3.21 ± 0.30^{ab}	3.40 ± 0.34^{b}
C 22:6n-3	4.25 ± 0.90^{a}	5.37 ± 0.73^{ab}	6.16 ± 1.52^{ab}	7.33 ± 1.11^{b}
N-3	**8.36 ± 1.67^{a}**	**11.05 ± 1.53^{ab}**	**12.98 ± 2.68^{bc}**	**15.93 ± 2.41^{c}**
PUFAs	**67.95 ± 11.86**	**85.52 ± 13.82**	**82.09 ± 17.67**	**96.95 ± 21.24**
HUFAs	**36.53 ± 6.24**	**41.01 ± 5.85**	**40.96 ± 7.46**	**43.41 ± 6.91**
EPA+DHA	**5.14 ± 1.18^{a}**	**7.10 ± 1.20^{ab}**	**8.87 ± 2.30^{bc}**	**11.44 ± 2.24^{c}**
N-6/N-3	**7.18 ± 0.72^{a}**	**6.74 ± 0.63^{a}**	**5.32 ± 0.29^{b}**	**5.07 ± 0.84^{b}**
%n-3 HUFA in total HUFA	**21.11 ± 1.79^{a}**	**24.91 ± 1.55^{b}**	**29.47 ± 1.19^{c}**	**34.35 ± 1.63^{d}**
Total	**173.38 ± 35.96**	**210.90 ± 32.91**	**209.85 ± 52.47**	**217.96 ± 42.15**

Saturated fatty acids (SFAs); Mono-unsaturated fatty acids (MUFAs); Omega-6 fatty acids (N-6); Omega-3 fatty acids (N-3); Polyunsaturated fatty acids (PUFAs); Highly unsaturated fatty acids (HUFAs); Eicosapentaenoic acid (EPA); Docosahexaenoic acid (DHA). Omega-6:Omega-3 ratio (N-6/N-3). Superscript differences represent significantly different values after one-way ANOVA + Tukey HSD ($p < 0.05$).

* supporting data from Dr. Ashley Patterson's Doctoral Thesis (Reference: Patterson, 2012)

Appendix D. Fish Oil Supplementation-Fatty Acid Composition of Lipid Pools (Chapter 8)

Table D.10. ***Fatty Acid Composition of Erythrocytes (n = 20)****

	Concentration (*µg fatty acid per 200 mg erythrocytes)*		
Fatty Acid	**Baseline**	**Week 4**	**Week 8**
C 12:0	0.37 ± 0.05[a]	0.17 ± 0.13[b]	0.23 ± 0.13[b]
C 14:0	2.38 ± 0.61[ab]	2.84 ± 0.79[a]	1.98 ± 0.48[b]
C 16:0	86.60 ± 7.29	79.99 ± 11.19	80.54 ± 15.37
C 18:0	52.56 ± 4.89	50.45 ± 7.44	52.82 ± 8.19
C 20:0	1.19 ± 0.19	1.16 ± 0.25	1.31 ± 0.35
C 22:0	4.54 ± 0.53	4.40 ± 0.76	4.40 ± 0.96
C 24:0	12.56 ± 1.72	12.24 ± 2.09	12.35 ± 2.45
SFAs	**179.77 ± 11.88**	**164.89 ± 21.05**	**170.60 ± 28.48**
C 12:1	0.01 ± 0.01	0.01 ± <0.01	0.04 ± 0.08
C 14:1	0.02 ± 0.01	0.02 ± 0.02	0.08 ± 0.13
C 16:1	1.11 ± 0.48	0.97 ± 0.29	1.01 ± 0.31
C 18:1n-7	5.06 ± 0.52[a]	4.49 ± 0.60[b]	4.52 ± 0.70[b]
C 18:1n-9	49.83 ± 4.91[a]	45.52 ± 6.48[ab]	44.93 ± 7.50[b]
C 20:1n-9	1.06 ± 0.23	0.97 ± 0.25	0.96 ± 0.26
C 22:1n-9	0.57 ± 0.07[a]	0.42 ± 0.06[b]	0.59 ± 0.18[a]
C 24:1n-9	13.06 ± 1.69	12.67 ± 1.37	12.59 ± 1.98
MUFAs	**73.35 ± 6.29[a]**	**66.77 ± 8.28[b]**	**66.99 ± 10.18[b]**
C 18:2n-6	40.82 ± 5.38	37.39 ± 6.57	36.49 ± 6.58
C 18:3n-6	0.19 ± 0.06	0.14 ± 0.06	0.18 ± 0.10
C 20:2n-6	0.98 ± 0.16	0.89 ± 0.20	0.98 ± 0.17
C 20:3n-6	6.20 ± 1.69	5.49 ± 1.51	5.22 ± 1.32
C 20:4n-6	54.40 ± 6.02[a]	49.12 ± 5.97[b]	48.29 ± 7.35[b]
C 22:2n-6	0.27 ± 0.08	0.25 ± 0.08	0.27 ± 0.13
C 22:4n-6	12.90 ± 2.04[a]	11.39 ± 2.11[b]	10.44 ± 1.80[b]
C 22:5n-6	2.28 ± 0.37[a]	1.98 ± 0.31[b]	1.76 ± 0.28[b]
N-6	**118.03 ± 9.42[a]**	**106.67 ± 13.48[b]**	**103.63 ± 14.12[b]**
C 18:3n-3	0.60 ± 0.18[a]	0.59 ± 0.13[b]	0.82 ± 0.23[b]
C 20:3n-3	0.07 ± 0.03	0.08 ± 0.03	0.11 ± 0.10
C 20:5n-3	1.89 ± 0.65[a]	2.46 ± 0.59[a]	3.98 ± 1.00[b]
C 22:5n-3	8.44 ± 1.39	8.33 ± 1.48	9.31 ± 1.84
C 22:6n-3	13.61 ± 2.76	13.58 ± 3.35	15.08 ± 2.73
N-3	**24.62 ± 3.37[a]**	**25.04 ± 4.78[a]**	**29.29 ± 4.97[b]**
PUFAs	**142.65 ± 12.15**	**131.70 ± 17.89**	**132.92 ± 18.55**
HUFAs	**99.79 ± 9.08**	**92.43 ± 12.04**	**94.17 ± 12.55**
EPA+DHA	**15.50 ± 2.92[a]**	**16.04 ± 3.73[a]**	**19.05 ± 3.52[b]**
N-6/N-3	**4.84 ± 0.46[a]**	**4.32 ± 0.40[b]**	**3.57 ± 0.30[c]**
%n-3 HUFA in total HUFA	**24.03 ± 2.05[a]**	**26.30 ± 2.15[b]**	**30.15 ± 2.10[c]**
Total	**395.77 ± 26.49**	**363.36 ± 45.50**	**370.52 ± 55.65**

Saturated fatty acids (SFAs); Mono-unsaturated fatty acids (MUFAs); Omega-6 fatty acids (N-6); Omega-3 fatty acids (N-3); Polyunsaturated fatty acids (PUFAs); Highly unsaturated fatty acids (HUFAs); Eicosapentaenoic acid (EPA); Docosahexaenoic acid (DHA). Omega-6:Omega-3 ratio (N-6/N-3). Superscript differences represent significantly different values after one-way ANOVA + Tukey HSD ($p < 0.05$).

* supporting data from Dr. Ashley Patterson's Doctoral Thesis (Reference: Patterson, 2012)

Appendix D. Fish Oil Supplementation-Fatty Acid Composition of Lipid Pools (Chapter 8)

Table D.11. ***Fatty Acid Composition of Erythrocytes (n = 5)****

	Concentration (*µg fatty acid per 200 mg erythrocytes)*			
Fatty Acid	**Baseline**	**Week 4**	**Week 8**	**Week 12**
C 12:0	0.34 ± 0.04[a]	0.09 ± 0.01[b]	0.15 ± 0.02[c]	0.03 ± 0.01[d]
C 14:0	2.07 ± 0.29[a]	2.75 ± 0.41[b]	1.89 ± 0.44[a]	1.46 ± 0.19[a]
C 16:0	81.90 ± 3.96	74.43 ± 5.68	68.19 ± 15.09	68.63 ± 4.79
C 18:0	54.44 ± 4.59[a]	47.86 ± 2.07[ab]	47.28 ± 5.83[b]	49.10 ± 1.61[ab]
C 20:0	1.19 ± 0.19[a]	1.11 ± 0.09[ab]	1.15 ± 0.14[ab]	0.93 ± 0.10[b]
C 22:0	4.69 ± 0.56[a]	4.42 ± 0.47[ab]	4.38 ± 0.87[ab]	3.34 ± 0.50[b]
C 24:0	11.83 ± 2.47	11.17 ± 2.12	11.49 ± 2.39	8.30 ± 1.23
SFAs	**177.94 ± 10.94[a]**	**155.49 ± 9.93[ab]**	**150.30 ± 27.27[ab]**	**144.06 ± 7.67[b]**
C 12:1	0.01 ± <0.01	0.01 ± <0.01	0.01 ± 0.01	0.01 ± <0.01
C 14:1	0.03 ± 0.01	0.03 ± 0.02	0.03 ± 0.02	0.04 ± 0.02
C 16:1	1.06 ± 0.68	0.85 ± 0.29	0.83 ± 0.44	0.71 ± 0.18
C 18:1n-7	5.03 ± 0.39[a]	4.33 ± 0.43[ab]	4.09 ± 0.52[b]	4.40 ± 0.55[ab]
C 18:1n-9	47.63 ± 5.06	41.99 ± 4.45	39.95 ± 8.47	41.78 ± 3.24
C 20:1n-9	0.95 ± 0.06	0.82 ± 0.06	0.82 ± 0.13	0.82 ± 0.12
C 22:1n-9	0.54 ± 0.06[ab]	0.47 ± 0.08[a]	0.65 ± 0.12[b]	0.40 ± 0.09[a]
C 24:1n-9	12.58 ± 1.86[a]	11.85 ± 0.87[a]	12.14 ± 1.09[a]	8.63 ± 0.86[b]
MUFAs	**70.72 ± 5.89[a]**	**62.03 ± 4.83[ab]**	**60.55 ± 10.34[ab]**	**57.76 ± 3.34[b]**
C 18:2n-6	36.45 ± 3.38	32.66 ± 1.55	31.07 ± 6.16	32.51 ± 3.20
C 18:3n-6	0.19 ± 0.08	0.14 ± 0.08	0.17 ± 0.08	0.12 ± 0.03
C 20:2n-6	0.86 ± 0.07[ab]	0.75 ± 0.03[a]	0.96 ± 0.19[b]	0.78 ± 0.09[ab]
C 20:3n-6	5.42 ± 1.39	4.61 ± 1.12	4.45 ± 1.31	4.28 ± 0.96
C 20:4n-6	56.08 ± 3.47[a]	47.70 ± 3.51[b]	45.96 ± 5.84[b]	46.96 ± 2.33[b]
C 22:2n-6	0.23 ± 0.06	0.22 ± 0.03	0.21 ± 0.04	0.23 ± 0.04
C 22:4n-6	13.58 ± 2.02[a]	11.57 ± 1.72[ab]	11.08 ± 1.92[ab]	9.82 ± 1.74[b]
C 22:5n-6	2.25 ± 0.37[a]	1.85 ± 0.32[ab]	1.78 ± 0.41[ab]	1.53 ± 0.28[b]
N-6	**115.05 ± 3.60[a]**	**99.51 ± 3.78[b]**	**95.67 ± 13.25[b]**	**96.23 ± 4.87[b]**
C 18:3n-3	0.48 ± 0.08	0.47 ± 0.04	0.64 ± 0.14	0.47 ± 0.11
C 20:3n-3	0.06 ± 0.01	0.07 ± 0.02	0.07 ± 0.01	0.07 ± 0.01
C 20:5n-3	1.72 ± 0.40[a]	2.21 ± 0.32[ab]	3.35 ± 0.87[b]	5.21 ± 0.84[c]
C 22:5n-3	8.39 ± 0.35[ab]	7.76 ± 0.34[a]	8.75 ± 1.06[ab]	9.53 ± 0.87[b]
C 22:6n-3	11.86 ± 2.34[ab]	11.20 ± 1.82[a]	13.12 ± 2.29[ab]	15.29 ± 1.44[b]
N-3	**22.51 ± 2.89[a]**	**21.70 ± 2.15[a]**	**25.93 ± 3.81[ab]**	**30.57 ± 2.36[b]**
PUFAs	**137.56 ± 5.42**	**121.21 ± 5.28**	**121.60 ± 16.61**	**126.80 ± 6.73**
HUFAs	**99.36 ± 5.17[a]**	**86.96 ± 4.71[b]**	**88.55 ± 10.93[ab]**	**92.70 ± 3.99[ab]**
EPA+DHA	**13.58 ± 2.73[a]**	**13.41 ± 2.09[a]**	**16.46 ± 3.02[ab]**	**20.50 ± 2.04[b]**
N-6/N-3	**5.17 ± 0.59[a]**	**4.61 ± 0.35[a]**	**3.70 ± 0.26[b]**	**3.16 ± 0.17[b]**
%n-3 HUFA in total HUFA	**22.11 ± 1.79[a]**	**24.38 ± 1.50[b]**	**28.51 ± 1.11[b]**	**32.44 ± 1.20[c]**
Total	**386.23 ± 21.35[a]**	**338.73 ± 19.31[ab]**	**332.45 ± 53.88[ab]**	**328.63 ± 16.86[b]**

Saturated fatty acids (SFAs); Mono-unsaturated fatty acids (MUFAs); Omega-6 fatty acids (N-6); Omega-3 fatty acids (N-3); Polyunsaturated fatty acids (PUFAs); Highly unsaturated fatty acids (HUFAs); Eicosapentaenoic acid (EPA); Docosahexaenoic acid (DHA). Omega-6:Omega-3 ratio (N-6/N-3). Superscript differences represent significantly different values after one-way ANOVA + Tukey HSD ($p < 0.05$).

* supporting data from Dr. Ashley Patterson's Doctoral Thesis (Reference: Patterson, 2012)

Appendix D. Fish Oil Supplementation-Fatty Acid Composition of Lipid Pools (Chapter 8)

Table D.12. ***Fatty Acid Composition of Plasma Phospholipids (n = 20)****

	Concentration (*µg fatty acid per 100 µL plasma)*		
Fatty Acid	**Baseline**	**Week 4**	**Week 8**
C 12:0	0.05 ± 0.02[a]	0.18 ± 0.20[ab]	0.19 ± 0.22[b]
C 14:0	0.53 ± 0.16[a]	0.66 ± 0.23[ab]	0.75 ± 0.21[b]
C 16:0	26.93 ± 5.93[a]	30.31 ± 5.30[ab]	32.84 ± 7.82[b]
C 18:0	15.52 ± 3.15[a]	18.58 ± 4.34[b]	19.02 ± 5.01[b]
C 20:0	0.55 ± 0.10	0.57 ± 0.09	0.54 ± 0.08
C 22:0	1.45 ± 0.33[a]	1.35 ± 0.37[ab]	1.18 ± 0.31[b]
C 24:0	1.31 ± 0.31	1.23 ± 0.37	1.09 ± 0.31
SFAs	**47.92 ± 9.54[a]**	**54.65 ± 10.09[ab]**	**57.32 ± 12.78[b]**
C 12:1	0.01 ± 0.01[a]	0.01 ± 0.01[a]	0.06 ± 0.05[b]
C 14:1	0.01 ± 0.01	0.02 ± 0.02	0.02 ± 0.01
C 16:1	0.44 ± 0.30	0.56 ± 0.19	0.55 ± 0.29
C 18:1n-7	1.72 ± 0.35	1.97 ± 0.54	2.08 ± 0.54
C 18:1n-9	9.55 ± 2.91[a]	13.76 ± 8.66[ab]	16.47 ± 7.42[b]
C 20:1n-9	0.21 ± 0.05	0.26 ± 0.16	0.29 ± 0.11
C 22:1n-9	0.32 ± 0.11[a]	0.40 ± 0.28[a]	0.49 ± 0.19[b]
C 24:1n-9	2.29 ± 0.40[a]	1.97 ± 0.64[a]	1.66 ± 0.45[b]
MUFAs	**14.68 ± 3.66[a]**	**19.08 ± 9.45[ab]**	**21.78 ± 8.36[b]**
C 18:2n-6	20.44 ± 3.74	23.36 ± 6.15	23.74 ± 5.17
C 18:3n-6	0.11 ± 0.08	0.10 ± 0.07	0.12 ± 0.07
C 20:2n-6	0.37 ± 0.12	0.35 ± 0.10	0.34 ± 0.09
C 20:3n-6	3.37 ± 1.27	3.12 ± 1.17	3.20 ± 1.17
C 20:4n-6	11.83 ± 3.05	10.66 ± 2.40	10.67 ± 3.14
C 22:2n-6	0.05 ± 0.02	0.06 ± 0.05	0.06 ± 0.05
C 22:4n-6	0.46 ± 0.12[a]	0.38 ± 0.10[ab]	0.31 ± 0.09[b]
C 22:5n-6	0.35 ± 0.10[a]	0.26 ± 0.07[b]	0.21 ± 0.07[b]
N-6	**36.99 ± 6.84**	**38.29 ± 8.01**	**38.64 ± 8.85**
C 18:3n-3	0.30 ± 0.17[a]	0.76 ± 1.19[ab]	1.04 ± 0.96[b]
C 20:3n-3	0.05 ± 0.02	0.04 ± 0.02	0.04 ± 0.01
C 20:5n-3	0.72 ± 0.41[a]	1.22 ± 0.27[b]	2.09 ± 0.68[c]
C 22:5n-3	1.04 ± 0.34[a]	1.13 ± 0.34[ab]	1.37 ± 0.49[b]
C 22:6n-3	3.37 ± 0.70[a]	3.75 ± 0.75[ab]	4.28 ± 0.86[b]
N-3	**5.48 ± 1.21[a]**	**6.91 ± 1.52[b]**	**8.82 ± 2.25[c]**
PUFAs	**42.47 ± 7.60**	**45.20 ± 9.26**	**47.46 ± 10.89**
HUFAs	**21.20 ± 4.82**	**20.57 ± 3.87**	**22.18 ± 5.58**
EPA+DHA	**4.09 ± 0.98[a]**	**4.98 ± 0.88[b]**	**6.38 ± 1.43[c]**
N-6/N-3	**6.89 ± 1.06[a]**	**5.59 ± 0.74[b]**	**4.43 ± 0.50[c]**
%n-3 HUFA in total HUFA	**24.62 ± 3.64[a]**	**30.04 ± 2.58[b]**	**35.47 ± 3.65[c]**
Total	**105.07 ± 20.17[a]**	**118.93 ± 23.55[ab]**	**126.57 ± 28.18[b]**

Saturated fatty acids (SFAs); Mono-unsaturated fatty acids (MUFAs); Omega-6 fatty acids (N-6); Omega-3 fatty acids (N-3); Polyunsaturated fatty acids (PUFAs); Highly unsaturated fatty acids (HUFAs); Eicosapentaenoic acid (EPA); Docosahexaenoic acid (DHA). Omega-6:Omega-3 ratio (N-6/N-3). Superscript differences represent significantly different values after one-way ANOVA + Tukey HSD ($p < 0.05$).

* supporting data from Dr. Ashley Patterson's Doctoral Thesis (Reference: Patterson, 2012)

Appendix D. Fish Oil Supplementation-Fatty Acid Composition of Lipid Pools (Chapter 8)

Table D.13. ***Fatty Acid Composition of Plasma Phospholipids (n = 5)****

	Concentration (*µg fatty acid per 100 µL plasma)*			
Fatty Acid	**Baseline**	**Week 4**	**Week 8**	**Week 12**
C 12:0	0.07 ± 0.02	0.20 ± 0.31	0.13 ± 0.03	0.11 ± 0.06
C 14:0	0.62 ± 0.24	0.61 ± 0.33	0.77 ± 0.23	0.88 ± 0.27
C 16:0	29.66 ± 9.72	27.17 ± 8.92	36.28 ± 13.28	34.05 ± 9.27
C 18:0	17.28 ± 5.02	16.45 ± 4.70	23.82 ± 7.97	24.02 ± 8.93
C 20:0	0.59 ± 0.10	0.53 ± 0.11	0.57 ± 0.11	0.64 ± 0.18
C 22:0	1.48 ± 0.39	1.30 ± 0.31	1.15 ± 0.46	1.26 ± 0.27
C 24:0	1.33 ± 0.41	1.21 ± 0.28	1.06 ± 0.44	1.23 ± 0.28
SFAs	**52.89 ± 15.71**	**48.97 ± 15.29**	**65.78 ± 21.83**	**64.76 ± 19.61**
C 12:1	0.01 ± <0.01[a]	0.01 ± 0.01[a]	0.07 ± 0.04[b]	0.01 ± <0.01[a]
C 14:1	0.01 ± 0.01	0.02 ± 0.01	0.01 ± <0.01	0.02 ± 0.02
C 16:1	0.58 ± 0.57	0.53 ± 0.25	0.62 ± 0.51	0.42 ± 0.13
C 18:1n-7	1.95 ± 0.60	2.06 ± 0.81	2.27 ± 0.70	2.01 ± 0.35
C 18:1n-9	10.91 ± 5.29	15.40 ± 13.09	19.75 ± 8.06	9.55 ± 3.35
C 20:1n-9	0.20 ± 0.07	0.28 ± 0.21	0.33 ± 0.12	0.19 ± 0.05
C 22:1n-9	0.33 ± 0.15	0.29 ± 0.13	0.56 ± 0.18	0.47 ± 0.15
C 24:1n-9	2.51 ± 0.32	2.02 ± 0.42	1.69 ± 0.64	1.96 ± 0.45
MUFAs	**16.63 ± 6.54**	**20.70 ± 14.29**	**25.49 ± 9.66**	**14.89 ± 4.17**
C 18:2n-6	20.09 ± 5.93	20.95 ± 9.24	25.25 ± 8.20	23.22 ± 6.69
C 18:3n-6	0.16 ± 0.12	0.12 ± 0.09	0.14 ± 0.08	0.18 ± 0.04
C 20:2n-6	0.36 ± 0.16	0.30 ± 0.10	0.33 ± 0.14	0.32 ± 0.10
C 20:3n-6	3.54 ± 1.96	2.94 ± 1.17	3.24 ± 1.41	2.68 ± 1.04
C 20:4n-6	14.58 ± 3.31	11.93 ± 3.11	12.16 ± 3.99	12.51 ± 2.82
C 22:2n-6	0.05 ± 0.02	0.04 ± 0.05	0.04 ± 0.03	0.05 ± 0.02
C 22:4n-6	0.53 ± 0.16[a]	0.38 ± 0.11[ab]	0.33 ± 0.12[ab]	0.26 ± 0.04[b]
C 22:5n-6	0.43 ± 0.14[a]	0.26 ± 0.09[ab]	0.22 ± 0.12[b]	0.21 ± 0.10[b]
N-6	**39.75 ± 10.85**	**36.93 ± 13.29**	**41.72 ± 13.74**	**39.43 ± 10.15**
C 18:3n-3	0.35 ± 0.21	0.87 ± 1.61	1.65 ± 1.04	0.23 ± 0.11
C 20:3n-3	0.05 ± 0.01	0.04 ± 0.01	0.04 ± 0.02	0.05 ± 0.01
C 20:5n-3	0.77 ± 0.42[a]	1.19 ± 0.40[ab]	2.51 ± 1.17[bc]	2.81 ± 1.03[c]
C 22:5n-3	1.18 ± 0.34	1.19 ± 0.27	1.69 ± 0.73	1.36 ± 0.31
C 22:6n-3[#]	3.21 ± 1.07	3.83 ± 1.02	4.28 ± 1.59	5.37 ± 1.39
N-3	**5.56 ± 1.64**	**7.11 ± 2.95**	**10.16 ± 3.66**	**9.82 ± 2.73**
PUFAs	**45.31 ± 12.40**	**44.04 ± 16.22**	**51.88 ± 17.25**	**49.24 ± 12.81**
HUFAs	**24.30 ± 6.88**	**21.76 ± 5.95**	**24.47 ± 8.95**	**25.24 ± 6.43**
EPA+DHA	**3.98 ± 1.38[a]**	**5.01 ± 1.39[ab]**	**6.79 ± 2.74[ab]**	**8.18 ± 2.35[b]**
N-6/N-3	**7.21 ± 0.68[a]**	**5.30 ± 0.44[b]**	**4.19 ± 0.58[c]**	**4.06 ± 0.41[c]**
%n-3 HUFA in total HUFA	**21.28 ± 1.37[a]**	**28.79 ± 1.17[b]**	**34.42 ± 1.63[c]**	**37.83 ± 1.92[d]**
Total	**114.82 ± 34.41**	**113.72 ± 45.28**	**143.15 ± 43.42**	**128.90 ± 35.30**

Saturated fatty acids (SFAs); Mono-unsaturated fatty acids (MUFAs); Omega-6 fatty acids (N-6); Omega-3 fatty acids (N-3); Polyunsaturated fatty acids (PUFAs); Highly unsaturated fatty acids (HUFAs); Eicosapentaenoic acid (EPA); Docosahexaenoic acid (DHA). Omega-6:Omega-3 ratio (N-6/N-3). Superscript differences represent significantly different values after one-way ANOVA + Tukey HSD ($p < 0.05$).

* supporting data from Dr. Ashley Patterson's Doctoral Thesis (Reference: Patterson, 2012)

[#] baseline DHA and week 12 DHA trend towards significance; $p = 0.07$.

Appendix E. Lipidomics of Whole Blood, Plasma and Erythrocytes (Chapter 9)

Table E.1. ***Characterization of Omega-3 HUFA-Containing Complex Lipids in Whole Blood, Plasma and Erythrocytes (n = 9)***

			Lipid Abundance, n = 9 (*Arbitrary Units*, Average ± SD)		
Observed *m/z*	**Lipid**	**Adduct**	**Whole Blood**	**Plasma**	**Erythrocytes**
780.5536	PC 16:0/20:5	$[M+H]^+$	64.19 ± 36.70	57.74 ± 32.66	16.68 ± 8.41
806.5693	PC 16:0/22:6	$[M+H]^+$	95.54 ± 39.75	130.36 ± 56.51	28.91 ± 7.27
812.6159	PC 18:0/20:3	$[M+H]^+$	35.44 ± 13.97	42.54 ± 12.97	7.91 ± 1.83
810.6002	PC 18:0/20:4	$[M+H]^+$	126.79 ± 32.62	178.91 ± 59.73	40.29 ± 8.12
808.5851	PC 18:0/20:5	$[M+H]^+$	17.38 ± 12.81	23.51 ± 21.15	6.12 ± 4.62
838.6322	PC 18:0/22:4	$[M+H]^+$	2.73 ± 0.49	3.14 ± 0.67	0.82 ± 0.10
834.6009	PC 18:0/22:6	$[M+H]^+$	28.71 ± 11.97	39.29 ± 17.54	7.47 ± 1.80
832.5853	PC 18:1/22:6	$[M+H]^+$	4.36 ± 1.86	5.54 ± 2.87	1.16 ± 0.24
740.5227	PE 16:0/20:4	$[M+H]^+$	13.26 ± 1.88	0.77 ± 0.30	18.60 ± 2.33
738.5069	PE 16:0/20:5	$[M+H]^+$	1.13 ± 0.71	0.06 ± 0.06	1.48 ± 0.75
764.5225	PE 16:0/22:6	$[M+H]^+$	8.43 ± 2.93	1.96 ± 1.00	17.99 ± 4.75
722.5114	Plasmenyl-PE P-16:0/20:5	$[M+H]^+$	1.44 ± 0.81	0.41 ± 0.28	1.67 ± 0.87
748.5273	Plasmenyl-PE P-16:0/22:6	$[M+H]^+$	2.97 ± 0.77	1.36 ± 0.54	3.89 ± 0.90
812.5437	PS 18:0/20:4	$[M+H]^+$	10.92 ± 1.93	0.10 ± 0.07	26.52 ± 5.13
836.5434	PS 18:0/22:6	$[M+H]^+$	7.11 ± 1.51	0.09 ± 0.04	19.11 ± 2.45
922.7861	TAG 16:0/18:1/22:6	$[M+NH_4]^+$	5.24 ± 4.02	9.12 ± 5.19	<0.01 ± <0.01
922.7861	TAG 18:1/18:1/20:5	$[M+NH_4]^+$	1.36 ± 0.86	2.43 ± 1.42	<0.01 ± <0.01
690.6186	CE 20:4	$[M+NH_4]^+$	5.90 ± 2.68	10.48 ± 2.86	<0.01 ± <0.01
688.6029	CE 20:5	$[M+NH_4]^+$	0.80 ± 1.04	2.53 ± 2.94	<0.01 ± <0.01
714.6175	CE 22:6	$[M+NH_4]^+$	0.43 ± 0.24	2.07 ± 1.31	<0.01 ± <0.01

Mass-to-charge ratio (*m/z*); Phosphatidylcholine (PC); Phosphatidylethanolamine (PE); Phosphatidylserine (PS); Triacylglycerol (TAG); Cholesteryl ester (CE).